UNIVERSITY OF OKLAHOMA

GRADUATE COLLEGE

USE OF POST-CONSUMER RECYCLED (PCR) PLASTICS IN ASPHALT MIXES: A LABORATORY STUDY

A DISSERTATION

SUBMITTED TO THE GRADUATE FACULTY

in partial fulfillment of the requirements for the

Degree of

DOCTOR OF PHILOSOPHY

By

SAGAR GHOS

Norman, Oklahoma

2024

USE OF POST-CONSUMER RECYCLED (PCR) PLASTICS IN ASPHALT MIXES: A LABORATORY STUDY

A DISSERTATION APPROVED FOR THE

SCHOOL OF CIVIL ENGINEERING AND ENVIRONMENTAL SCIENCE

BY THE COMMITTEE CONSISTING OF

Dr. Musharraf Zaman, Chair

Dr. Gerald A. Miller

Dr. Kianoosh Hatami

Dr. Liangliang Huang

Dr. Arif Sadri

Dedicated

to

My Beloved Parents

ACKNOWLEDGEMENTS

First and foremost, I would like to express my deep and sincere gratitude to God, The Almighty, for His countless blessings in every step of my life. Secondly, I would like to thank my parents and uncle who have always encouraged me and sacrificed everything for fulfilling my goals.

I would like to express my sincerest appreciation, deepest gratitude, and heartiest thanks to my supervisor and the Chair of my doctoral committee, Professor Dr. Musharraf Zaman, for his guidance, encouragement, and unparalleled support throughout my graduate studies at the University of Oklahoma. His deep insights, critical comments, edits, and valuable suggestions contributed greatly to the completion of this study. It was him who helped me to grow into a researcher. His mentoring style, high expectations and trust greatly elevated my critical thinking, writing skills, and confidence.

I would like to acknowledge and thank Dr. Liangliang Huang for serving on my dissertation committee. He has trained me on a very sophisticated analytical tool "Atomistic Modelling and Molecular Dynamic Simulation." I have learned a lot from him, which enabled me to examine material from the fundamental level. I am grateful to him for providing me with his valuable knowledge and input for completing this research.

I would like to thank Dr. Gerald A. Miller for serving on my dissertation committee. I have learned a lot from his "Forensic Geotechnical Engineering" class. I would like to thank him for sharing his knowledge, ideas and providing valuable input for completing this dissertation. Also, I wish to thank Dr. Kianoosh Hatami for serving on my doctoral committee. His valuable comments and ideas helped finalize this study. I would like to thank Dr. Arif Sadri for serving on my doctoral committee. His valuable insights helped me in finalizing this dissertation. I want to thank all the professors at the School of Civil Engineering and Environmental Science for helping me with their knowledge and experience through their courses at OU. I would like to express my deepest gratitude to all the staff of the School of Civil Engineering and Environmental Science and the Southern Plains Transportation Center (SPTC) for their help and support. I would also like to extend my gratitude to Dr. Michael Molina for his help in reviewing manuscripts.

I would like to acknowledge and thank every member of Dr. Zaman's research group, especially Dr. Syed Ashik Ali, for his enormous help and guidance throughout my research. He is an excellent example of a mentor, good friend, sincere researcher, and a fine person. He was always there to guide me in the field and laboratory testing and to help me in developing ideas throughout my graduate study here at OU. His valuable comments and suggestions helped me to improve my research and writing skills. I want to extend my gratitude to Dr. Matias Larrain Mendez, Mr. Kenneth R. Hobson, Mr. Luis Urbina and Mr. Axel Segura for their help in the field and laboratory work throughout my thesis research.

I must thank Dr. Nazimuddin Wasiuddin and his research group from the Louisiana Tech University for sharing their knowledge and help with the Fourier Transform Infrared Spectroscopy (FTIR) data collection and analysis. Special thanks to Md Reazul Islam for his help with the FTIR data collection. Special thanks to Mr. Greg Kaliki, Mr. Darrain Metzer, Silver Star Construction Inc., and EST Engineering Inc., now WSB, for help in collecting materials.

The financial support provided by the Oklahoma Center for Advancement of Science and Technology (OCAST), Oklahoma Department of Transportation, and Southern Plains

Transportation Center are greatly acknowledged. I am thankful to ODOT Asphalt Branch Manager, David Vivanco, for his support with this study. I wish to express my sincere gratitude to Avengard Innovative Inc. and Hite Plastics Inc. for their help and support with this study.

Finally, I want to thank my beautiful wife, Shoumita Ghosh and my daughter, Srijita Ghosh for their love, inspiration, encouragement, prayers, and support.

TABLE OF CONTENTS

LIST OF TABLES

LIST OF FIGURES

ABSTRACT

In recent years, the use of recycled materials in asphalt mixes has gained popularity among asphalt producers and users to reduce environmental pollution, enhance sustainability, and conserve natural resources. Among different recycled materials, the use of Post-Consumer Recycled (PCR) plastic poses several challenges. These challenges stem from the processes used to incorporate PCR plastic, mixing protocol, sample preparation, testing, and field implementation. Asphalt mixes containing PCR plastic pose several challenges both from the volumetric properties and performance standpoints. Specifically, this study investigates the changes in the volumetric properties and performance of PCR plastic-modified asphalt mixes designed using the Balanced Mix Design (BMD) approach. For this purpose, a control mix (0% plastic) was designed using the BMD approach. This mix was modified using different percentages of two PCR plastics, namely Low-Density Polyethylene (LDPE) and Linear Low-Density Polyethylene (LLDPE). The PCR plastics were added using the dry process. A suitable mixing protocol was developed for incorporating PCR plastics by simulating the production process used for incorporation of Reclaimed Asphalt Pavement (RAP) in an asphalt plant. Volumetric properties, namely maximum theoretical specific gravity of the mix, bulk specific gravity, voids in mineral aggregate (VMA), voids filled with asphalt (VFA), air void contents, and densities were determined for both control (0% plastic) and plastic-modified mixes. Also, Indirect Tensile Strength (ITS), Indirect Tensile Asphalt Cracking Test (IDEAL-CT), and Hamburg Wheel Track (HWT) tests were performed to assess performance of these mixes. Changes in the volumetric and performance properties of asphalt mixes due to plastic modification were studied and are reported in this dissertation.

To study the cracking behavior of plastic-modified mixes, effect of loading rate and notch depths on fracture properties was evaluated using Illinois Flexibility Index Test (IFIT), Louisiana Semicircular Bend (L-SCB) and IDEAL-CT. Fracture properties, specifically, fracture energy, Flexibility Index (FI), Cracking Tolerance Index (CT_{Index}), Strain Energy at Failure (SEF), and Critical Strain Energy Release Rate (*J-integral*) were evaluated.

In addition, the effect of aging conditions on the performance of plastic-modified mixes was evaluated in this study. For this purpose, asphalt mixes without plastic (control mix) and with (LDPE and LLDPE) modification were subjected to three aging conditions, namely short-, medium- and long-term aging. Mechanical tests, including IDEAL-CT and Dynamic Modulus (DM), were conducted to evaluate the effect of aging on cracking resistance and stiffness. Additionally, binders were extracted and recovered from all aged mixes and the extracted aggregates were visually inspected. The effect of aging on the rheological properties of the recovered binder was assessed using Rotational Viscosity (RV), Dynamic Shear Rheometer (DSR), and Multiple Stress Creep Recovery (MSCR) tests. The impact of aging was further examined by identifying changes in chemical functional groups using Fourier Transform Infrared Spectroscopy (FTIR) tests. Finally, AASHTOWare Pavement ME Design (PMED) simulations were used to evaluate the effect of aging on the field performance.

Over stiffening of plastic-modified mixes was observed due to the higher amounts of plastics, which resulted in reduced cracking resistance. Consequently, this study aimed at increasing the percentage of plastic in asphalt mixes by incorporating a bio-rejuvenator. The plastic-modified mixes were modified by adding bio-rejuvenator modified binder. The volumetric properties were determined and the mechanical performance, namely rutting, cracking and moisture induced damage resistance, of the asphalt mixes were evaluated using the

HWT and IDEAL-CT tests. The optimum dosage of plastics was determined using the BMD criteria. Moreover, the environmental impact analysis was performed on plastic-modified mixes. A significant reduction in Greenhouse Gas (GHG) emissions was observed from the use of plastic in asphalt mixes. Knowledge gained from this study on the effect of addition of PCR plastic on the performance of asphalt mixes designed using the BMD approach is expected to be helpful in incorporating waste plastic in future asphalt mix designs.

CHAPTER 1 INTRODUCTION

1.1 BACKGROUND

The utilization of recycled materials in asphalt mixes has gained popularity across the globe in recent years. Different recycled materials such as Reclaimed Asphalt Pavement (RAP), Recycled Asphalt Shingles (RAS), Post-Consumer Recycled (PCR) plastics and Ground Tire Rubber (GTR) are being used in asphalt mixes to reduce environmental pollution and conserve natural resources (Leng et al. 2018; Adegoke et al. 2019; Dalhat et al. 2019). In 2018, the USA generated 37.5 million tons of waste plastics (EPA 2020). According to the United States Environmental Protection Agency EPA (EPA 2020), only 8.7-percent of waste plastic was recycled, and the remaining was either burned for fuel value or landfilled. The recycling rate further went down to approximately 5% by the end of 2019 (Milbrandt et al. 2022). This trend of recycling of waste plastics remained unchanged till this date (The Guardian 2024). To reduce the impact of plastic pollution on the environment, the Plastic Industry Association (PLASTICS) conducted a study to identify potential New End Market Opportunities (NEMO) for recycling waste plastic. Incorporation of waste plastics in asphalt pavement construction was reported as one of the potential new end markets for waste plastics (PLASTICS 2020). In 2021 approximately 430 million tons of asphalt mixes were produced in the U.S. (Williams et al. 2022). Therefore, the use of PCR plastic in asphalt mixes even at a rate of 0.5%, as a replacement of aggregate (by weight), will reduce landfilling of waste plastic by approximately 8% (2 million tons). Thus, reusing PCR plastic in asphalt mixes is a win-win proposition for asphalt producers, construction companies, and the state Department of Transportations (DOTs) to enhance the durability and service life of pavements, while safeguarding the environment.

Asphalt mixes consist of two primary components, namely mineral aggregates and asphalt binder. Asphalt binders are blends of complex hydrocarbons and their derivatives (Wang et al. 2022). The binder is primarily composed of carbon (80-88%), hydrogen (8-12%), sulfur (0-9%), oxygen (0-2%), nitrogen (0-2%) and traces of some heavy metals (Lesueur 2009). Despite the presence of various chemical species, the main components of asphalt binder are categorized into four chemical groups namely, asphaltene, resins, aromatics and saturates (Lesueur 2009; Wang 2022). Asphaltenes are mainly composed of polyaromatics, n-alkanes and a few porphyrins. Resins are structurally similar to asphaltenes except they contain fewer aromatic rings and heteroatoms (Wang 2022). Aromatics contain aliphatic-like structure and sporadic condensed aromatic rings. Saturates are composed of long aliphatic chains with naphthenic hydrocarbons (Wang et al. 2022). Collectively, these four groups are referred to as the SARA fractions of asphalt binder. In asphalt mixes (also known as asphalt concrete), the binder acts as the binding agents for the aggregates.). Asphalt mixes are produced by mixing pre-heated aggregates with hot liquid asphalt binder.

As noted previously, asphalt agencies are trying to utilize waste plastics in asphalt mixes. The incorporation of waste plastics in asphalt mixes poses several challenges. These challenges stem from the processes used to incorporate PCR plastic, mixing protocol, sample preparation, and testing. Unlike some other recycled materials, asphalt mixes containing PCR plastic pose challenges both from the volumetric properties and performance standpoint. Most state DOTs use balanced mix designs, adding to these challenges. The types and quality of PCR plastics add to the challenge even more.

The waste plastic stream is generally composed of different resins, namely Polypropylene (PP) (32.1%), Low-Density Polyethylene (LDPE) and Linear Low-Density Polyethylene

(LLDPE) (17.5%), High-Density Polyethylene (HDPE) (11.5%), and others including Polyvinyl Chloride (PVC), Polystyrene (PS), and Polyethylene Terephthalate (PET) (38.6%) (EPA 2020). A recent study conducted by Willis et al. (2020) suggested using Polyethylene (PE) i.e., LDPE, LLDPE, and HDPE in the production of asphalt mixes as other plastics can produce toxic gases or are incompatible with asphalt mixes.

Until now, waste plastics have been incorporated in asphalt mixes using one of two processes, namely the wet process involving modification of binder with plastic and the dry process in which plastics are added directly to the mix (Abukhettala 2016; Angelone et al. 2016; Ranieri et al. 2017; Dalhat et al. 2019; Martin-Alfonso et al. 2019). The incorporation of waste plastics in asphalt mixes has been mostly studied with the wet process. A limited number of studies have been conducted using the dry process. Previous studies have reported improvements in the performance properties of asphalt mixes with the addition of plastic using both processes (Vasudevan et al. 2010; Angelone et al. 2016; Lastra-González et al. 2016; Dalhat et al. 2019). Improvement in asphalt binder and mix performances, specifically, rutting (Vasudevan et al. 2010; Angelone et al. 2016; Lastra-González et al. 2016; Dalhat et al. 2019), stiffness (Angelone et al. 2016; Zhang et al. 2011;) and moisture induced damage resistance (Leng et al. 2018; Haider et al. 2020). However, contradictory results were reported for fatigue cracking resistance after plastic addition in several previous studies (Angelone et al. 2016; Costa et al. 2017; Suaryana et al. 2018). Also, previous studies have reported some other issues, namely phase separation, storage stability, reduced workability, and incompatibility of plastic particles with asphalt binder (Fang et al. 2014; Nouali et al. 2020).

The ease of the addition of waste plastic in asphalt mixes makes the dry process popular among researchers and asphalt producers (Angelone et al. 2016; Lastra-Gonzalez et al. 2016;

Martin-Alfonso et al. 2019). However, very limited information is available about the incorporation of plastic in asphalt mixes using the dry process. Also, previous studies related to plastic-modified mixes using the dry process were primarily focused on the changes in performance properties, such as rutting, cracking, and resistance to moisture-induced damage. To the authors' knowledge, no previous studies have reported both volumetric properties and performance of plastic-modified asphalt mixes using the BMD approach and the dry process.

Several studies have evaluated the effect of waste plastics on the cracking performance of asphalt mixes (Modarres and Hamedi 2014; Radeef et al. 2021; Goli et al. 2023; Radeef et al. 2023). For example, Modarres and Hamedi (2014) and Radeef et al. (2023) reported an increase in the fatigue cracking resistance of plastic-modified mixes. However, Zhang et al. (2020a) and Almeida et al. (2020) reported a decrease in the fatigue cracking resistance of asphalt mixes containing waste plastics. Therefore, based on the existing literature, the fatigue cracking resistances of plastic-modified asphalt mixes are inconclusive and require further investigation. Also, the results were found to vary with the testing methods used.

Most of the existing studies were focused on evaluating the volumetric properties and performance of plastic-modified asphalt mixes under short-term aging conditions. Only a limited number of studies on the long-term aging of plastic-modified asphalt mixes could be found in the literature (Kumar et al., 2021; Mashaan et al., 20211; Radeef et al., 2022). For example, Mashaan et al. (2021) evaluated the effect of 20 hours of Pressure Aging Vessel (PAV) aging on the performance of Polyethylene Terephthalate (PET)-modified asphalt binder. The PET-modified binder was found to exhibit a lower Aging Index (AI) compared to the neat binder. Radeef et al. (2022) assessed the impact of aging on the fracture properties of LDPE-modified asphalt mixes. The Indirect Tensile Asphalt Cracking Test (IDEAL-CT) was performed on short-and long-term aged asphalt mixes to evaluate the fracture properties. The addition of LDPE resulted in higher fatigue cracking resistance after long-term aging compared to the control mix (Radeef et al. 2022). However, the increase in aging resistance mechanism due to plastic addition was not fully understood from the IDEAL-CT. Therefore, more studies are needed to characterize the long-term aging performance of asphalt mixes containing recycled plastics. The current study aims to evaluate the impact of long-term aging on asphalt mixes containing two different types of PCR plastics, namely LDPE and Linear Low-Density Polyethylene (LLDPE). In the current study, a hybrid approach was used by integrating the aging of asphalt mixes with performance testing, as well as the extraction and recovery of binders from the aged mixes for rheological and chemical characterization.

Overall, waste plastics were found to improve the rutting resistance, stiffness, and volumetric properties of asphalt mixes (Suaryana et al. 2018; Haider et al. 2020; Ghos et al. 2022a). However, plastic-modified mixes were found to adversely affect the fatigue cracking resistance (Suaryana et al. 2018; Haider et al. 2020; Ghos et al. 2022a; Ghos et al. 2022b; Ghos et al. 2024a; Ghos et al. 2024b; Ghos et al. 2024c). Also, the incorporation of waste plastics using the wet process was found to increase the viscosity of the blends which results in a stiff binder having reduced workability. Consequently, a high mixing and compaction temperature is required during the production of asphalt mix (Abdelaziz & Mohamed 2010; Al-Abdul Wahhab et al. 2017). Over stiffening of asphalt mixes limits the plastic percentage to a lower dose. The current study is aimed at increasing the plastic content in asphalt mixes without sacrificing the cracking resistance. Incorporation of bio-rejuvenators in asphalt mixes can be an excellent solution for lowering the stiffness of asphalt mixes (Zhou et al. 2018; Behnood 2019). The purpose of using a rejuvenator is to restore the rheological and chemical properties of the aged binder to a level close to the virgin binder (Zhou et al. 2018). Rejuvenators can also be added to highly viscous binders to reduce stiffness and improve engineering properties (Behnood 2019). The use of bio-rejuvenators in asphalt mixes containing PCR plastics is expected to improve cracking performance and results in economic and environmental benefits. The current study used Waste Cooking Oil (WCO) as a softening agent for reducing stiffness and increasing the resistance to cracking of plastic-modified asphalt mixes.

In addition to performance evaluation, assessing environmental impact is equally important to use waste plastics and bio-rejuvenators in asphalt mixes. Environmental impacts of asphalt mixes were determined in the past studies using reduced energy generation and CO_2 emission approach (also known as the Greenhouse Gas (GHG) emission approach) and the Life Cycle Assessment (LCA) (Wu et al. 2021; Belc et al. 2021; Santos et al. 2021; Yao et al. 2022). In the current study, the GHG emission approach was used for evaluating the environmental impact of plastic-modified mixes.

1.2 OBJECTIVES

Based on the reviews and gap in the literature noted above and detailed in subsequent chapters, the specific objectives of this study are:

a) To identify a suitable mixing protocol for incorporating waste plastic using the dry process;
b) To evaluate the effect of plastic on volumetrics properties and mechanical performance of a surface mix designed using the BMD approach;
c) To study the fracture properties of plastic-modified asphalt mixes using different available cracking tests;

d) To evaluate the effect of long-term aging on the performances of plastic-modified asphalt mixes;

e) To evaluate the impact of bio-rejuvenator on the performance of plastic-modified asphalt mixes; and

f) To determine the environmental impact of plastic-modified asphalt mixes.

1.3 OUTLINE

This dissertation consists of six chapters, each of chapters 2 -5 representing a journal paper either published or processed for publication. An overview of each chapter is given in this section.

Chapter 1: This chapter provides the overall background and a brief overview of using PCR plastics in asphalt mixes. The objectives of the dissertation are also included in this chapter.

Chapter 2: This chapter presents the findings of a study conducted to incorporate PCR plastics in asphalt mixes using dry process and BMD. Impact of two different types of plastics with three different percentages on volumetric properties and mechanical performance are presented in this chapter. Performance of plastic-modified mixes with respect to the BMD criteria used by the Oklahoma Department of Transportation (ODOT) is also presented in this chapter.

Chapter 3: This chapter includes the findings of a study focused on the evaluation of the fatigue cracking resistance of asphalt mixes containing PCR plastics using three commonly used fracture test methods, namely Illinois Flexibility Index Test (IFIT), Louisiana Semi-Circular Bend Test (L-SCB), and IDEAL-CT. Specifically, fracture energy, flexibility index, critical strain energy release rate, and cracking tolerance index were used as cracking indices for evaluating the fracture properties of seven asphalt mixes containing two different post-consumer recycled plastics. These mixes were ranked for their cracking resistance using a scale of 1 to 7 (1 being the best and 7 being the worst). The relationships among fracture energy, flexibility index and cracking tolerance index with notch depths and loading rates are also presented in this chapter. In addition, a loading rate-dependent parameter for flexibility index was developed in this study and is presented in this chapter.

Chapter 4: This chapter presents the results of a study conducted to investigate the effect of aging on the performance of asphalt mixes containing PCR plastics. Asphalt mixes with and without LDPE and LLDPE were subjected to three different aging protocols, namely short-term, mid-term and long-term laboratory aging. The effect of these aging protocols on the cracking performance was evaluated using IDEAL-CT tests. Binders were extracted from these aged mixes and recovered for further study. The results of both rheological and chemical analysis of extracted binders are presented in this chapter.

Chapter 5: This chapter presents the results of a study conducted to increase the percentage of PCR plastics in asphalt mixes. For this purpose, a bio-rejuvenator was used to lower the high-temperature performance grade of the control binder. The effects of bio-rejuvenator on rutting, cracking and moisture-induced performance of asphalt mixes containing are presented in this chapter. In addition, an environmental impact assessment was conducted on plastic-modified mixes. Impact on the GHG generation is also presented in Chapter 5.

Chapter 6: The overall conclusions of this study are presented in this chapter along with pertinent recommendations. The recommendations are focused on the direction of future work related to the use PCR plastics in asphalt pavement construction.

CHAPTER 2 PERFORMANCE OF ASPHALT MIXES CONTAINING POST-CONSUMER RECYCLED (PCR) PLASTICS USING BALANCED MIX DESIGN APPROACH AND DRY PROCESS[*]

ABSTRACT

In recent years, use of Post-Consumer Recycled (PCR) plastics in asphalt mixes has been gaining popularity due to increased environmental awareness, promote sustainability, and conserve natural resources. When using the dry process, incorporation of PCR plastic in asphalt mixes poses several challenges including mixing, sample preparation, and testing. Use of balanced mix design (BMD) for asphalt mixes containing PCR plastic poses additional challenges that have not been adequately covered in previous studies. To this end, the changes in the volumetric properties and performance of PCR plastic modified asphalt mixes were investigated in this study. For this purpose, an asphalt mix having a Nominal Maximum Aggregate Size (NMAS) of 9.5 mm and PG 64-22 binder was designed using the BMD approach. Three different percentages (0.25%, 0.5%, and 1% by weight of aggregate) and two different PCR plastics, namely Low-Density Polyethylene (LDPE) and Linear Low-Density Polyethylene (LLDPE) were incorporated in the mix using the dry process. Volumetric properties, namely maximum theoretical specific gravity, bulk specific gravity, Voids in Mineral Aggregate (VMA), Voids Filled with Asphalt (VFA), air void contents, and densities were determined for both control (0% plastic) and modified mixes. Also, Indirect Tensile Strength (ITS), Indirect Tensile Asphalt Cracking Test (IDEAL-CT), and Hamburg Wheel Tracking (HWT) tests were performed to assess performance of these mixes. A comparison of

[*] This chapter has been published in the Transportation Research Record (TRR) Journal of the Transportation Research Board (TRB) under the title "Performance of Asphalt Mixes Containing Post-Consumer Recycled (PCR) Plastic using Balanced Mix Design Approach and Dry Process." The current version has been formatted for this dissertation.

performance for both plastic type and amount and issues related to the incorporation of PCR plastic using the dry process are discussed in this chapter.

Keyword: Transverse Cracking; LDPE; LLDPE; BMD

2.1 INTRODUCTION

Utilization of recycled materials in asphalt mixes has gained popularity across the globe in the last few decades. Different recycled materials such as Recycled Asphalt Pavement (RAP), Reclaimed Asphalt Shingles (RAS), Post-Consumer Recycled (PCR) plastics and Ground Tire Rubber (GTR) are being used in asphalt mixes to reduce environmental pollution and conserve natural resources (Leng et al. 2018; Adegoke et al. 2019; Dalhat et al. 2019). In 2018, the USA generated 35.7 million tons of waste plastics (EPA 2020). According to Environmental Protection Agency (EPA), only 8.7-percent of waste plastic was recycled, and the remaining was either burned for fuel value or landfilled (EPA 2020). In order to reduce the impact of plastic pollution on the environment, the Plastic Industry Association (PLASTICS) conducted a study to identify potential New End Market Opportunities (NEMO) for recycling waste plastic. Incorporation in asphalt pavement was reported as one of the potential new end markets for waste plastics (PLASTICS 2020).

The waste plastic stream is generally composed of different resins, namely Polypropylene (PP) (32.1%), Low-Density Polyethylene (LDPE) and Linear Low-Density Polyethylene (LLDPE) (17.5%), High-Density Polyethylene (HDPE) (11.5%), and others including Polyvinyl Chloride (PVC), Polystyrene (PS), and Polyethylene Terephthalate (PET) (38.6%) (EPA 2020). A recent study conducted by Willis et al. (2020) suggested using Polyethylene (PE) i.e. LDPE, LLDPE and HDPE in the production of asphalt mixes as other plastics can produce toxic gases or are incompatible with asphalt mixes.   Several studies have evaluated the basic properties, namely melting point, decomposition point, relative density, particle sizes of PE plastics for potential use in asphalt mixes (Vasudevan et al. 2010; Angelone et al. 2016; Lastra-Gonzalez et al. 2016; Ranieri et al. 2017; Suaryana et al. 2018). Typically, the melting points and decomposition temperatures of the PE plastic used in asphalt research are in the range of 100-120°C and 270-350°C, respectively (Vasudevan et al. 2010; Menaria et al. 2015). Also, the densities of the PE plastic were found to vary between 0.857gm/cm^3 and 0.975gm/cm^3 (Plastic Technology 2021). Several studies have used PE plastic of different particle sizes ranging from 9.5mm to 425µm for modifying asphalt mixes. Also, different shapes of plastic, such as granulates, flakes and pellets have been used in asphalt mixes (Angelone et al. 2016; Lastra-Gonzalez et al. 2016; Ranieri et al. 2017; Suaryana et al. 2018). The properties of the PCR plastics were reported to influence the properties of the asphalt mixes (Vasudevan et al. 2010; IRC 2013).

Until now, waste plastics have been incorporated in asphalt mixes using one of the two processes, namely the wet process involving modification of binder with plastic and the dry process in which plastics are directly to the mix (Abukhettala 2016; Angelone et al. 2016; Ranieri et al. 2017; Dalhat et al. 2019; Martin-Alfonso et al. 2019). Previous studies have reported improvements in performance properties of asphalt mixes with the addition of plastic using both processes (Khan et al. 2009; Vasudevan et al. 2010; Zhang et al. 2011a; Angelone et al. 2016; Lastra-Gonzalez et al. 2016; Costa et al. 2017; Ranieri et al. 2017; Suaryana et al. 2018; Haider et al. 2020). For example, Khan et al. (2009) evaluated the performance of PP-modified asphalt mixes. Addition of 15% PP by the weight of the binder was reported to improve the rutting resistance (Khan et al. 2009). Angelone et al. (2016) conducted a comparative study by adding recycled waste plastics from silo bags (consisting of LDPE and HDPE) and recycled PP at a rate of 2%, 4% and 6% by the weight of the mix. Increased rutting resistance and stiffness were reported with the addition of waste plastic. Also, 2% of plastic by the weight of mix was reported as the optimum amount of waste plastic that can be incorporated in the production of asphalt mixes (Angelone et al. 2016). Lastra-González et al. (2016) evaluated the performance of plastic-modified asphalt mixes using the dry process in regard to rutting, stiffness, fatigue cracking and workability. Four different types of waste plastic, namely PE, PP, PS and End-of-Life Tires (ELT) were used for modifying a surface course mix. These waste plastics were used as aggregate replacement (1% by weight of the aggregate). The addition of waste plastic was reported to improve the resistance to rutting without compromising the fatigue performance (Lastra-González et al. 2016). Ranieri et al. (2017) evaluated the performance of a surface course mix modified with HDPE and Ethylene Vinyl Acetate (EVA) by using both the wet and dry processes. The mixes produced using the dry process were found to exhibit more moisture resistance and higher stiffness than the mixes produced using the wet process. The addition of HDPE plastic did not show any improvement in resistance to the fatigue cracking (Ranieri et al. 2017). Suaryana et al. (2018) reported significant improvement in rutting and fatigue resistances after modification of mixes with LDPE. Haider et al. (2020) evaluated the properties of LDPE- and HDPE-modified mixes. In that study, rutting resistance was found to improve after LDPE- and HDPE addition using dry process (Haider et al. 2020). Mishra et al. (2020) evaluated the performance of LDPE-modified mixes. In that study, dry processed mixes were found to sustain higher loads as compared to wet processed mixes (Mishra et al. 2020). The ease of the addition of waste plastic in asphalt mixes makes the dry process has the potential to make this process popular among the researchers and asphalt producers (Angelone et al. 2016; Lastra-González et al. 2016; Martin-Alfonso et al. 2019). However, very limited information is available about the incorporation of plastic in asphalt mixes using the dry process. Also, previous studies related to plastic-modified mixes using the dry process were primarily focused on the changes in performance properties, such as rutting, cracking or resistance to moisture-induced damage. To the authors' knowledge, no previous studies have reported both volumetric properties and performance of plastic-modified asphalt mixes using the balanced mix design approach and the dry process.

According to the Federal Highway Administration (FHWA) Expert Task Group (ETG) on Mixtures and Construction, BMD is defined as the design of asphalt mixtures using performance tests that address multiple modes of distresses. Generally, BMD incorporates at least two performance tests, namely rutting and cracking, to assess the performance of an asphalt mix (West et al. 2018). Currently, three different approaches are available for designing BMD mixes, as shown in Figure 2.1 (Buchanan 2017; West et al. 2018). Approach 1 is volumetric design with performance verifications, as illustrated in Figure 2.1(a). It is a Superpave volumetric design with verifying performance properties. The mix needs to be redesigned if the performance is not satisfactory. Currently, six states in U.S. are using this approach. Approach 2 is based on the performance-modified volumetric design, as shown in Figure 2.1(b). In this approach, the binder content in the initial design is selected using AASHTO M323 (AASHTO 2017a) prior to performance testing. The results of the performance tests are used to modify the mix proportions and adjust the binder content. Currently, the California Department of Transportation (CALTRANS) and Oklahoma Department of Transportation (ODOT) are using this approach (Buchanan 2017; ODOT 2020). Approach 3 is the performance-based design (Figure 2.1(c)). In this approach, performance tests are conducted at varying binder contents and the design binder content is selected based on these results. Volumetric properties are determined as the last step (Buchanan 2017; West et al. 2018). As previously mentioned, ODOT uses the BMD Approach 2 for designing a BMD (ODOT 2020). ODOT requires that the design be prepared following the AASHTO R35 method (AASHTO 2022c), except density is allowed to vary from 96 to 97%. Rutting and cracking performances are measured by HWT and IDEAL-CT tests, respectively. An asphalt mix with a rut depth of 12.5-mm or less and a Cracking Tolerance Index (CT_{Index}) of 80 or more is considered as a balanced mix (ODOT 2020).

A number of studies have used recycled materials, such as RAP, RAS and GTR in BMD mixes (Zhang et al. 2020b; Meroni et al. 2020; Sabouri et al. 2020). However, to the authors' knowledge, no studies have reported the performance of PCR plastic-modified asphalt mixes relative to BMD. In the present study, volumetric and performance properties of PCR plastic-modified mixes were evaluated in the laboratory using the BMD criteria followed by the ODOT. Two different PCR plastics, namely LDPE and LLDPE were added to the asphalt mixes using the dry process. The specific objectives of this study are:

g) To identify the changes in the volumetric properties of asphalt mixes due to the addition of LDPE and LLDPE PCR plastics using the dry process;

h) To evaluate the relative effect of LDPE and LLDPE plastic on the performance properties, namely rutting, cracking and moisture-induced damage of a surface mix;

i) To evaluate the performance of plastic-modified asphalt mixes with respect to the balanced mix design approach.

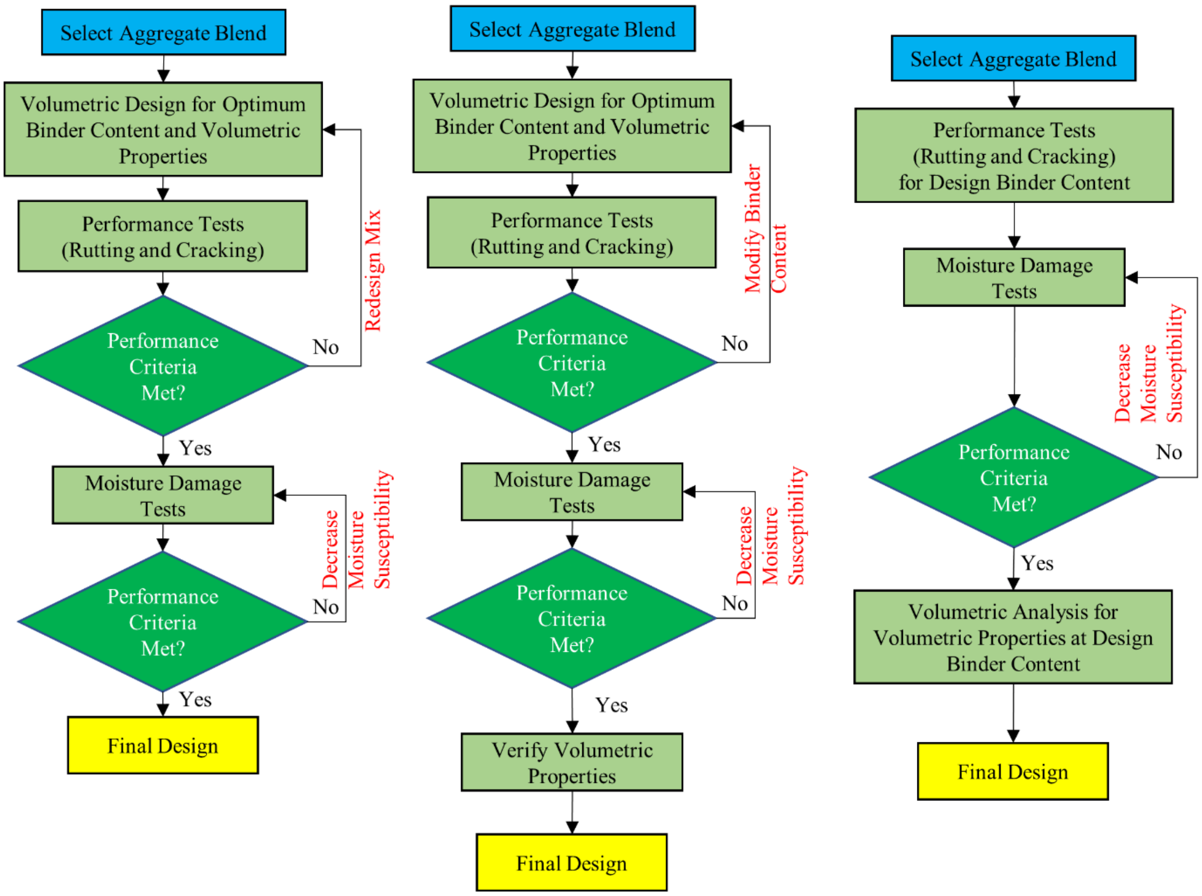

(a) (b) (c)

Figure 2.1 Balanced Mix Design (BMD) approaches: (a) Approach 1; (b) Approach 2; and (c) Approach 3 (West et al. 2018)

2.2 MATERIALS AND METHODS

Figure 2.2 shows the work-flow diagram used in this study. For the purpose of this study, an aggregate gradation with a Nominal Maximum Aggregate Size (NMAS) of 9.5-mm was selected. The mineral aggregates consisted of 3/8-inch (9.5-mm) crushed stone chips, manufactured sand, 3/16-inch (4.76-mm) screenings and local sand. Gradations of the individual mineral aggregates are presented in Table 2.1 along with the ODOT requirements for a surface course mix with NMAS of 9.5-mm. A PG 64-22 asphalt binder was used as the base binder. Required amounts of aggregates and binder were collected from a local plant in Oklahoma. As noted previously, in this study, two different types of PCR plastics, namely LDPE and LLDPE were collected from an industry vendor. Both the LDPE and LLDPE PCR plastics were received in the form of 5-mm diameter pellets. A summary of the properties of the PCR plastics is presented in Table 2.2. The properties include Melt Flow Index (MFI) (ASTM D1238 (ASTM 2020a)), relative density (ASTM D792 (ASTM 2020b)), ash content (ASTM D5630-13 (ASTM 2013)) and moisture content (ASTM D6980 (ASTM 2017)). From Table 2.2, both the LDPE and LLDPE plastics exhibited very similar relative densities. However, the LLDPE plastic had a significantly higher MFI than the LDPE plastic. The linear structure of LLDPE plastic is responsible for this higher MFI than the LDPE plastic, which contains a complex branched structure.

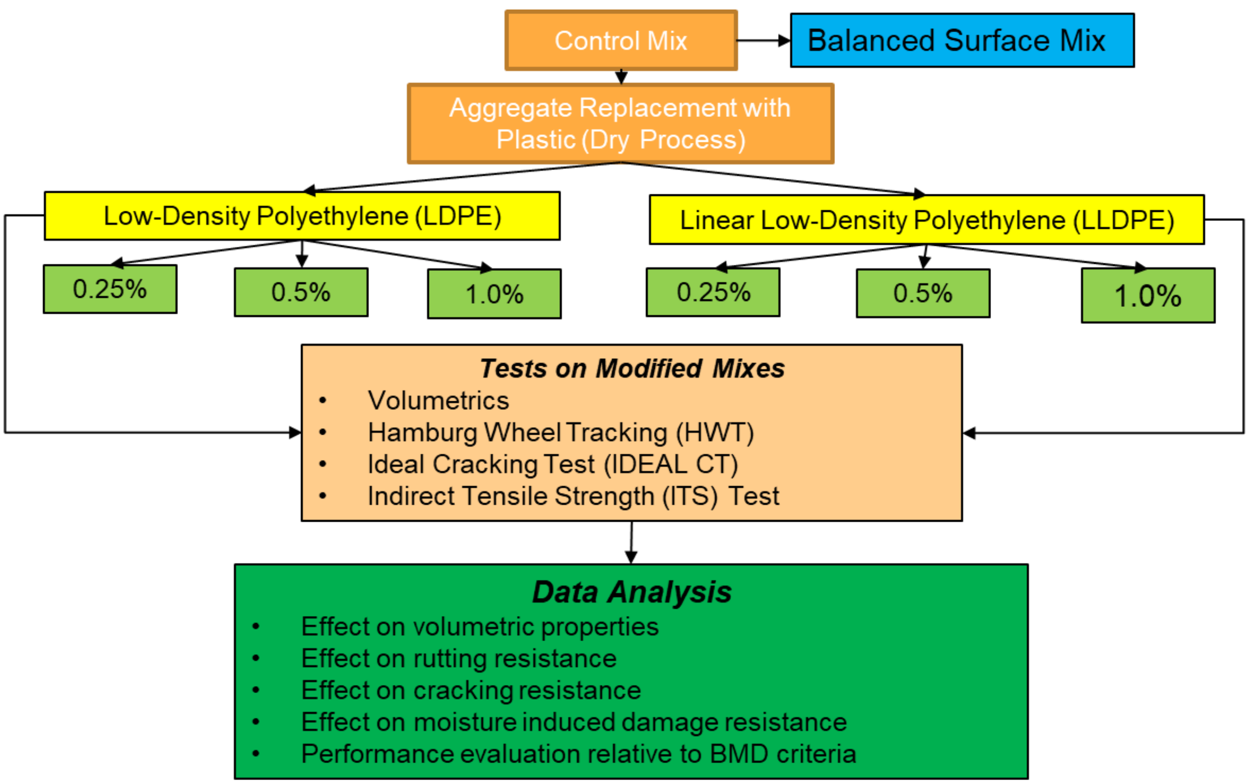

Figure 2.2 Workflow diagram

Table 2.1 Gradation of collected aggregates

Sieve	Percent Passing (%)					
	3/8" Chips	Man. Sand	3/16" Scrns	Sand (GMI)	Combined Gradation	ODOT Requirements
3/4"	100.0	100.0	100.0	100.0	100.0	100.0
1/2"	100.0	100.0	100.0	100.0	100.0	100.0
3/8"	93.8	99.5	100.0	100.0	97.0	90.0-100.0
No. 4	27.6	65.6	95.4	100.0	66.0	59.0-73.0
No. 8	7.4	33.5	59.4	100.0	41.0	36.0-46.0
No. 16	5.3	19.1	36.9	99.0	30.0	26.0-34.0
No. 30	4.2	11.9	24.1	91.0	23.0	19.0-27.0
No. 50	3.2	7.3	15.4	60.0	15.0	11.0-19.0
No. 100	2.5	4.8	10.6	15.0	7.0	4.0-10.0
No. 200	2.0	3.7	7.6	5.0	5.0	3.0-7.0

Table 2.2 Properties of PCR plastics

Property	**Test Method**	**Low-Density Polyethylene (LDPE)**	**Linear Low-Density Polyethylene (LLDPE)**
Melt Flow Index, MFI (gm/10 min) (kg/10 min) at 190°C	ASTM D1238 (ASTM 2020a)	0.7412 (0.0007412)	2.3173 (0.0023173)
Relative Density (gm/cm^3) (km/m3)	ASTM D792 (ASTM 2020b)	0.927 (927)	0.915 (915)
Ash Content (%)	ASTM D5630-13 (ASTM 2013)	1.1795	0.4116
Moisture Content (%)	ASTM D6980 (ASTM 2017)	0.0400	0.0400

The control mix was designed with the PG 64-22 binder following the BMD approach, but without any plastic. The BMD Approach 2, as proposed by FHWA (West et al. 2018), was followed for this purpose. At first, the design binder content of the mix was determined by satisfying the volumetric requirements, as specified in the AASHTO M323 (AASHTO 2017a) and ODOT Specification (ODOT 2020). Then the rutting and cracking performance of the mix was used to modify the mix proportions and adjust the binder content. The final control mix consisted of 40% 3/8-inch (9.5-mm) crushed stone chips, 10% manufactured sand, 38% 3/16-inch (4.76-mm) screenings and 12% local sand. An optimum binder content of 6.0% was required to satisfy both the volumetric properties and the performance criteria relative to rutting and fatigue cracking.

The plastic modified mixes were produced by adding LDPE and LLDPE plastics using the dry process. As noted earlier, three different percentages of plastics, namely 0.25%, 0.5% and 1.0% by the weight of aggregates, were added into the mixes. In 2018, approximately, 390 million tons of asphalt mixes were produced in the USA (Williams et al. 2020). Therefore, use of waste plastic in asphalt mixes at a rate of 0.25%, 0.5% and 1.0%, as a replacement of aggregate (by weight), corresponds to approximately 1, 2 and 4 million tons of plastic wastes, respectively. Also, according to EPA (EPA, 2020), 26.9 million tons of plastic wastes were landfilled in 2018. Using plastic at a rate of 0.25%, 0.5% and 1.0% of aggregate replacement will reduce landfilling of waste plastic by approximately 4%, 8% and 16%, respectively. Therefore, reusing waste plastics in asphalt mixes is a win-win proposition for removing plastic from the environment and enhancing pavement performance.

Plastics were incorporated into the mix as a replacement of aggregate. The proportions of different aggregates were adjusted to incorporate plastic into the mix. In order to reduce the amount of variables and to evaluate the effect of the addition of LDPE and LLDPE plastics, all the plastic modified mixes were produced using the same binder content (6% by weight of the mix) as the control mix. To determine the most suitable protocol, the following three different methods of incorporating plastics into asphalt mixes in the laboratory setting were explored:

Method #1: Aggregates were heated in the oven at 163°C for two hours. The heated aggregates were taken out of the oven and blended with plastic at room temperature before adding the binder. The required amount of heated binder was then added to the aggregate-plastic blend and mixed using a mixer. Figure 2.3(a) shows the preparation of aggregate-plastic blend following Method #1.

Method #2: An Aggregate-plastic blend was prepared before heating the aggregate in the oven. The aggregate-plastic blend was then heated at the mixing temperature (i.e., 163°C) for two hours. Figure 2.4(a) shows a pictorial view of the heated aggregate-plastic blend. The heated binder was then added to the heated aggregate-plastic blend to produce plastic-modified mixes.

Method #3: Aggregates were heated in the oven at 163°C for two hours. Room-temperature plastics and heated asphalt binder were added to the heated aggregates simultaneously and mixed using a mixing equipment. Figure 2.5(a) presents the mixing process used in Method#3.

The mixes produced using these three methods were observed physically, and the challenges associated with each method were identified. A number of studies have used Method #1, i.e., blending plastics with heated aggregates at room temperature and reported coating on aggregate surface with plastic (Vasudevan et al. 2010; Angelone et al. 2016). In this study, careful observations did not reveal any visible coating of plastic on any aggregate surface, as shown in Figure 2.3 (b). Rather plastic particles remained separated like aggregates. Evidently, the amount of heat and the time necessary for melting plastic were not enough in Method #1. Also, the heat loss during the mixing process was not favorable to coating. In addition, mixing PCR plastic with aggregates without any binder made mixing difficult and not representative of mixing in an asphalt plant. In Method #2, the plastic particles were observed to melt (Figure 2.4 (a)), as the aggregate-plastic blend was heated to 163°C for 2 hours. Also, a paper-like film was found to form inside the aggregate-plastic blend, as shown in Figure 2.4 (b). Some plastics were lost in this method as the melted plastics got stuck to the bottom and sides of the pan (Figure 2.4 (c)). The problem with the formation of paper-like films and sticking with the pan was eliminated in Method #3, as shown in Figure 2.5 (b). Also, a uniform distribution was seen as the plastics were added while the mixture was constantly stirred in the mixing equipment. In addition, this method simulates the mixing process used in the asphalt plant where the plastics are introduced through the RAP port. In Oklahoma, high RAP drum mix plants have two RAP ports. These are readily seen at the top of the drum. RAP is added directly using these ports and heated indirectly with superheated aggregates. A similar procedure can be applied to incorporate waste plastics using the dry process. Therefore, Method #3 was selected in this study for producing plastic-modified mixes for further testing. Changes in the volumetric, rutting, cracking and moisture-induced damage potential of plastic-modified mixes were evaluated with respect to the control mix. Finally, the performance of the plastic-modified mixes was used to evaluate if they satisfied the BMD criteria.

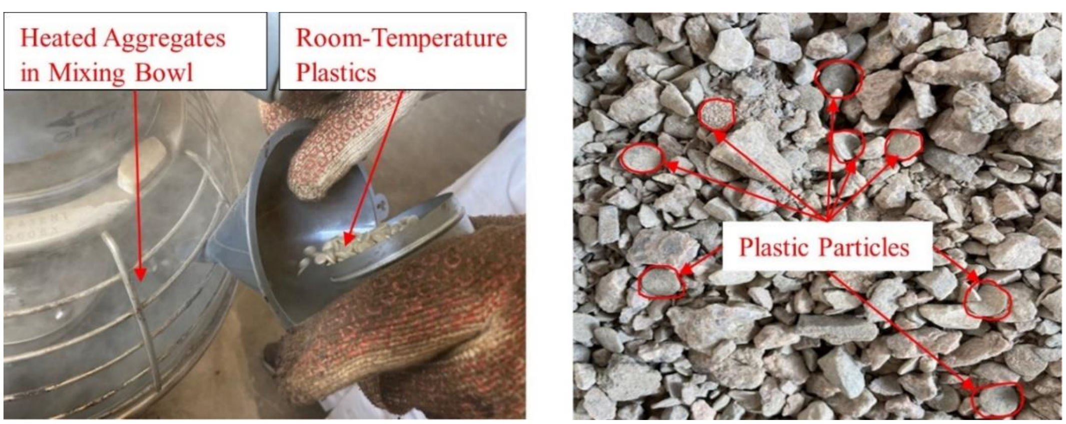

(a) (b)

Figure 2.3 Mixing of plastic with heated aggregates: (a) Adding plastic at room temperature to heated aggregates; and (b) Aggregate-Plastic mix

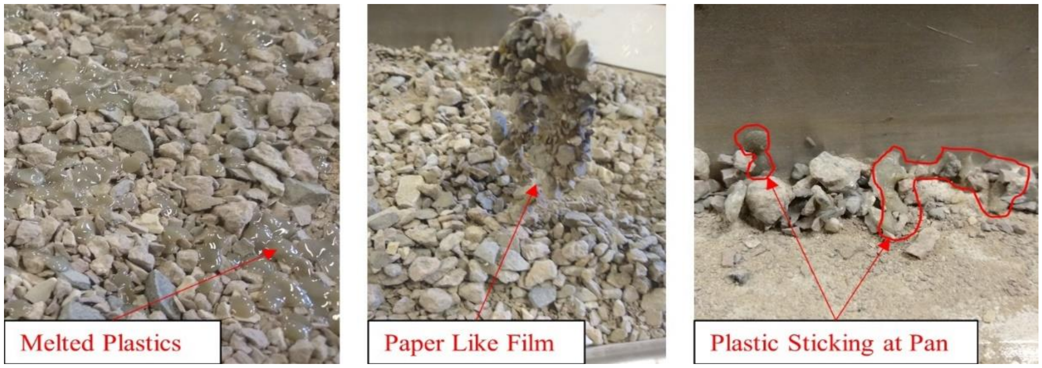

(a) (b) (c)

Figure 2.4 Adding plastic at room temperature with aggregate at room temperature and then heating: (a)Heated aggregate + plastic mix; (b) Paper like film; and (c) Plastic sticking with the pan

(a) (b)

Figure 2.5 Addition of plastic with the heated aggregate-binder mix: (a) Plastic mixing; and (b) Final mix

2.2.1 **Test Methods**

2.2.1.1 ***Volumetrics***

For evaluating the volumetric properties, the theoretical maximum specific gravity of asphalt mix (G_{mm}) was determined for each mix following AASHTO T209-12 (AASHTO 2016b). For this purpose, approximately 1500-gm of loose, oven-dried samples were placed in a tared vacuum flask at 25°C. Sufficient water of the same temperature was added to the flask so that the asphalt sample was completely submerged. Vacuum was applied for 15±2-mintues. The flask was then filled completely by adding water. The mass of the flask filled with the mix and water was measured in air. From these data, the G_{mm} was calculated. The bulk specific gravity (G_{mb}) was determined for each mix following AASHTO T166 (AASHTO 2016c). For this purpose, compacted samples having a diameter of 150-mm, and a height of 115-mm were prepared from each mix using a Superpave Gyratory Compactor (SGC). These samples were prepared using 50-gyrations. The mass of the sample in dry, submerged, and saturated conditions was measured, and G_{mb} was calculated from these data. Using the G_{mm} and G_{mb} values, % densities, air voids, Voids in Mineral Aggregates (VMA), and Voids Filled with Asphalt (VFA) were calculated for each mix.

2.2.1.2 ***Hamburg Wheel Tracking (HWT) Test***

For evaluating rutting performance, HWT tests were conducted on a pair of 150-mm diameter and 60-mm thick saw-cut specimens from the laboratory produced mixes, following the AASHTO T 324 (AASHTO 2011) and OHD L-55 (ODOT 2014) method. The specimens for the HWT tests were compacted at 7±0.5% air voids. The tests were conducted at 50 °C with a wheel pass frequency of 52 passes/minute. The tests were terminated after reaching a maximum rut depth of 20-mm or 20,000-wheel passes, whichever reached first. From wheel-pass vs rutting plot, the rut depth at specified number of wheel pass and stripping inflection point were determined to evaluate the resistance to rutting and moisture-induced damage, respectively.

2.2.1.3 ***Indirect Tensile Asphalt Cracking Test (IDEAL-CT)***

Indirect Tensile Asphalt Cracking Tests (IDEAL-CT) were performed to evaluate the cracking resistance of cylindrical specimens (150-mm in diameter and 62-mm height) for all mixes, following the ASTM D 8225-19 (ASTM 2019) test method. For this purpose, four cylindrical specimens of each mix were prepared at 7±0.5% air voids after 4 hours of aging. The IDEAT-CT test was conducted by applying a load at 50-mm/min at room temperature (25°C) until failure. The load-displacement data were recorded for the entire duration of the test. The CT_{Index} was calculated from the load-displacement curve. Generally, a higher CT_{Index} indicates a better cracking resistance for a mix.

2.2.1.4 ***Tensile Strength Ratio (TSR) Test***

In this study, resistance to moisture-induced damage was evaluated for all mixes following the AASHTO T 283 (AASHTO 2007) test method. For this purpose, six specimens with a diameter of 150-mm and a height of 95-mm were prepared from each mix. Three out of the six specimens were tested in dry condition for Indirect Tensile Strength (ITS). The other three specimens were vacuum saturated and placed for a freezing cycle for at least 16 hours at -18°C. These frozen specimens were then placed in a warm (60°C) water bath for 24 hours for thawing. After thawing, these specimens were conditioned at room temperature (25°C) and then tested for ITS. The Tensile Strength Ratio (TSR) was calculated from the ratio of indirect tensile strength at wet (ITS_{wet}) and dry (ITS_{dry}) conditions.

2.3 RESULTS AND DISCUSSION

2.3.1 **Effect on Volumetric Properties**

The effect of the addition of LDPE and LLDPE plastic on the volumetric properties of the aforementioned mixes were evaluated in this study. The following properties were included: G_{mm}, G_{mb}, VMA, VFA, percent density and air void content. Figure 2.6 (a) shows the variation of G_{mm} with the plastic percentage. The G_{mm} reduced with an increase in the amount of LDPE and LLDPE plastic. This is primarily caused by the low specific gravity of plastics as compared to the aggregate. As the lighter-weight plastic particles replaced the heavier-weight aggregate particles, the G_{mm} was reduced. For example, the relative density of the LDPE was 0.927 that is significantly lower than the relative density of the combined aggregate (2.572). This reduction in G_{mm} was higher for the LLDPE plastic than the LDPE plastic. A lower relative density of LLDPE (0.915) compared to LDPE (0.927) was responsible for this phenomenon.

Figure 2.6 (b) presents the variation of the G_{mb} with the amount of LDPE and LLDPE plastic. Overall, the G_{mb} was found to decrease with an increase in the plastic percentage in the mix. As previously noted, the low specific gravities of the plastics are responsible for this reduction in the G_{mb} values.

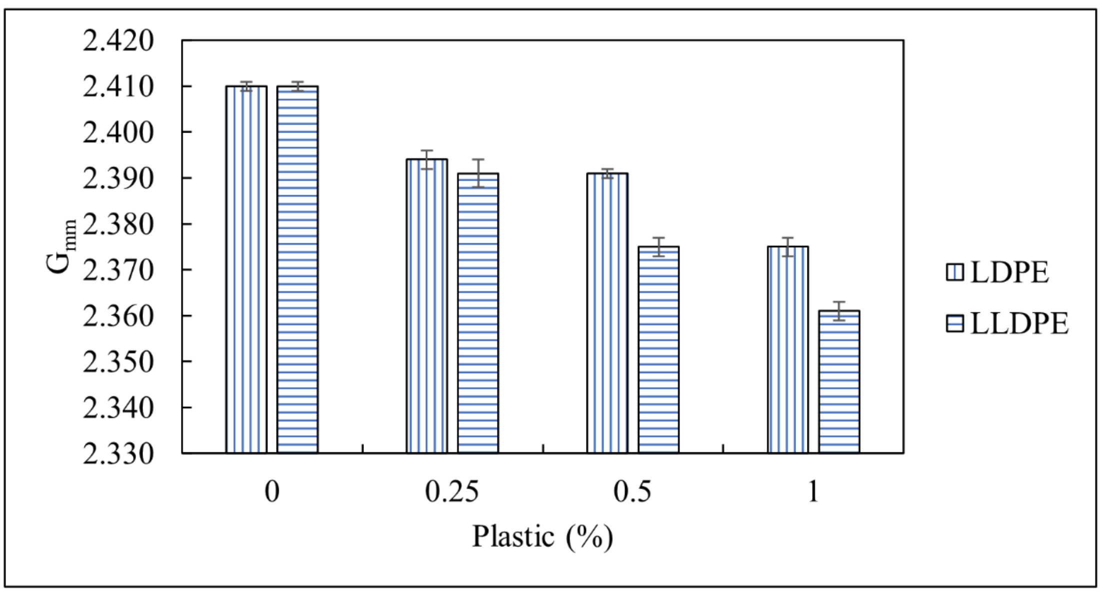

(a)

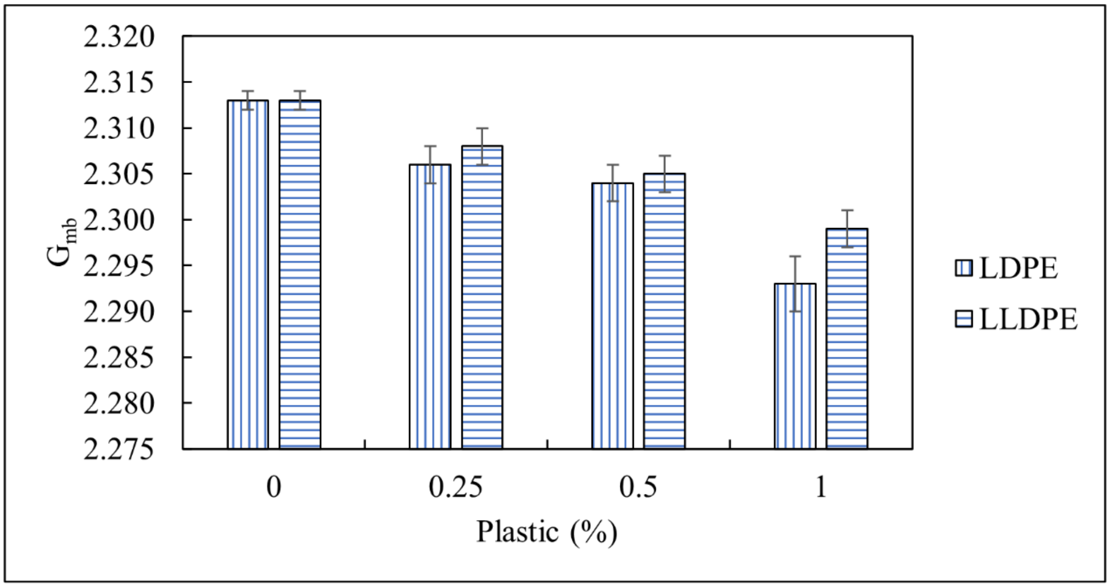

(b)

Figure 2.6 Variation of (a) G_{mm}, and (b) G_{mb} density of mixes with the amount of LDPE and LLDPE plastics

A summary of the volumetric properties of all mixes is presented in Table 2.3. According to the ODOT BMD Special Provision (ODOT 2020), the density of a balanced mix should lie in the range of 96.0-97.0%. From Table 2.4, it was found that all mixes, except 0.5%-LLDPE- and 1.0%-LLDPE-modified mixes satisfied this requirement. For both LDPE and LLDPE plastic-modified mixes, the density (% of G_{mm}) was observed to increase with an increase in the amount of plastic. The density of a mix is calculated as a ratio of the G_{mb} and G_{mm} of that mix. It was observed that the addition of plastic reduced both the G_{mb} and G_{mm} of the mixture. However, the reduction in the G_{mm} was higher than the reduction in the G_{mb}. As a result, the density of the mix was observed to increase with the increased amount of plastic. Also, the increase in the density for the LLDPE-modified mixes was higher compared to that of the LDPE-modified mixes. The higher reduction in G_{mm} value for the LLDPE-modified mixtures is responsible for this phenomenon.

For both LDPE and LLDPE, effective binder content (P_{be}) was found to increase with an increase in the amount of plastic. For example, P_{be} increased from 5.00 to 5.28% with an increase in LDPE from 0 to 0.25%, respectively. The results indicated that plastics used in the mix partly acted as a binder extender. Similar findings were also reported by Vasudevan et al. (2010). However, it was difficult to quantify the amount of plastic contributed to binder extension.

All plastic-modified mixes were found to satisfy the ODOT's requirement for VMA. The control mix, 0.25%-LDPE-, 0.5%-LDPE-, 1.0%-LDPE- and 0.25%-LLDPE-modified mixes exhibited a VFA ranging from 70 to 80, which is a requirement for ODOT BMD mixes (ODOT 2020). Therefore, considering volumetric requirements, the control mix, 0.25%-LDPE-, 0.5%-LDPE- and 0.25%-LLDPE mixes satisfied the requirements for ODOT BMD mixes.

Table 2.3 Summary of volumetric properties of plastic-modified mixes

Parameter	ID						
	Control	0.25-LDPE	0.5-LDPE	1.0-LDPE	0.25-LLDPE	0.5-LLDPE	1.0-LLDPE
G_{mm}	2.41	2.394	2.391	2.375	2.391	2.375	2.361
G_{mb}	2.313	2.306	2.304	2.293	2.308	2.305	2.299
Density (%)	96	96.3	96.4	96.5	96.5	97.1	97.4
Air Voids (%)	4	3.7	3.6	3.5	3.5	2.9	2.6
VMA	15.5	15.7	15.8	16.2	15.6	15.8	16
VFA	74	76.6	77	78.7	77.8	81.3	83.6
P_{be} (%)	5	5.28	5.33	5.61	5.33	5.6	5.87
ODOT Density Criteria: 96.0-97.0	Satisfied	Satisfied	Satisfied	Satisfied	Satisfied	Not Satisfied	Not Satisfied
ODOT VMA Criteria: ≥15	Satisfied	Satisfied	Satisfied	Satisfied	Satisfied	Satisfied	Satisfied
ODOT VFA Criteria: 70-80	Satisfied	Satisfied	Satisfied	Satisfied	Satisfied	Not Satisfied	Not Satisfied

2.3.2 **Effect on Rutting Resistance**

The HWT test was conducted to evaluate the rutting and moisture-induced damage resistance of plastic-modified asphalt mixes. The variation of rut depth with the number of wheel passes for the plastic-modified mixes is presented in Figure 2.7. From Figure 2.7, the rut depths at 10,000-wheel passes were determined for all mixes and are summarized in Table 2.4. Also, stripping inflection points were calculated from the rut depth vs. wheel passes curve to evaluate the resistance to moisture-induced damage. A rut depth of 12.5-mm or less (at 10,000-wheel pass) is required for a mix by the ODOT BMD Special Provision for surface mixes having PG 64-22 binder (ODOT 2020). For other mixes with PG 70-22, PG 76-22 binders, the maximum allowable rut depth by the ODOT BMD Special Provision is 12.5-mm at 15,000 and 20,000-wheel passes (ODOT 2020). Overall, the rutting resistance was observed to improve with the addition of both the LDPE and LLDPE plastic, as evident from Figure 2.7 and Table 2.4. A similar reduction in rutting with the addition of the LDPE and LLDPE plastics was reported by several studies (Suaryana et al. 2018; Haider et al. 2020). Also, the creep slope of the rutting plot was found to reduce with the increase in the amount of plastic. The reduction in rut depth and creep slope is primarily caused by the increase in stiffness contributed by the plastic particles. Also, from Figure 2.7, the moisture-induced damage potential of the mixes was improved after adding plastic. Moisture resistance is evaluated using the stripping inflection points of the rut curve. The stripping inflection points get delayed as the stiffness increases (Yin et al. 2014). The stripping inflection points were found to increase as the mixes stiffened with the increase in the amount of plastic. The HWT test did not exhibit any stripping inflection points for the 0.5% LDPE-, 1% LDPE- and 0.5% LLDPE-modified mixes as the specimens did not pass the creep phase and reach the stripping phase after 20,000-wheel passes. The increased stiffness of these mixes with the addition of plastic was likely responsible for this longer creep phase. The LDPE-modified mixes were found to exhibit better rutting and moisture-induced damage resistance as compared to the LLDPE-modified mixes. The MFI indicated a higher viscosity of the LDPE plastic than the LLDPE plastic (Kumar et al. 2020). This increased viscosity of the LDPE plastic could be the potential contributing factor for improving the rutting performance.

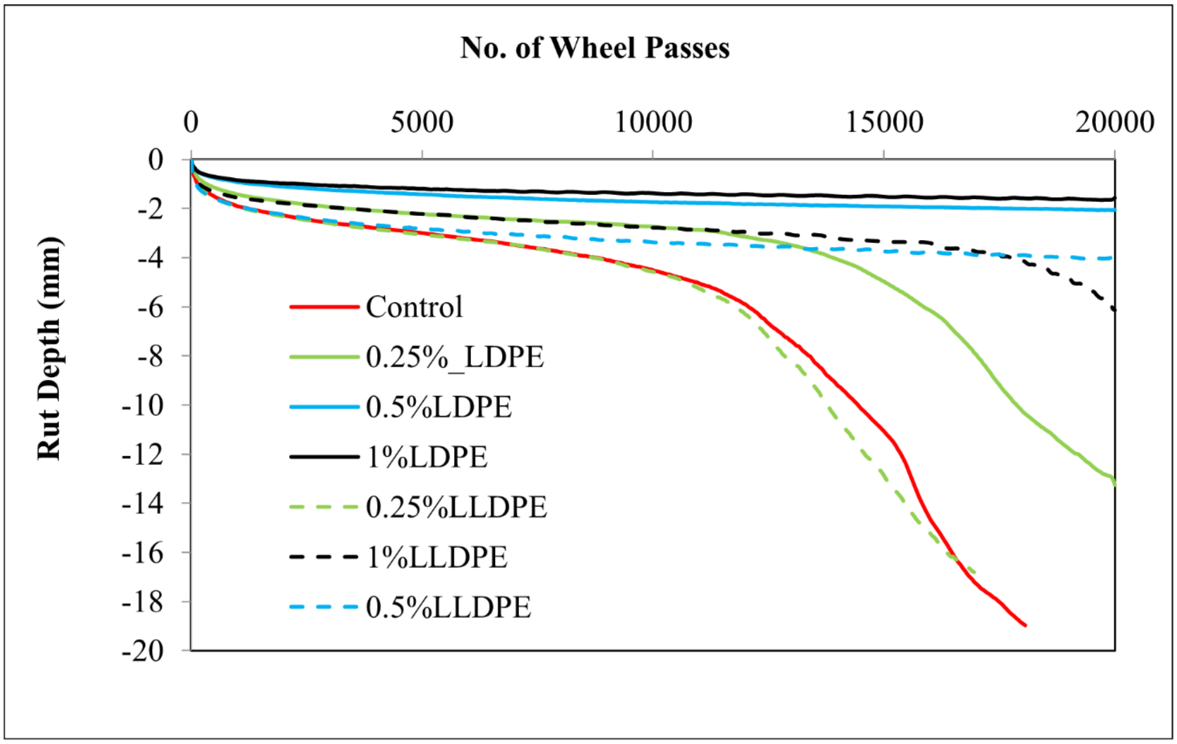

Figure 2.7 Variation of rut depth with the number of wheel passes

Table 2.4 Summary of HWT results

Plastic Percentage	Rut Depth @ 10,000-Wheel Pass		Stripping Inflection Point (SIP)		Creep Slope		Stripping Slope	
	LDPE	LLDPE	LDPE	LLDPE	LDPE	LLDPE	LDPE	LLDPE
0	4.10	4.10	12,000	12,000	0.00027	0.00027	0.0018	0.0018
0.25	2.40	4.10	13,200	12,000	0.00013	0.00027	0.002	0.0022
0.5	1.75	3.4	--	--	4.4E-05	0.00012	--	--
1.0	1.30	2.8	--	18,000	2.2E-05	0.000075	--	0.0008

2.3.3 **Effect on Cracking Resistance**

Figure 2.8 shows the variation of the CT_{Index} with the addition of different percentages of plastic in the asphalt mixes. From Figure 2.8, it was observed that both the LDPE and LLDPE plastics reduced the cracking resistance of the asphalt mixes. The CT_{Index} value was found to decrease with an increase in the amount of plastic. For example, for an increase in the plastic percentage of 0.25% to 0.5%, CT_{Index} was found to reduce from 81 to 56 for the LDPE- and from

137 to 92 for the LLDPE-modified mixes, respectively. Increased stiffness of mixes due to the addition of plastic is expected to be responsible for the reduction in the cracking resistance. Also, from Figure 2.8, the LLDPE-modified mixes were found to provide better cracking resistance than the LDPE-modified mixes. As mentioned earlier, lower viscosity of the LLDPE plastic contributed to lower stiffness as compared to that of the LDPE plastic. Several previous studies have reported a reduction in cracking resistance with the increase in the amount of plastic in the mixture (Costa et al. 2017; Ranieri et al. 2017).

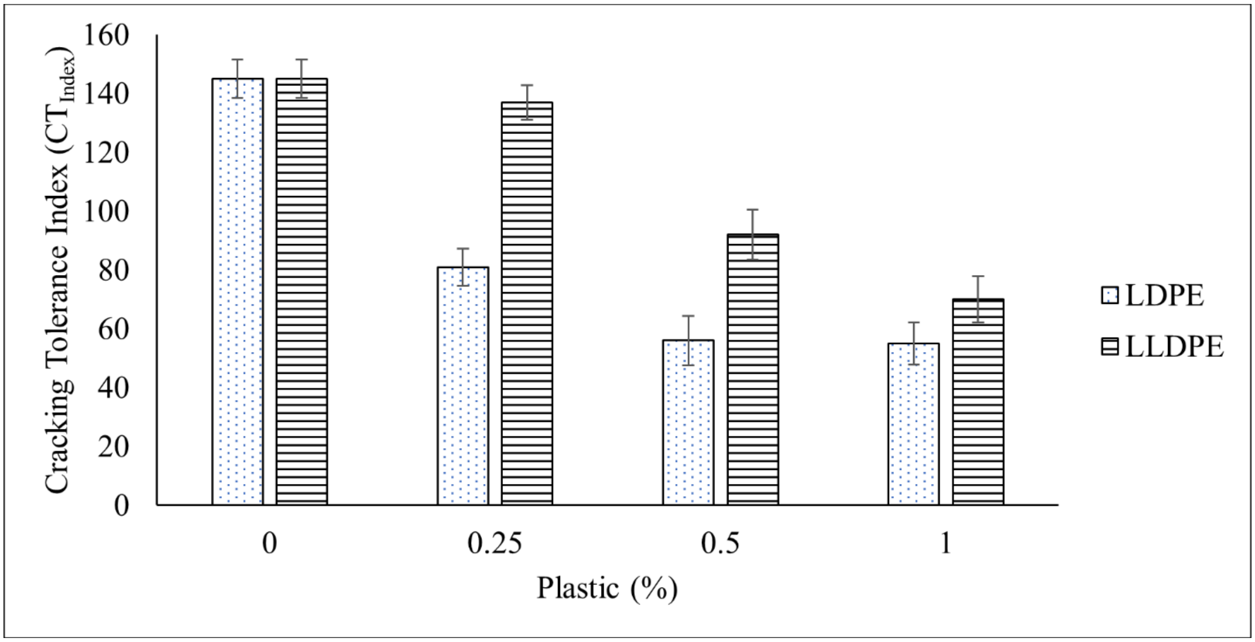

Figure 2.8 Variation of CT_{Index} with the amount of LDPE and LLDPE plastics

2.3.4 **Effect on Moisture-Induced Damage**

The changes in the moisture-induced damage potential of the asphalt mixes with the addition of the LDPE and LLDPE plastic were evaluated using the TSR values and results are presented in Figure 2.9. A TSR of 0.8 is required for a mixture to provide sufficient resistance to moisture-induced damage (ODOT 2009). From Figure 2.9, all mixes were observed to satisfy the moisture-induced damage criteria for TSR of at least 0.8. However, The TSR value was found to reduce with an increase in the plastic percentage, as shown in Figure 2.9. For example, for an increase in the plastic percentage from 0.25% to 0.5%, the TSR decreased from 0.92 to 0.88 for the LDPE and from 0.85 to 0.82 for the LLDPE-modified mixes, respectively. A similar decrease in TSR was observed by other researchers (Azam et al. 2019; Almeida et al. 2020). It was observed that the changes in the TSR value after 0.5% plastic, for both LDPE and LLDPE plastics, were less prominent as compared to that for 0 to 0.5% plastics. Also, from Figure 2.9, the LLDPE-modified mixes were found to be more prone to moisture-induced damage than that of the LDPE-modified mixes.

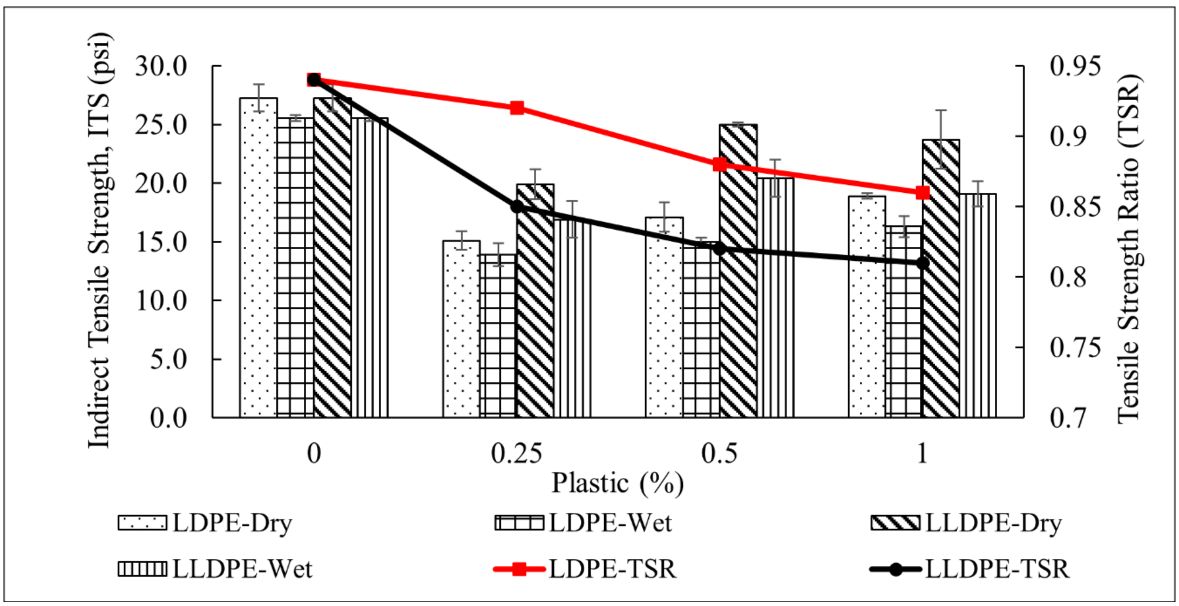

Figure 2.9 Variation of TSR with plastic percentages

2.3.5 **Performance of Plastic-Modified Mixes Relative to Balanced Mix Design Approach**

According to ODOT BMD specifications, a mix must meet both volumetrics and performance related specifications for satisfying BMD requirements (ODOT 2020). It was observed that the control mix, 0.25%-LDPE-, 0.5%-LDPE- and 0.25%-LLDPE satisfied the volumetric requirements for ODOT BMD mixes. The performance related criteria for BMD were evaluated using the BMD quadrant plot. Figure 2.10 presents the BMD quadrant plot prepared following the ODOT BMD Special Provision (ODOT 2020). As noted earlier, the ODOT specification requires a rut depth of 12.5-mm or less and a CT_{Index} of 80 or more. Therefore, a mix plotted on the top left quadrant of Figure 2.10 will satisfy the performance requirements specified in ODOT BMD special provision. From Figure 2.10, the 0.25%-LDPE-, 0.25%-LLDPE- and 0.5%-LLDPE-modified mixes were found to satisfy both rutting and cracking criteria for BMD. The other mixes, namely 0.5%-LLDPE-, 1.0%-LDPE- and 1.0%-LLDPE-modified mixes satisfied the rutting criterion but did not meet the cracking criterion. Considering both volumetrics and performance criteria, only two plastic-modified mixes, namely 0.25%-LDPE- and 0.25%-LLDPE-modified mixes satisfied the criteria for BMD. Also, these two mixes satisfied the moisture-induced damage requirement of TSR greater than 0.8. Therefore, mixes with 0.25% LDPE and 0.25% LLDPE plastic are expected to exhibit balanced performance pertaining to rutting, cracking and moisture-induced damage in their service lives. Modifications, such as changes in binder type and content, and use of an additive or rejuvenator may be needed to obtain a balanced rutting and cracking performance from mixes with higher amounts of plastics.

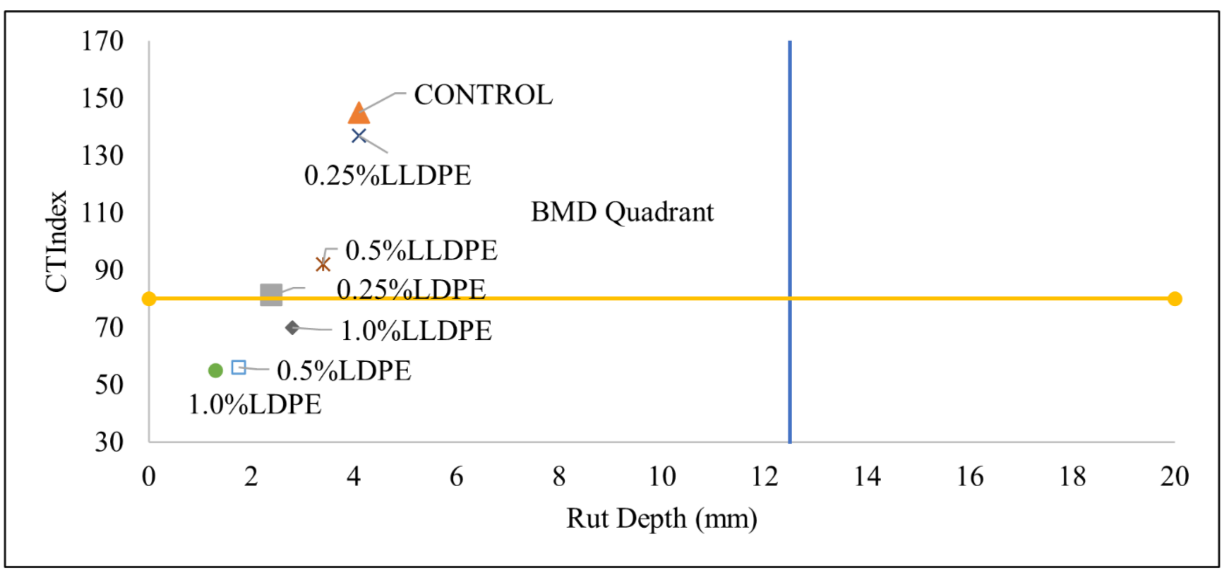

Figure 2.10 BMD quadrant plot showing relative positions of plastic-modified mixtures

2.4 CONCLUSIONS

In this study, the effects of incorporating two types of PCR plastics, namely LDPE and LLDPE, in asphalt mixes were evaluated with respect to changes in volumetric properties, rutting, cracking and moisture-induced damage. Also, the suitability of the plastic-modified mixes as a BMD was evaluated. Based on the results presented in the preceding sections, the following conclusions were drawn:

a) Adding PCR plastic at room-temperature during mixing with heated aggregate and binder was found as a feasible way for incorporation of plastic in asphalt mixes using the dry process.

b) The addition of LDPE and LLDPE plastics increased the density (% of G_{mm}) and decreased the G_{mm} and G_{mb} of the mixes.

c) Rutting resistance improved with the use of the LDPE and LLDPE plastics. The LDPE-modified mixes exhibited a better rutting resistance than the LLDPE-modified mixes.

d) Incorporation of plastic reduced the cracking resistance as indicated by the lower CTIndex in IDEAL-CT tests. However, the LLDPE-modified mixes performed better than the LDPE-modified mixes.

e) Based on the TSR values, the addition of LDPE and LLDPE reduced the resistance to moisture-induced damage of asphalt mixes. However, the LDPE-modified mixes were found to have a higher resistance to moisture-induced damage compared to the LLDPE-modified mixes.

f) The mixes with 0.25%-LLDPE and 0.25%-LLDPE satisfied the requirements for a balanced mix, as per ODOT specification for BMD.

In this study, it was assumed that the plastic particles will act as a replacement of aggregate. However, in reality, a portion of the plastic is expected to melt during the mixing and compaction process. Due to the limited scope of this study, the amount and the effect of melted plastic was not investigated in this study. Also, for the purpose of this study, all the plastic modified mixes were considered uniform, i.e., similar distribution of materials though out the compacted samples. It should be noted that the findings presented in this study were based on a surface mix (NMAS of 9.5-mm) and two types of PCR plastics (LDPE and LLDPE). Effects of PCR plastics on mixes with different aggregate gradations and different grades of binder may be evaluated in future studies. Several previous studies have reported the presence of microplastics in road runoff as one of the potential environmental concerns (Kole et al. 2017; Unice et al. 2019; Vogelsang et al. 2019). Microplastics mainly come from the degradation of tire edges and road-wear particles from road-markings (Kole et al. 2017; Unice et al. 2019; Vogelsang et al. 2019). However, to the best of the authors' knowledge, no tests or specific standards have been developed until now to address the issue related to the release of microplastics from plastic-modified asphalt mixes. Due to the limited scope, authors did not address environmental concerns related to the release of microplastics from asphalt mixes. A future study can be conducted to address this issue.

CHAPTER 3 FRACTURE CHARACTERIZATION OF ASPHALT MIXES CONTAINING POST-CONSUMER RECYCLED (PCR) PLASTICS USING DIFFERENT CRACKING TESTS[†]

ABSTRACT

Cracking is one of the most common forms of distress in asphalt pavements. Selection of a suitable cracking test is essential to evaluate the performance of asphalt mixes during the design as well as under in-service condition. Cracking performance of plastic-modified asphalt mixes is even more critical as addition of plastic stiffens the mix. This paper focuses on the evaluation of the fatigue cracking resistance of asphalt mixes containing Post-Consumer Recycled (PCR) plastics using three commonly used fracture test methods, namely Illinois Flexibility Index Test, Louisiana Semi-Circular Bend Test, and Indirect Tensile Asphalt Cracking Test. Specifically, fracture energy, flexibility index, critical strain energy release rate, and cracking tolerance index were used as cracking indices for evaluating the fracture properties of seven asphalt mixes containing two different post-consumer recycled plastics. These mixes were ranked for their cracking resistance from 1 to 7 (1 being the best and 7 being the worst) using each parameter. Also, load-displacement relationships and cracking indices of these three tests were compared. It was found that the post-peak portion of the load-displacement curve had a significant impact on the cracking resistance. The relationships of fracture energy, flexibility index and cracking tolerance index with notch depths and loading rates were evaluated. Also, a loading rate-dependent parameter for flexibility index was developed in this study. Findings

[†] This chapter has been submitted to the International Journal of Pavement Research and Technology under the title "Fracture Characterization of Asphalt Mixes Containing Post-Consumer Recycled (PCR) Plastics using Different Cracking Tests." The current version has been formatted for this dissertation.

from this study are expected to provide an insight of these three commonly used tests and can be used in selecting a suitable test for plastic-modified mixes for characterization of fracture.

Keywords**:** Transverse Cracks; Post-Consumer Recycled (PCR) Plastics; Plastic-Modified Asphalt Mix; Fracture; Cracking Tolerance Index; Flexibility Index; Fracture Energy; Critical Strain Energy Release Rate.

3.1 INTRODUCTION

In recent years, Balanced Mix Design (BMD) is gaining momentum nationally for elevating asphalt mix designs to a new level in which screening of mixes for both volumetric properties and performance (rutting, cracking, moisture damage, etc.) requirements are addressed at the design stage. State Departments of Transportation (DOTs) are emphasizing incorporating recycled materials, namely, Reclaimed Asphalt Pavement (RAP), Recycled Asphalt Shingles (RAS), Ground Tire Rubber (GTR) and waste plastics in asphalt mixes for sustainable construction. However, incorporation of such recycled materials is adding more challenges for BMD implementation. Specifically, the problem becomes more complicated when waste plastic is used in asphalt mixes. Waste plastics are incorporated in asphalt mixes either by modifying asphalt binder with plastics (also known as wet method) or adding plastics during the mixing by replacing a certain amount of aggregates (dry method) (Costa et al. 2013; Dalhat et al. 2017; Ghos et al. 2022a; Ghos et al. 2022b; Radeef et al. 2023. Heydari et al. 2024). Several studies have evaluated the performance of wet-processed plastic-modified asphalt mixes (Costa et al. 2013; Dalhat et al. 2017; Costa et al. 2019; Mashaan et al. 2021). For example, Dalhat et al. (2017) evaluated the performance of Polypropylene (PP), High-Density Polyethylene (HDPE) and Low-Density Polyethylene (LDPE)-modified binder and mixes. In that study, asphalt binders were modified with these three types of waste plastics using wet process. These plastic-modified binders were tested for the rheological properties, namely, complex modulus (G*), phase angle (δ), and non-recoverable creep compliance (J_{nr}). Also, asphalt mixes produced with plastic-modified binders were tested for resilient modulus (M_R). A significant improvement in the fatigue cracking and rutting resistance was reported in that study (Dalhat et al. 2017). Costa et al. (2019) evaluated the performance of HDPE, Ethylene Vinyl Acetate (EVA) and Styrene-Butadiene-Styrene (SBS)-modified binders. In that study, binder modification with HDPE was reported to reduce the fatigue cracking resistance (Costa et al. 2019). Mashaan et al. (2021) evaluated the performance of Polyethylene Terephthalate (PET)-modified binders. Fatigue cracking resistance was evaluated by DSR test on Pressure Aging Vessel (PAV) conditioned samples. It was reported that modification of binder with PET (8% by the weight of binder) improved fatigue cracking resistance (Mashaan et al. 2021). Several other studies have evaluated the effect of waste plastics on the cracking performance of asphalt mixes (Modarres and Hamedi 2014; Radeef et al. 2021; Goli et al. 2023; Radeef et al. 2023). For example, Modarres and Hamedi (2014) evaluated the fatigue cracking properties of PET-modified asphalt mixes. In that study, asphalt mixes were produced using dry process by varying the PET contents from 2 to 10% by the weight of asphalt binder. Indirect tensile strength tests were conducted to evaluate the fatigue cracking resistance of PET-modified mixes. It was reported that PET increased the stiffness and fatigue cracking resistance of asphalt nixes (Modarres and Hamedi 2014). Zhang et al. (2020a) evaluated the effect of HDPE on the fatigue cracking resistance of asphalt mixes. In that study, Four-Point Bending Beam Fatigue Tests (BBFT) were conducted on asphalt mixes containing HDPEs. The number of cycles to failure was used as an indicator of fatigue performance. The number of cycles to fatigue failure dropped by more than a factor of 5 with the addition of 7% HDPE (Zhang et al. 2020a). Almeida et al. (2020) evaluated the fatigue cracking resistance of asphalt mixes containing Low-Density Polyethylene (LDPE). In that study, adding 6% waste LDPE plastic was found to reduce the number of cycles to fatigue failure by 33% for both aged and unaged samples (Almeida et al. 2020). In a similar study, Martin-Alfonso et al. (2019) evaluated the fatigue resistance of asphalt mixes containing LDPE. The addition of 0.5% waste LDPE reduced the fatigue resistance by a factor of ~3 for asphalt mixes (Martin-Alfonso et al. 2019). However, Radeef et al. (2023) reported that fatigue cracking resistance of asphalt mixes increased with the addition of waste plastics. In that study, repeated load Semi-Circular Bend (SCB) test was used to evaluate the fatigue cracking resistance of plastic-modified asphalt mixes (Radeef et al. 2023). Therefore, based on the current literature, the fatigue cracking resistances of plastic-modified asphalt mixes are inconclusive and require further investigation. Also, the results were found to vary with the testing methods used. To this end, the current study is aimed at evaluating the fatigue cracking resistance of asphalt mixes containing two different types of post-consumer recycled plastics and using three different test methods. A summary of cracking mechanism of asphalt mix, different available cracking tests and their key parameters is summarized and presented in the following section.

3.2 BACKGROUND

According to West et al. (2018), more than 85% of asphalt pavements in the United States experience various forms of cracks, including transverse crack, reflective crack, fatigue crack, and longitudinal crack. Cracking of asphalt mixes is a process of energy dissipation (Zhou et al. 2020). In this process, the work of stress is converted into elastic strain energy, which is stored within the asphalt mix. When the stored strain energy exceeds the capacity of an asphalt mix, it results in cracking (Zhou et al. 2020). Several studies have been conducted to evaluate the cracking resistance of asphalt mixes using different fracture tests (Zhou et al. 2020; Abdulshafi and Majidzadeh 1985; Haslett 2018). In the early days, Abdulshafi and Majidzadeh (1985) used the Semi-Circular Bend (SCB) test for evaluating the fracture properties of the asphalt mixes. It was concluded that the Critical Strain Energy Release Rate (J-integral or J_c) can be used as an index parameter for evaluating the fracture properties of asphalt mixes (Abdulshafi and Majidzadeh 1985). Louisiana Transportation Research Center (LTRC) has been using the SCB test since 2004 to evaluate the fracture properties of asphalt mixes at an intermediate temperature (Cooper et al. 2016). This test is also known as the Louisiana Semi-Circular Bend (L-SCB) test. This method uses J-integral as the cracking index parameter for evaluating the fracture properties. In determining the J-integral value, the area of the load-displacement curve up to peak load is used, and the post-peak portion of the load-displacement curve is ignored (ASTM 2016). El Khatib (2016) developed a performance-based test method for quantifying the cracking potential of asphalt mixes by modifying the SCB test. This test method is also known as Illinois Flexibility Index Test (IFIT). In that study, Flexibility Index (FI) was recommended for evaluating the cracking potential of asphalt mixes (El Khatib 2016). Zhou et al. (2017) developed an indirect tensile cracking test for designing asphalt mixes and using it as a quality control/quality assurance tool for field cores and laboratory compacted samples. This test is known as Indirect Tensile Asphalt Cracking Test (IDEAL-CT) and can be run at room temperature. In IDEAL-CT, an index parameter known as Cracking Tolerance Index (CT_{Index}) is used for characterizing the cracking resistance of asphalt mixes. This test is less time consuming and requires no cutting and notching. Also, this test is relatively easy to perform and requires a minimum amount of training (Zhou et al. 2017). The working principles of L-SCB, IFIT and IDEAL-CT are discussed in detail in the following sub-section. Several other tests are also available for determining the cracking resistance of asphalt mixes including the Dissipated Creep

Strain Energy (DCSE), Texas Overlay (OT), Four-Point Bending Beam test, Disk-Shaped Compaction Test (DCT), and Indirect Tensile Test (IDT) (Zhou et al. 2020; Elseifi et al. 2012).

It is important to select a suitable test method for characterizing the cracking resistance of asphalt mixes depending on the purpose and availability of resources. To this end, several studies have been conducted in recent years to identify the most suitable cracking tests for asphalt mixes. For example, Haslett (2018) conducted a study to explore the temperature and loading rate interdependency of fracture properties of the asphalt mixes. In that study, six different cracking indices namely, Fracture Energy ($\boldsymbol{G_f}$), FI, Fracture Strain Tolerance (FST), Cracking Resistance Index (CRI), Toughness Index (TI) and N_{flex} factor were evaluated at four different temperature and loading rate combinations. These cracking indices were used to rank the performances of five asphalt mixes. It was found that the load-displacement curves varied significantly with temperature. Also, it was recommended that the climatic regions should be considered in selecting test temperatures and loading rates (Haslett 2018). Zhou et al. (2020) conducted a study to compare the commonly used fracture test methods, namely IDT, Single Edge Notch Beam test (SENB), SCB and DCT. In that study, the stress intensity factors for these test methods were compared and the appropriate range of notch depth was evaluated. The SCB test (with a loading rate of 5 mm/min) was finally recommended as the test method for evaluating the cracking resistance of asphalt mixes. Also, the fracture energy was recommended as the most suitable cracking index for evaluating the cracking resistance. Specifically, the fracture energy at the contra flexure point was suggested as the cracking index to evaluate the ultimate cracking resistance of asphalt mixes (Zhou et al. 2020).

3.2.1 **Illinois Flexibility Index Test (IFIT)**

Illinois Flexibility Index Test (IFIT) determines the cracking resistance of asphalt mixes, following AASHTO T 393-22 (AASHTO 2022d). The IFIT is based on the Linear Elastic Fracture Mechanics (LEFM), a method of fracture analysis for determining the stress required to induce fracture instability in a structure containing a crack-like flaw (notch) of known size and shape (Zhou et al. 2020; AASHTO 2022d). In this test, asphalt mix samples are compacted using Superpave Gyratory Compactor (SGC). The cylindrical specimens are then trimmed and cut into half to produce semi-circular test specimens. The thickness of each specimen is kept at 50-mm. A 15-mm notch is cut in the flat side of the semi-circular specimen, opposite to the curved edge. The specimen is loaded monotonically at a displacement rate of 50-mm/min until failure in a three-point bending configuration. The load and load line displacement are measured during the entire duration of the test. A typical load- displacement curve along with its important features is presented in Figure 3.1. The G_f and FI were calculated from this diagram using Equations 3.1 and 3.2, respectively.

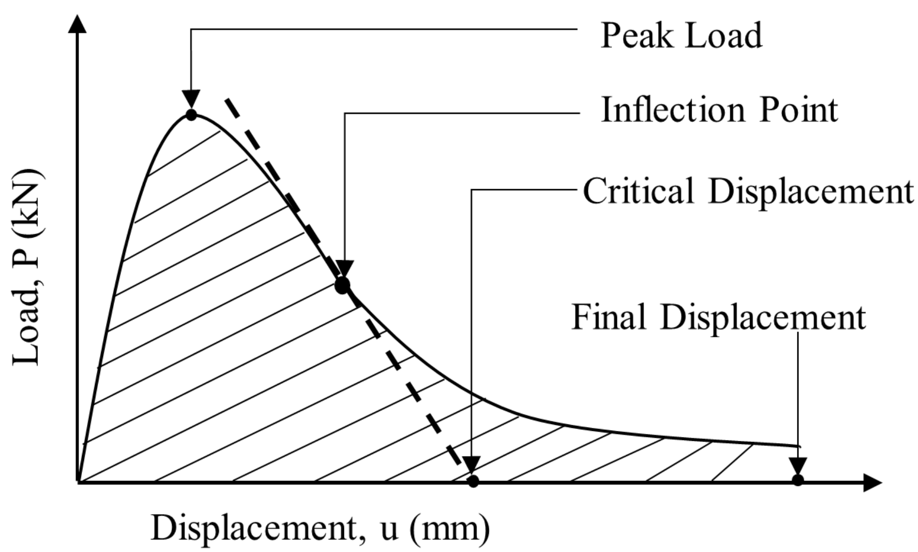

Figure 3.1 Typical load-displacement diagram of IFIT

$$G_f = \frac{W_f}{Area_{lig}} \times 10^6 \quad (3.1)$$

where,

G_f = fracture energy (J/m^2);

W_f = work of fracture (J);

$Area_{lig}$ = ligament area (mm^2) = (r-a) ×t;

r = specimen radius (mm);

a = notch depth (mm);

t = specimen thickness.

$$FI = \frac{G_f}{|m|} \times A \quad (3.2)$$

where,

FI = flexibility index;

$|m|$ = absolute value of the post-peak load slope (kN/m) at the inflection point;

A = unit conversion factor (0.01).

3.2.2 **Louisiana Semi-Circular Bend Test (L-SCB)**

Louisiana Semi-Circular Bend (L-SCB) tests are performed following ASTM D 8044 (ASTM 2016). This test is based on the Elasto-Plastic Fracture Mechanics (EPFM) (ASTM 2016; Yang 2016). In this test, 50-mm thick semi-circular specimens are loaded monotonically under a constant rate of deformation of 0.5-mm/min in a three-point bending configuration. The load and deformation data are continuously recorded and used to compute the intended parameters. In this test, only the pre-peak portion of the load displacement curve (i.e., up to peak load) is used for evaluating the cracking resistance. SGC compacted specimens of 150-mm diameter are prepared. Each specimen is then saw cut to produce 150-mm diameter and 50-mm thick four semi-circular specimens. These tests are conducted at three notch depths, namely 25.4-mm, 31.8-mm and 38-mm.

In this method, the cracking resistance of asphalt mixes is evaluated using the critical strain energy release rate (*J-integral* also known as J_c). The *J-integral* reflects the strength of stress-strain field at the crack tip. The J_c value was calculated using Equation 3.3.

$$J_c = -\left(\frac{1}{b}\right)\frac{dU}{da} \tag{3.3}$$

where,

J_c = critical strain energy release rate (kJ/m^2);

b = thickness of the specimen (m);

a = notch depth (m);

U = strain energy (area under the stress-strain curve) (N-m).

3.2.3 **Indirect Tensile Asphalt Cracking Test (IDEAL-CT)**

The IDEAL-CT is similar to IDT and performed on a cylindrical specimen (150-mm diameter and 62-mm high) at a loading rate of 50-mm/min (Zhou et al. 2017). This method is based on the Paris Law of Crack Propagation. The Paris Law developed the relationship between crack growth and the stress intensity factor under the LEFM (Zhou et al. 2017; Yang 2016). This test is run at room temperature i.e, 25°C in a typical IDT fixture. This is a relatively simple test with no requirement for cutting, gluing, or notching of the specimen. During the test, the load and displacement data are recorded during the entire duration. A typical load-displacement curve is shown in Figure 3.2. The load-displacement curve is used to calculate the cracking resistance of the asphalt mixes in terms of fracture energy and CT_{Index}. The CT_{Index} is defined by Equation 3.4.

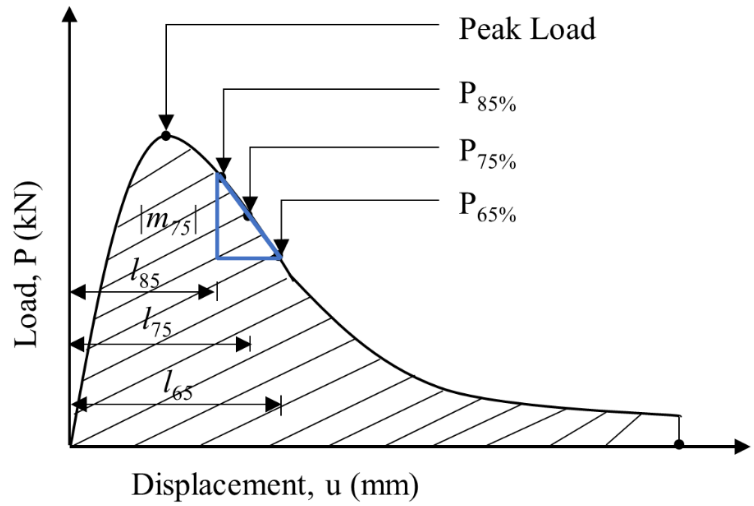

Figure 3.2 Typical load-displacement diagram of IDEAL-CT

$$CT_{Index} = \frac{G_f}{|m_{75}|} \times \left(\frac{l_{75}}{D}\right) \tag{3.4}$$

where,

G_f = fracture energy = work of fracture (area under the load displacement curve) divided by the area of the cracking face;

$|m_{75}|$ = absolute value of the slope at the post-peak curve between 85% of the peak load and 65% of the peak load;

l_{75} = displacement at the 75% of the peak load at the post-peak curve;

D = diameter of the specimen.

The CT_{Index} can vary from 1 to 1000. The higher the CT_{Index} , the better the cracking resistance.

3.3 OBJECTIVES

Several studies have shown that the SCB test is the most suitable test method for evaluating the fracture properties of asphalt mixes (Zhou et al. 2020; Ameri et al. 2012; Aliha et al. 2014). Also, the IDEAL-CT test is gaining popularity among state DOTs to evaluate the cracking resistance for its simplicity. To this end, the current study was focused on understanding the cracking resistance of plastic-modified asphalt mixes by using two SCB tests, namely IFIT and L-SCB, and IDEAL-CT tests. Therefore, the specific objectives of this study were as follows:

a) To evaluate the cracking resistance of asphalt mixes containing post-consumer recycled plastics using three commonly used fracture test methods, namely IFIT, L-SCB and IDEAL-CT;

b) To compare the commonly used cracking indices obtained from these three tests methods;

c) To evaluate the effect of loading rate and notch depth on cracking indices of IFIT and L-SCB.

3.4 MATERIALS AND METHODS

In this study, an S5 asphalt mix designed using the BMD approach was used as the control mix. A total of 6 PCR plastic-modified mixes were produced using two different types of plastics, namely Low-Density Polyethylene (LDPE) and Linear Low-Density Polyethylene (LLDPE) at three different percentages (0.25%, 0.5% and 1.0% by the weight of the aggregate blend). The optimum binder content of the control mix was determined as 6%. Optimum LDPE and LLDPE dosage were determined using the BMD Quadrant Plot and found as 0.25% for LDPE and 0.5% for LLDPE. Detail description of the plastic properties, plastic addition process, mix volumetrics and performances were reported in Chapter 2 (Ghos et al. 2022a). In this paper, mixes are named as C, XX-LDPE and XX-LLDPE, where, C indicates control mix, XX indicates the percentage of plastics used in producing plastic-modified mixes. During compaction, these mixes were heated in the oven at 149°C for 2 hours. Eight SGC specimens of 150-mm diameter and 160-mm high were prepared for each mix to produce SCB samples. These specimens were then trimmed and saw cut to create semi-circular samples of 50-mm thick and 150-mm diameter as shown Figure 3.3. Although a L-SCB test requires 57-mm thick samples, 50-mm thick samples were used in this study for simplicity and better comparison. The SCB samples were prepared with four different notch depths namely, 15-mm, 25.4-mm, 31.8-mm and 38-mm. These samples were tested using both IFIT and L-SCB test methods. However, IFIT requires only 15-mm notch depth whereas L-SCB requires 25.4-mm, 31.8-mm and 38-mm notched samples. In this study, all four notch depths were used for both test methods for better comparison and analysis. In addition, IFIT tests were conducted on control, 0.25-LDPE and 0.5-LLDPE mixes at 4-different loading rates, namely 0.5-mm/min, 5-mm/min, 10-mm/min and 50-mm/min to evaluate the effect of loading rates on the fracture properties. An overview of the sampling and testing was provided in the test matrix in Table 3.1. Three 150-mm diameter and 62-mm high samples were prepared for each mix. These samples were used for the IDEAL-CT tests. All samples were conditioned at 25^{o}C before testing. In all cases, load and displacement data were recorded for the entire duration of these tests. These data were used to calculate the cracking indices, as discussed subsequently.

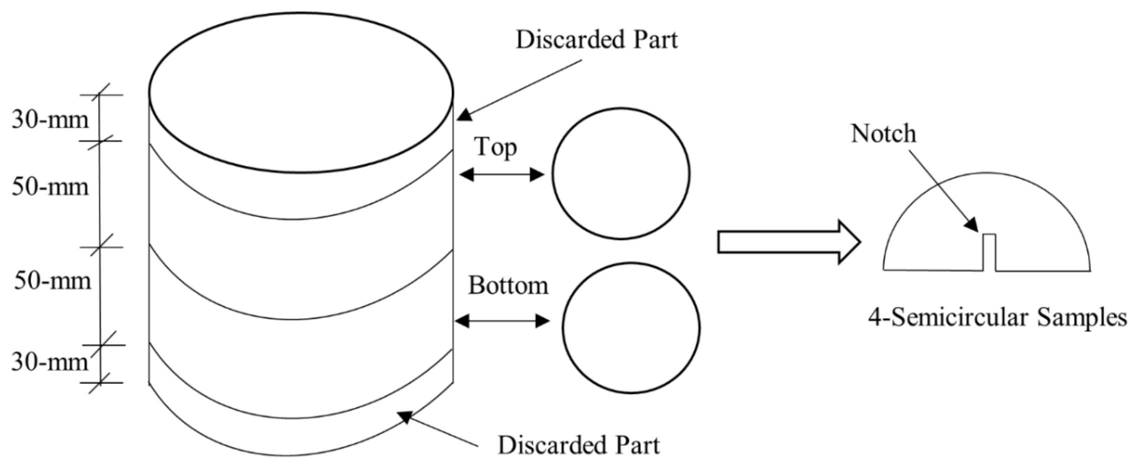

Figure 3.3 Sample preparation for IFIT and Louisiana SCB tests

Table 3.1 Test matrix

Mix ID	Notch Depth (mm)	Loading Rate (mm/min)	No. of Samples for Each Mix	Test Method
C, 0.25-LDPE, 0.5-LDPE, 1.0-LDPE, 0.25-LLDPE, 0.5-LLDPE, and 1.0-LLDPE	15	50	4	IFIT
	25.4	50	4	IFIT
	31.8	50	4	IFIT
	38	50	4	IFIT
	15	0.5	4	L-SCB
	25.4	0.5	4	L-SCB
	31.8	0.5	4	L-SCB
	38	0.5	4	L-SCB
	--	50	3	IDEAL-CT
C, 0.25-LDPE and 0.5-LLDPE	15	10	4	IFIT
	15	5	4	IFIT

3.5 RESULTS AND DISCUSSION

3.5.1 **Ranking of Mixes Based on IFIT**

As noted before, in this study, the IFIT tests were conducted on all seven mixes following the AASHTO T 393 (AASHTO 2022d). These tests were conducted by applying a monotonic load at 50-mm/min until failure. From these tests, FI values were calculated and used for ranking the mixes. The higher the FI value the better the cracking resistance (Haslett 2018; Ozer et al. 2016). Also, a higher FI value corresponds to the softer mix. For new asphalt pavements, a FI of 8 or more is considered good cracking resistance. A FI value of less than 6 is considered poor cracking resistance (Ozer et al. 2016). The IFIT test results are summarized in Table 2 for all seven mixes. All seven mixes were found to satisfy the cracking resistance criteria based on their FI values, as evident from Table 3.2. The FI of the control mix was found to vary from 36.1 to 28.5 with an average of 32.1 and a standard deviation of 3.1. Overall, FI values decreased with an increase in the plastic content. Based on these FI values, these mixes were ranked from 1 to 7, in which 1 being the best cracking resistance and 7 being the worst cracking resistance. As previously mentioned, a higher FI value corresponds to a softer mix. The control mix was found to be the best cracking resistant mix. An increase in the plastic content increased the stiffness of the asphalt mix. Asphalt mix with 1%-LDPE was found to show the worst-case scenario. The level of decrease in the FI value for plastic addition is higher for the LDPE mixes as compared to the LLDPE mixes.

3.5.2 **Ranking of Mixes based on the L-SCB**

L-SCB tests (also, known as crack propagation test) were conducted on all seven mixes following the ASTM D 8044 (ASTM 2016). The J_c-value was determined from the load-displacement curves to rank these mixes for cracking resistance. The higher the J_c-value the better the resistance to cracking. Although four notch depths, namely 15-mm, 25.4-mm, 31.7-mm and 38-mm were used in this study, the strain energy release rate for 25.4-mm, 31.7-mm and 38-mm were used at this stage for calculating the J_c-value. According to ASTM D 8044 (ASTM 2016), a J_c-value of 0.5-kJ/m^2 or higher is typically recommended to ensure adequate cracking resistances of asphalt mixes. The L-SCB test results are also summarized in Table 3.2 for all seven mixes. As previously mentioned, a higher *Jc*-value corresponds to a better cracking resistance. All mixes were found to satisfy the J_c-value criteria as evident from Table 3.2. It was observed that J_c-value increased with an increase in the plastic content. Mechanistically, J_c-value indicates the resistance of a material to crack initiation and propagation under a steady tensile deformation and a means of reporting the toughness of a material (Spiegelberg et al. 2016). Therefore, plastics were found to contribute to the tensile strength of asphalt mixes. From these results, the L-SCB, 1.0-LLDPE mix was found to be the best performing mix among the seven mixes tested here. However, a different ranking was found from the IFIT results, as discussed in the previous section. One possible reason for such difference ranking is that L-SCB only considers the load-displacement curve only up to the peak load. Also, from the mechanistic point of view, the J_c-value is not valid after the peak load (Zhou et al. 2020). A detailed comparison of IFIT and L-SCB is presented in the subsequent section.

3.5.3 **Ranking of Mixes based on the IDEAL-CT**

Finally, the IDEAL-CT tests were conducted on all seven mixes, and G_f and CT_{Index} were determined from load-displacement diagrams. Each mix was assigned a rank based on the CT_{Index} value. As previously discussed, the CT_{Index} can vary from 1 to 1,000. A larger value corresponds to a better cracking resistance of the asphalt mix (El Khatib 2016). The IDEAL-CT test results are summarized in Table 3.2 for all seven mixes. The CT_{Index} value of the control mix was found to vary from 115to 175 with an average of 145 and a standard deviation of 30.1. The CT_{Index} of 1.0-LDPE mix was found to vary from 50 to 61 with an average of 55 and standard deviation of 7.1. From the IDEAL-CT point of view, the control mix was found as the best performing mix and the 1.0-LDPE mix was found as the worst among the seven mixes tested here. It was found that the IDEAL-CT test results provided a different ranking than the IFIT and L-SCB results. However, the differences in ranking for IDEAL-CT and IFIT were minimal as compared to the differences between the IDEAL-CT and L-SCB rankings. Slight variations between IDEAL-CT and IFIT could result from the sample geometry, notching and distribution of plastic particles inside the mastic. On the other hand, the L-SCB test considered only the peak-portion of the load-displacement curve, and which created significant differences in ranking.

Table 3.2 Summary of IFIT, L-SCB and IDEAL-CT test results

Mix ID	FI				Rank
	Maximum	Minimum	Average	Standard Deviation	
C	36.1	28.5	32.1	3.1	1
0.25-LDPE	33.3	17.7	27.9	7.1	3
0.5-LDPE	27.5	22.1	27.0	4.1	5
1.0-LDPE	20.1	11.5	14.6	5.5	7
0.25-LLDPE	36.5	22.6	30.6	6.4	2
0.5-LLDPE	34.7	22.3	28.6	6.1	4
1.0-LLDPE	18.1	13.1	15.4	2.7	6
	Critical Strain Energy Release Rate, Jc (kJ/m^2)				
	Maximum	Minimum	Average	Standard Deviation	
C	0.68	0.54	0.65	0.07	7
0.25-LDPE	0.76	0.49	0.69	0.13	6
0.5-LDPE	0.98	0.87	0.90	0.06	4
1.0-LDPE	1.11	0.85	0.96	0.03	2
0.25-LLDPE	0.91	0.81	0.86	0.04	5
0.5-LLDPE	1.02	0.90	0.92	0.06	3
1.0-LLDPE	1.06	0.95	0.98	0.03	1
	CT_{Index}				
	Maximum	Minimum	Average	Standard Deviation	
C	175	115	145	30.1	1
0.25-LDPE	95	63	81	16.2	4
0.5-LDPE	65	50	56	8.4	6
1.0-LDPE	61	50	55	7.1	7
0.25-LLDPE	171	103	137	48.1	2
0.5-LLDPE	98	86	92	8.5	3
1.0-LLDPE	74	63	69	6.8	5

3.5.4 **Comparison between IFIT, Louisiana SCB and IDEAL-CT**

3.5.4.1 ***Cracking Pattern and Crack Propagation***

In this study, the crack growth and pattern were observed for all three methods. In addition, crack growths were observed at two more loading rates, namely 5-mm/min and 10-mm/min. For these two additional loading rates, the IFIT test setup was used, and tests were carried out only on 15-mm notched specimens. The cracks in the IFIT tests (50-mm/min) were more prominent as compared to the L-SCB tests (0.5-mm/min), as shown in Figures 3.4(a). The reason behind this phenomenon is the rapid loading rate and smaller notch depth (Aliha et al.

2014; Li and Marasteanu 2010). Also, the Fracture Processing Zones (FPZ) developed in the case of IFIT were much larger than in the case of L-SCB. The size of FPZ depends on the loading rate, test temperature, aggregates size, mix designs and notch depth (Aliha et al. 2014; Li and Marasteanu 2010). The size of FPZ decreased with a decrease in the loading rate. In this study, all three tests were conducted at 25°C. Although IFIT requires only one notch depth (15-mm), in this study IFIT tests were conducted on specimens with three other notch depths (25.4, 31.8 and 38 mm) to compare results with the L-SCB test results. It was observed that in all cases the FPZs were larger in IFIT as compared to that of the L-SCB. Also, the cracks were not initiated at the center of the notch depth due to the stress concentration, instead, these cracks were initiated at the corner. Furthermore, cracks were found to propagate through the mastic in the case of IFIT, whereas cracks were found to propagate through the binder in the case of L-SCB, as shown in Figures 3.4(a) and 3.4(b). For plastic-modified mixes, cracks propagated through mastics for all loading rates, as evident from Figures 3.4(b) and 3.4(c). The presence of plastic fibers was visually observed in the plastic-modified mixes. These fibers are expected to contribute to the strength of plastic-modified mixes. This phenomenon is in agreement with the L-SCB test results, as discussed in the previous section. It was observed that several aggregates were broken after IFIT tests due to rapid loading for all mixes (Li and Marasteanu 2010). However, the IDEAL-CT test is much more destructive in nature. In these tests, the cracks were even more prominent as compared to the IFIT test due to the nature of loading and loading rate. Also, several aggregates were found broken in IDEAL-CT testing due to rapid loading.

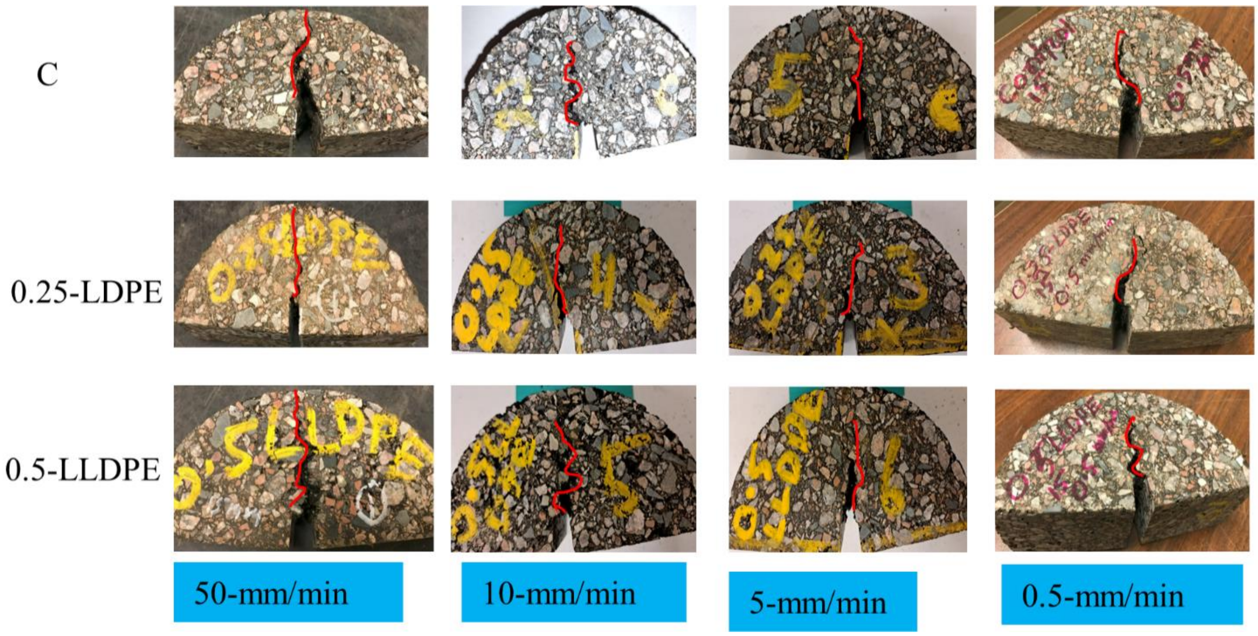
C
0.25-LDPE
0.5-LLDPE
50-mm/min
10-mm/min
5-mm/min
0.5-mm/min

(a)

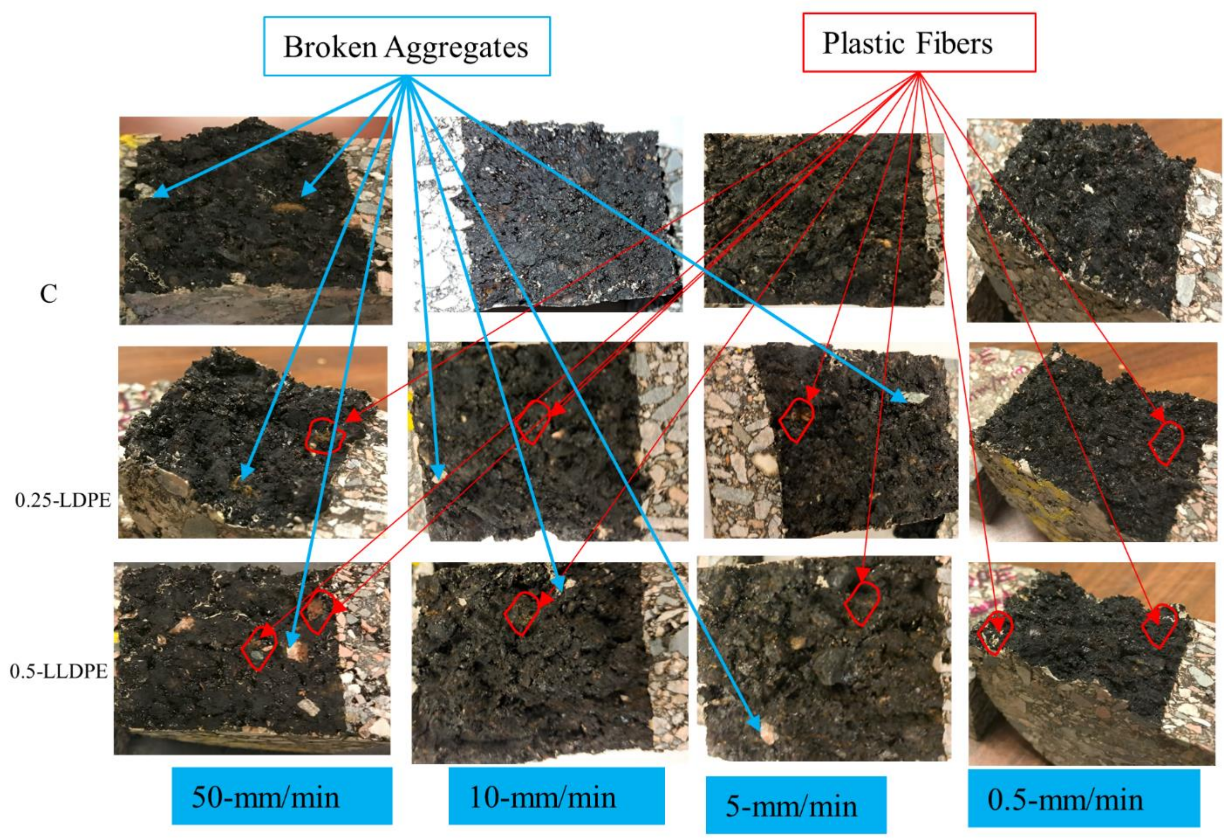
Broken Aggregates
Plastic Fibers
C
0.25-LDPE
0.5-LLDPE
50-mm/min
10-mm/min
5-mm/min
0.5-mm/min

(b)

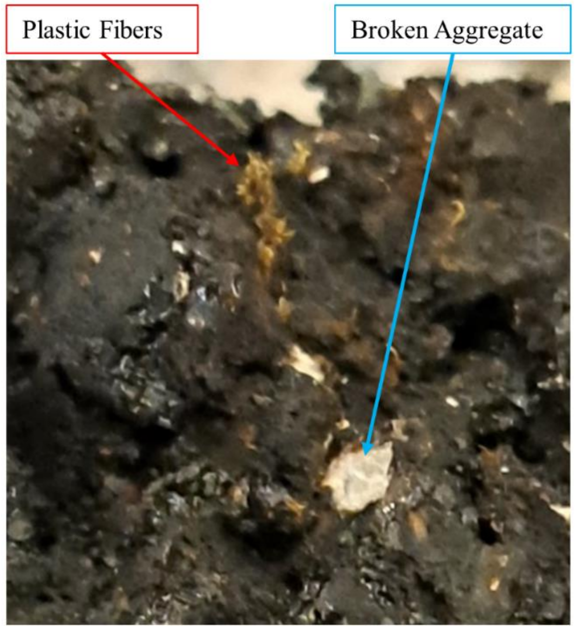

(c)

Figure 3.4 Cracking pattern at different loading rates: (a) Cracking pattern; (b) Cracks inside samples; and (c) Zoomed image of 0.5-LLDPE specimen at 50-mm/min loading rate

3.5.4.2 ***Load-Displacement Relationship***

In this study, load-displacement data from IFIT, L-SCB and IDEAL-CT tests for all seven mixes were carefully examined to evaluate the cracking behaviors. The load-displacement curves of all these mixes are shown in Figures 3.5 (a) to 3.5(g). Higher peak loads and stiffer slopes in the pre-peak portion of the load-displacement curves were observed for the IFIT tests as compared to the L-SCB tests for all seven mixes, as shown in Figure 3.5. Also, the IDEAL-CT tests were found to show the highest peak loads for 0.25-LDPE, 0.5-LDPE and 1.0-LDPE. However, the control and LLDPE-mixes were found to show different behavior in the IDEAL-CT test. The L-SCB tests were found to show flatter curves indicating more ductile behavior as compared to that of the IFIT tests. The reason behind this phenomenon is the rapid loading rate in IFIT and IDEAL-CT tests. The elastic component of a visco-elastic material becomes predominant under increased loading rates (Li and Marasteanu 2010). Also, the area under the load-displacement curve was higher in case of IDEAL-CT test, followed by IFIT and L-SCB tests. Based on these observations, it can be concluded that a higher toughness can be expected from the IDEAL-CT test, followed by IFIT and L-SCB tests.

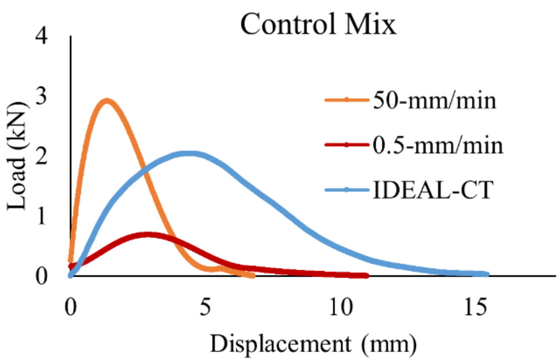

(a)

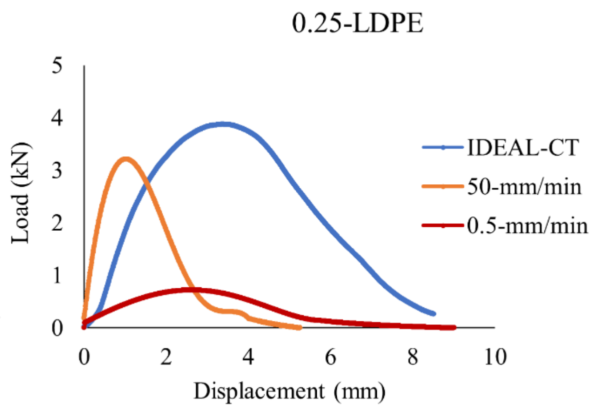

(b)

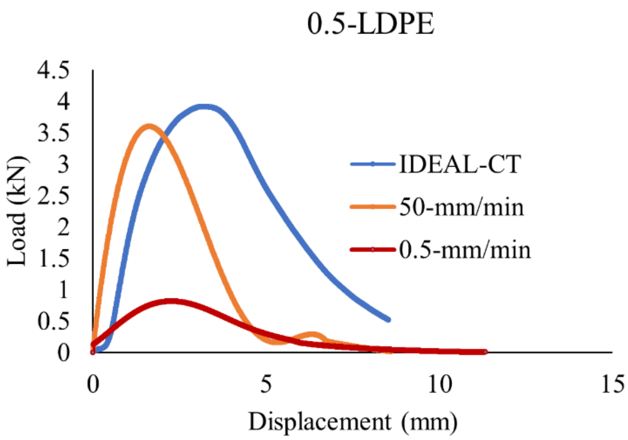

(c)

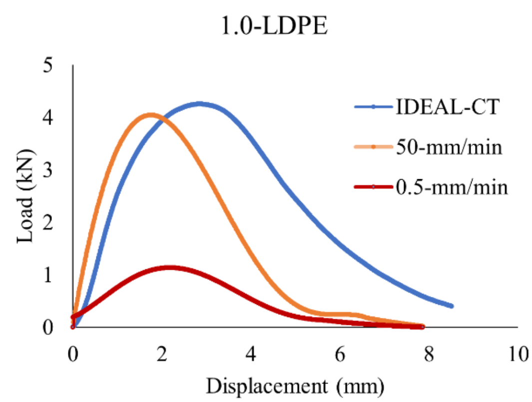

(d)

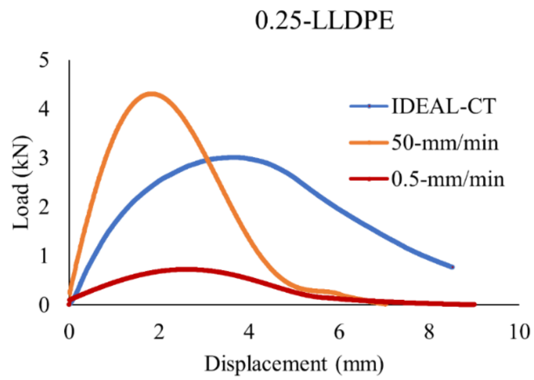

(e)

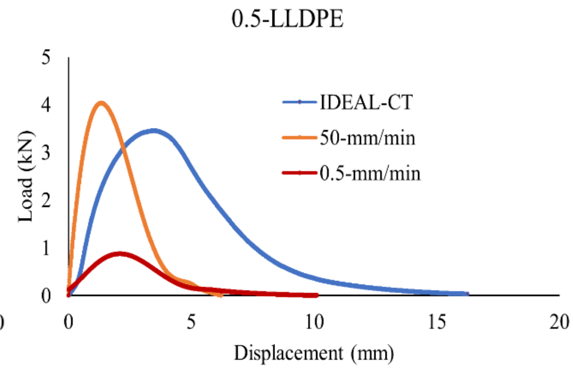

(f)

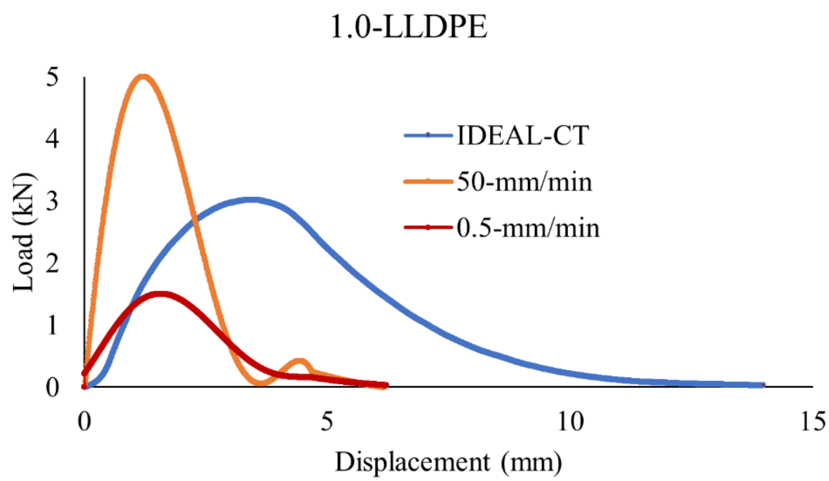

(g)

Figure 3.5 Load-displacement curves: (a) Control Mix; (b) 0.25-LDPE; (c) 0.5-LDPE; (d) 1.0-LDPE; (e) 0.25-LLDPE; (f) 0.5-LLDPE; and (g) 1.0-LLDPE

3.5.5 **Comparison of Cracking Indices for IFIT, Louisiana SCB and IDEAL CT**

3.5.5.1 ***Flexibility Index, J_c-Value and CT_{Index}***

To compare the results of these three test methods, it was necessary to use a common cracking index for all three methods. In this study, the *FI* values of all these three mixes were calculated from the load-displacement curves of these three test methods. As previously mentioned, the *FI* was developed using the LEFM for IFIT. In this study, the *FI* values were also calculated for L-SCB and IDEAL-CT tests for comparative analysis. In this section, *FI* values were calculated at 15-mm notch depth for 50-mm/min (IFIT) and 0.5-mm/min (L-SCB). The *FI* values calculated from the IFIT, L-SCB and IDEAL-CT tests are presented in Figure 3.6. All mixes were found to show the same trend in the *FI* value. This time, a similar ranking was found from all three test methods, as shown in Table 3.3. However, the ranking was different for each test method, as discussed previously. In the case of L-SCB test, the J_c-value was used for ranking these mixes. The *J*-integral is a path independent line integral around the crack which is used to measure the strain energy release rate (Saha and Biligiri 2016). One of the major differences between the LEFM and EPFM approaches to calculate J_c is the notch depth that is variable in the EPFM practice during the estimation process of J_c-value. There are some limitations of using the J_c-value (Zhou et al. 2020; ASTM 2016). Firstly, the J_c-value does not consider the post-peak portion of the-load displacement curve. Secondly, the J_c-value is not applicable to the case where the crack is stably spread. Finally, the *J*-integral criterion is meant to consider initiation of the crack. It is understood that certain strength remains after the initiation of crack, and crack instability expansion occurs subsequently. So, *J*-integral is a relatively conservative theory. Also, in the case of the IDEAL-CT, the CT_{Index} was used for ranking the performance of these three mixes. One important consideration for determination of CT_{Index} is that CT_{Index} uses post-peak slope at 75% of the peak load (m_{75}) for simplification (Zhou et al. 2017). On the contrary, *FI* uses the slope at the inflection point of the post-peak curve. The use of slope at the inflection point appears more mathematically sound than using the m_{75}. Mechanistically, the inflection point at the post-peak curve represents how the material is deteriorating under loading. Therefore, the *FI* can be used as a common cracking index for all these three test methods.

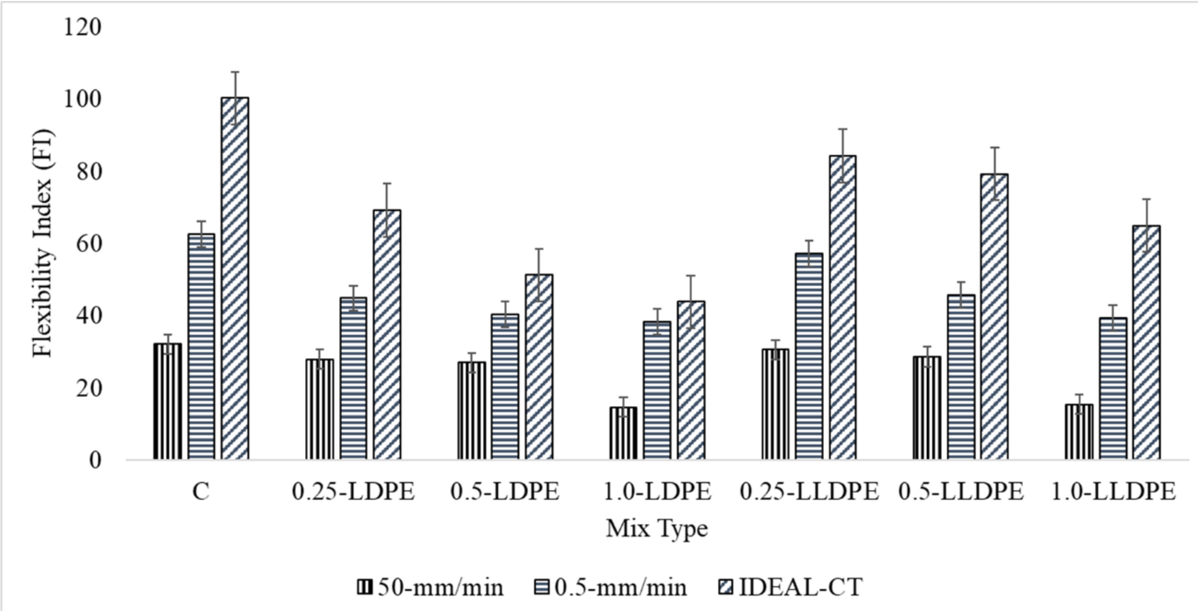

Figure 3.6 Variation of FI with the test methods

Table 3.3 Ranking of mixes based on FI

Test Method	Rank						
	1	2	3	4	5	6	7
IFIT	C	0.25-LLDPE	0.5-LLDPE	0.25-LDPE	0.5-LDPE	1.0-LLDPE	1.0-LDPE
L-SCB	C	0.25-LLDPE	0.5-LLDPE	0.25-LDPE	0.5-LDPE	1.0-LLDPE	1.0-LDPE
IDEAL-CT	C	0.25-LLDPE	0.5-LLDPE	0.25-LDPE	0.5-LDPE	1.0-LLDPE	1.0-LDPE

3.5.5.2 ***Fracture Energy (G_f)***

One of the important fracture properties evaluated in cracking test methods is the G_f of the specimen. The G_f is calculated by determining the area under the load-displacement curve. In this study, G_fs were calculated for all mixes using IFIT, L-SCB and IDEAL-CT tests. Figure 3.7 shows the average G_f of all seven mixes. Overall, G_f was found to increase with an increase in the plastic content. Tensile strength of plastic fibers might have contributed to this phenomenon.

Both IFIT and L-SCB were found to show a similar trend for all mixes. However, IDEAL-CT was found to show a slightly different trend. In IFIT and L-SCB, determination of G_f involves a notch of known size and shape. On the contrary, the IDEAL-CT specimens did not have any notch. The LEFM, the fracture mechanics used in IFIT, and IDEAL-CT tests use Mode-I stress intensity factor (requires a notch in the specimen). Also, the G_f is specimen size-dependent parameter (AASHTO 2022d). Therefore, using *FI* as a common cracking resistance index would be more reasonable than using G_f.

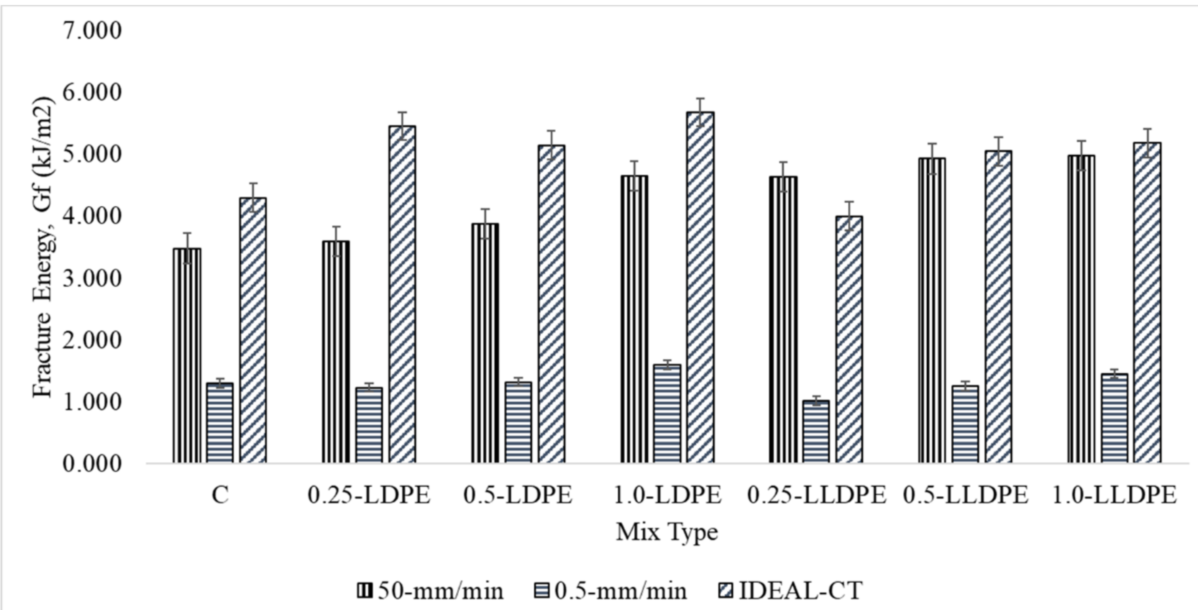

Figure 3.7 Variation of fracture energy with test methods

3.5.6 **Effect of Loading Rate and Notch Depth**

3.5.6.1 ***Strain Energy at Failure (SEF)***

To evaluate the effect of loading rate and notch depth, the strain energy at failure was determined for all the notch depths in both loading rates (i.e. 50-mm/min and 0.5-mm/min). Variations of SEF with notch depths and loading rates of all seven mixes are presented in Figure 3.8. The SEF was found to decrease with an increase in the notch depths and loading rates for all seven mixes. The low work of fracture required to initiate crack at higher notch depth might have contributed to this phenomenon (Spiegelberg et al. 2016). Also, SEF increased with an increase in the plastic contents at both loading rates which indicates more energy was required for initiating cracks in the plastic-modified mixes. However, the rate of change was found to vary from mix to mix. For example, for an increase in notch depth from 15-mm to 25.4-mm the SEF decreased to 37.4% and 53.6% for control and 0.25-LLDPE mixes, respectively, at 50-mm/min loading rate. For IDEAL-CT, all mixes were found to show higher SEFs as compared to the two other test methods because of the specimen size dependency of SEFs. However, a similar trend was observed for all three test methods for all mixes.

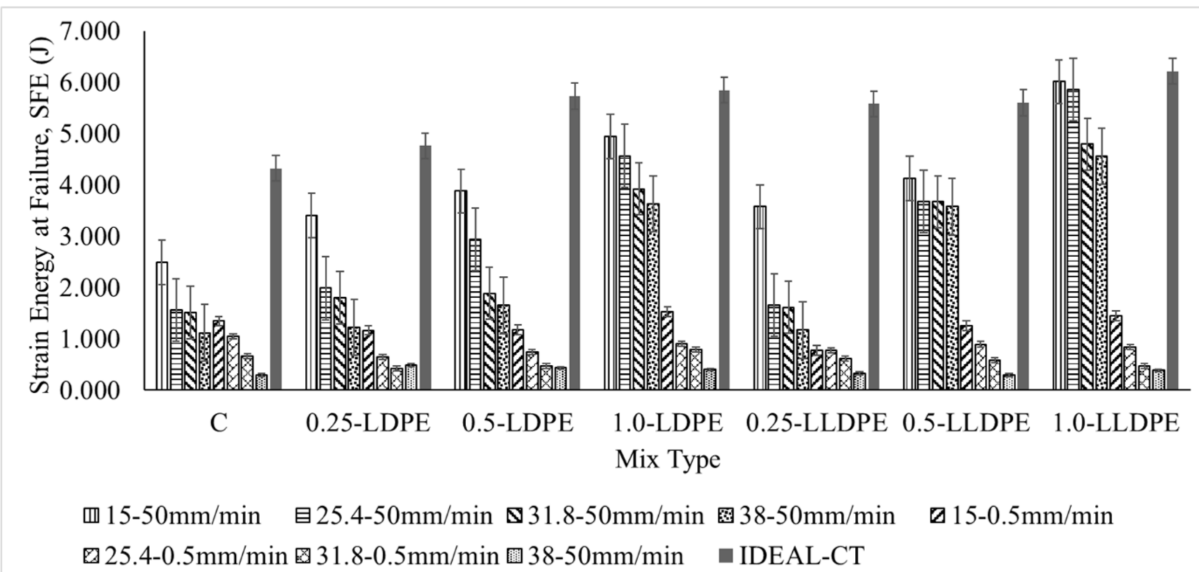

Figure 3.8 Variation of SEF with notch depth and loading rate

3.5.6.2 ***Critical Strain Energy Release Rate (Jc)***

To evaluate the effect of loading rates and notch depths, five different combinations of notch depths at each loading rate were used for calculating J_c-values. A summary of the combinations of notch depths is presented in Table 3.4. J_c-values were calculated for each combination and presented in Figure 3.9. shows the variations of J_c-value with loading rates and notch depths. The J_c-value was found to decrease with a decrease in the loading rate from 50-mm/min to 0.5-mm/min. This trend is valid for all seven mixes as evident from Figure 3.9. No proper trend was found for the rate of reduction of J_c-values for plastic modified mixes. Distribution of plastic particles inside the specimen and notch area could be responsible for this phenomenon. At higher loading rate (50-mm/min), higher fluctuations in J_c-values were observed with the notch depth combinations for LDPE-mixes. However, at slower loading rate (0.5-mm/min), a more consistent trend was found for all seven mixes as evident from Figure 3.9. As shown in Figure 3.9, the effect of notch depth was found as less distinguishable at 0.5-mm/min as evident from the J_c-values of high plastic content mixes (i,e. 1.0-LDPE and 1.0-LLDPE). The probable reason behind this phenomenon could be the elastic component of a visco-elastic material becomes dominant at higher loading rates whereas viscous component become dominant in lower loading rates (Khan 2016).

Table 3.4 Notch depth combinations

Combination ID	Notch Depths (mm)	Loading Rate (mm/min)
C1-50mm/min	15, 25.4 and 31.7	
C2-50mm/min	15, 25.4 and 38	
C3-50mm/min	15, 31.7 and 38	50
C4-50mm/min	25.4, 31.7 and 38	
C5-50mm/min	15, 25.4, 31.7 and 38	
C1-0.5mm/min	15, 25.4 and 31.7	
C2-0.5mm/min	15, 25.4 and 38	
C3-0.5mm/min	15, 31.7 and 38	0.5
C4-0.5mm/min	25.4, 31.7 and 38	
C5-0.5mm/min	15, 25.4, 31.7 and 38	

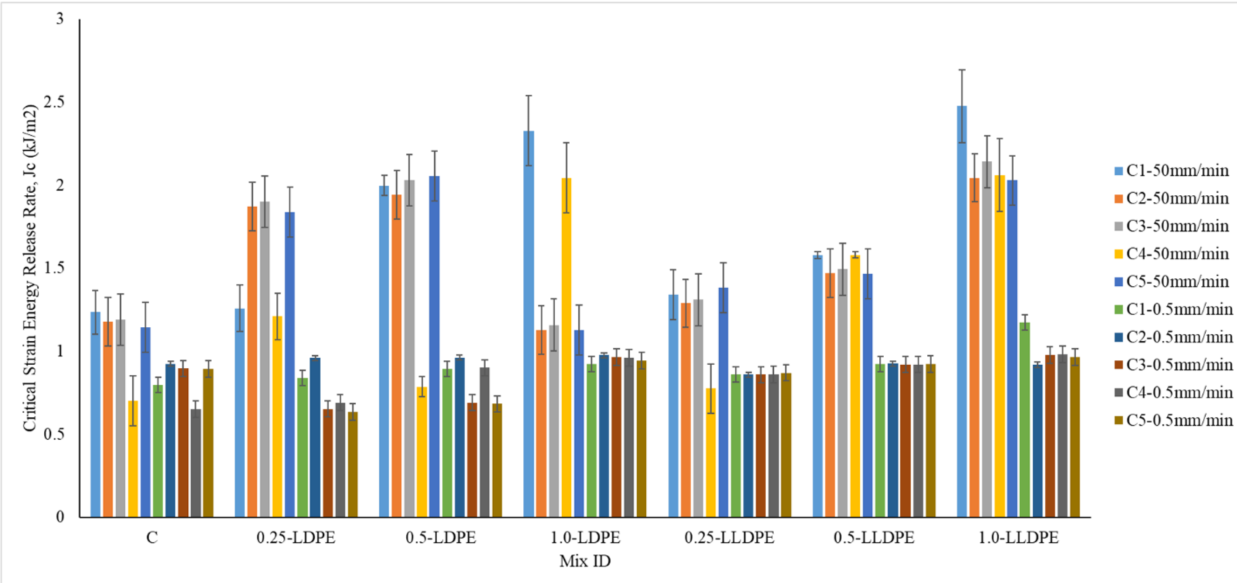

Figure 3.9 Variation of J_c-value with notch depth and loading rate

3.5.6.3 ***Flexibility Index (FI)***

Figure 3.10 shows the variations of *FI* with notch depths and loading rates. It was found that FI increased with an increase in the notch depth. At a higher notch depth, less energy was required to break the specimen. Highest *FI* values were observed for all mixes at 38-mm notch depth. Very large FI values at 38-mm notch depth implies the instability of test specimens. Similar trends were also observed for fracture energies at different notch depths and will be discussed in the subsequent section. Also, it was found that the *FI* increased with a decrease in the loading rate as shown in Figure 3.10. This is primarily caused by the flatter load-displacement curve for lower loading rate and the post-peak slope as discussed in the previous section. Moreover, *FI* decreased with an increase in the plastic contents. This trend is valid at all loading rates and notch depths. Higher stiffness of plastic particles might have resulted in stiffer mixes as compared to the control one.

To select a suitable loading rate for determining *FI* of plastic-modified mixes, control mix, 0.25-LDPE and 0.5-LLDPE mixes were tested for 2 more loading rates (i, e., 5- and 10-mm/min). These mixes were selected based on the ODOT BMD Criteria (ODOT 2023). The *FI*s of these three mixes were determined at four loading rates namely, 0.5-, 5-, 10- and 50-mm/min. Figure 3.11 shows the variations of *FI* with loading rates. It was observed that variations in *FI* were more distinguishable at slower loading rates. The *FI* values slowly become asymptomatic at higher loading rates. The probable reason behind this phenomenon could be the elastic component of a visco-elastic material becomes dominant at higher loading rates whereas viscous component becomes dominant in lower loading rates (Khan 2016).

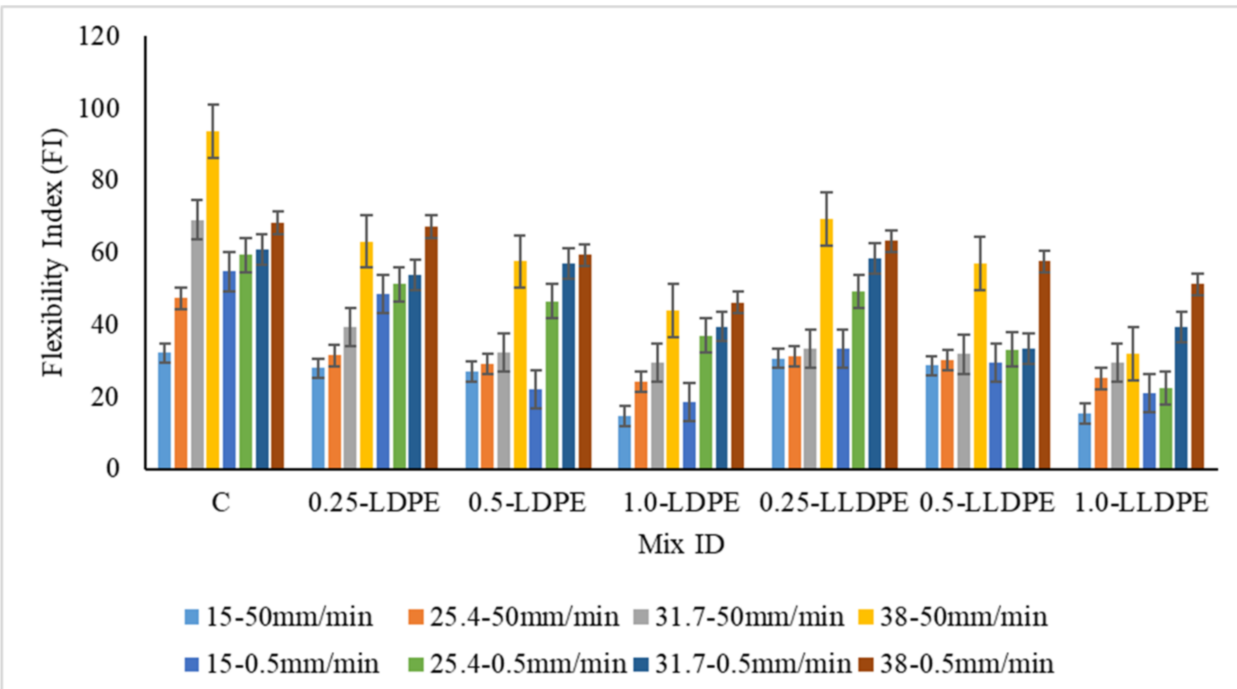

Figure 3.10 Variation of *FI* with notch depth and loading rate

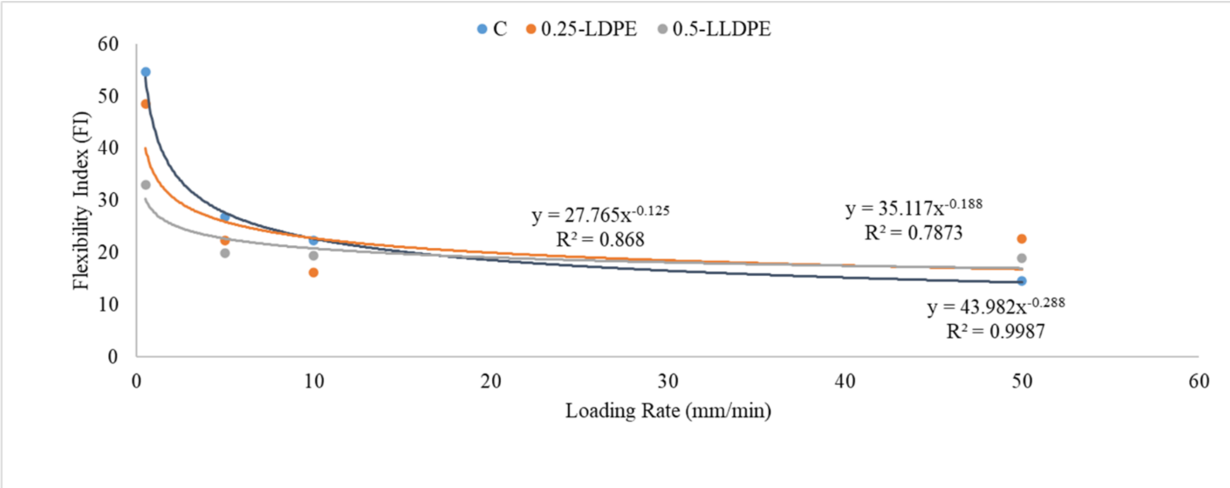

Figure 3.11 Variation of *FI* with loading rate

3.5.6.4 ***Fracture Energy (G_f)***

Figure 3.12 shows the variations of $G_{f\ with}$ notch depths and loading rates. It was found that fracture energy decreased with an increase in the notch depth and decrease in the loading rate. This is primarily caused by the larger area of the load-displacement curve for higher loading rate as discussed in the previous section (Khan 2016). Also, less energy is required to break a specimen having a larger notch depth as discussed in the previous section. Furthermore, the rate of change of fracture energy was found to be steeper for mixes with higher plastic content. Therefore, loss of plastic particles from mastic due to notching might have contributed to the loss of fracture energies for higher plastic content mixes.

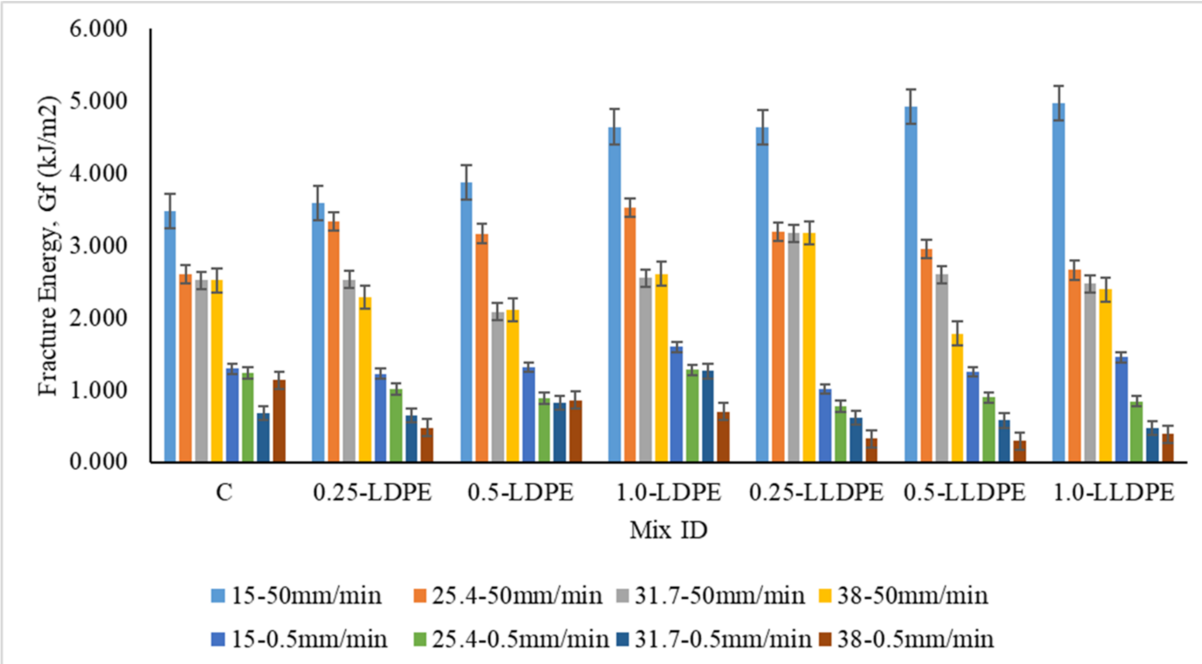

Figure 3.12 Variation of G_f with notch depth and loading rate

3.6 CONCLUSIONS

In this study, the fracture properties of seven plastic-modified mixes (0%, 0.25%-LDPE, 0.5%-LDPE, 1.0%-LDPE, 0.25%-LLDPE, 0.5%-LLDPE and 1.0%-LLDPE) were evaluated using three commonly used fracture test methods, namely IFIT, L-SCB and IDEAL-CT. Effects of both loading rate and notch depth on the fracture properties were examined. These mixes were ranked based on the cracking indices used in the three aforementioned test methods. The specific conclusions of this study are listed below:

- The IFIT, L-SCB and IDEAL-CT tests showed that the ranking of mixes for cracking resistance is different for different test methods.
- The post-peak behavior had a significant influence on the ranking of cracking performance of the mixes. The L-SCB test is much conservative in design. It only deals with the load-displacement curve up to crack initiations and does not account for the post-peak behavior. Situations where slower traffic loadings are expected, plastic-

modified mixes can be expected to provide superior performance as compared to the control mix as evident by the Jc-values from the L-SCB tests. The IDEAL-CT test is a more simplified test from practical considerations. It does not consider the post-peak slope at the inflection point, instead considers the post-peak slope at 75% of peak load. However, the post-peak behavior is well captured by the IFIT test.

- The results indicated that the *FI* can be used as a common cracking index for all these three test methods as it showed a common trend in all cases. However, based on the results of this study and from the fracture mechanics point of view, IFIT was found to be a good method for evaluating the cracking performance of asphalt mixes.
- The fracture parameters, namely SEF, J_c-value, *FI* and G_f, with loading rate and notch depth are influenced by the plastic contents, as evident from this study. At slower loading rate, the L-SCB was found to provide more consistent results as evident from the effect of loading rate and notch depths on SEF and J_c-value. Variations in *FI* with loading rates are more distinguishable at slower loading rates and *FI* become asymptomatic at higher loading rates. Therefore, *FI* may be a better parameter at higher loading rates and J_c-value may be a better parameter at slower loading rates regardless of plastic contents. The IDEAL-CT test, on the other hand, is a better option for rapid testing and assessment of cracking resistance.

The findings of this study are based on one control mix and two different plastic types. Expanding the database by including more plant and laboratory mixes is recommended for future work. Also, the incorporation of Finite Element Analysis (FEA) would be more helpful in understanding these test methods.

CHAPTER 4 AGING OF POST-CONSUMER RECYCLED (PCR) PLASTIC-MODIFIED ASPHALT MIXES AND BINDERS: A LABORATORY STUDY‡

ABSTRACT

Oxidative aging significantly influences the performance of asphalt mixes over time. This aging process becomes more critical when the mixes contain recycled materials, such as reclaimed asphalt pavement, recycled roofing shingles, and waste plastics. Until now, the aging of asphalt mixes containing waste plastics has not been studied widely. This study aims to investigate the aging behavior of two types of post-consumer recycled plastic-modified asphalt mixes, namely Low-Density Polyethylene (LDPE) and Linear Low-Density Polyethylene (LLDPE). To this end, asphalt mixes without plastic (control mix) and with (LDPE and LLDPE) were prepared in the laboratory and subjected to three aging conditions, namely short-, medium- and long-term aging. Mechanical tests, including Indirect Asphalt Tensile Cracking Test (IDEAL-CT) and Dynamic Modulus (DM) tests, were conducted to evaluate the effect of aging on cracking resistance and stiffness. Additionally, binders were extracted and recovered from all aged mixes, and the extracted aggregates were visually inspected. The effect of aging on the rheological properties of the recovered binder was assessed using Rotational Viscosity (RV), Dynamic Shear Rheometer (DSR), and Multiple Stress Creep Recovery (MSCR) tests. The impact of aging was further examined by identifying changes in chemical functional groups using Fourier Transform Infrared Spectroscopy (FTIR) tests. Finally, AASHTOWare Pavement ME Design simulations were used to evaluate the effect of aging on the field performance. This study provides a comprehensive framework for evaluating the aging characteristics of plastic-

‡ This chapter has been submitted to the Transportation Geotechnics under the title “Aging of Post Consumer Recycled (PCR) Plastic-Modified Asphalt Mixes and Binders: A Laboratory Study.” The current version has been formatted for this dissertation.

modified mixes through mechanical, rheological, and chemical testing, as well as structural simulations.

Keywords: Aging, Post-Consumer Recycled (PCR) Plastics, Low-Density Polyethylene (LDPE), Linear Low-Density Polyethylene (LDPE), Stiffness, Rheology, Fourier Transform Infrared Spectroscopy (FTIR).

4.1 INTRODUCTION

The utilization of waste plastics in asphalt mixes has gained popularity worldwide in recent years. The addition of plastic has been found to improve the performance properties of asphalt mixes (Khan et al., 2009; Angelone et al., 2016; Lastra-González et al., 2016; Ghos et al., 2022a). Most of the existing studies were focused on evaluating the volumetric properties and performance of plastic-modified asphalt mixes at short-term aging condition. Only a limited number of studies on the long-term aging of plastic-modified asphalt mixes could be found in the literature (Kumar et al., 2021; Mashaan et al., 2021; Radeef et al., 2022). For example, Mashaan et al. (2021) evaluated the effect of 20 hours of Pressure Aging Vessel (PAV) aging on the performance of Polyethylene Terephthalate (PET)-modified asphalt binder. The PET-modified binder was found to exhibit a lower Aging Index (AI) compared to the neat binder. Radeef et al. (2022) assessed the impact of aging on the fracture properties of waste plastic-modified asphalt mixes. In that study, 1% Low-Density Polyethylene (LDPE) (by the weight of the total mix) was used to modify the control mix using the dry process. Both control and LDPE-modified mixes were subjected to long-term laboratory aging by keeping in an oven at 85°C for 120 hours. The Indirect Tensile Asphalt Cracking Test (IDEAL-CT) was performed on short- and long-term aged asphalt mixes to evaluate the fracture properties. The addition of LDPE resulted in higher fatigue cracking resistance after long-term aging compared to the control mix (Radeef et al.

2022). However, the increase in aging resistance mechanism due to plastic addition was not fully understood from the IDEAL-CT. Therefore, more studies are needed to characterize the long-term aging performance of asphalt mixes containing recycled plastics. The current study aims to evaluate the impact of long-term aging on asphalt mixes containing two different types of Post-Consumer Recycled (PCR) plastics, namely LDPE and Linear Low-Density Polyethylene (LLDPE).

Performance of asphalt mixes deteriorates as they age over time. Aging increases the stiffness of asphalt mixes and consequently reduces their cracking resistance (Paul et al., 2016; Saleh et al., 2020; Ziari et al., 2020). According to Lee et al. (2009), the aging process of asphalt mixes can be divided into three phases. Phase 1 involves the aging of original binder during transporting, storing, and handling prior to mixing with the aggregates. Phase 2 refers to the aging of the asphalt binder during mix production and construction. Phase 3 involves aging of the asphalt binder/mix during its service life (Lee et al., 2009). In general, the aging of asphalt has been studied using two approaches, namely laboratory aging of asphalt binder and laboratory aging of asphalt mixes (Saleh et al., 2020). Laboratory aging of asphalt binders involves aging of the binder using the Rolling Thin Film Oven (RTFO) and the PAV (AASHTO 2016a; AASHTO 2017c). The RTFO aging simulates short-term aging, i.e., the aging of asphalt binder during mix production and compaction (AASHTO 2017c). PAV aging simulates the oxidative aging of asphalt binder after 5 to 10 years of service (AASHTO 2016a). According to Domke et al. (2000), Jin et al. (2011), and Saleh et al. (2020), studies on binder aging do not account for the effects of mineral aggregates on the oxidation mechanism and, consequently, do not accurately reflect asphalt mix aging. The study of asphalt mix aging involves aging in a forced draft oven following the AASHTO R 30 (AASHTO 2015) method. According to the AASHTO R30 method short-term aging is simulated by conditioning the asphalt mix at 135°C for 4 hours. Long-term aging involves conditioning a compacted specimen at 85°C for 120 hours (AASHTO 2015). Several studies have expressed concern about this long-term aging procedure for compacted specimens due to its inability to simulate aging at pavement depths and have suggested aging loose mixes before compaction (Kim et al., 2018; Newcomb et al., 2019; Saleh et al., 2020). Therefore, in the current study, loose mixes were conditioned for long-term aging before compaction. Additionally, a hybrid approach was used by integrating the aging of asphalt mixes with performance testing, as well as the extraction and recovery of binders from the aged mixes for rheological and chemical characterization.

Several studies have been conducted to understand the effects of aging on asphalt mix properties (Baek et al., 2012; Islam et al., 2015; Paul et al., 2016; Saleh et al., 2020; Ziari et al., 2020). For example, Baek et al. (2012) evaluated the effect of aging on the Dynamic Modulus (DM) and fatigue properties of asphalt mixes. In that study, asphalt mixes were aged at four different levels, and DM tests, constant crosshead rate tests, and cyclic fatigue tests were performed to evaluate the viscoelastic properties of the aged asphalt mixes. A significant increase in stiffness and a decrease in fatigue cracking resistance after aging were reported (Baek et al., 2012). Islam et al. (2015) investigated the effects of asphalt aging using the Indirect Tensile Strength (ITS) test. The ITS tests were conducted on compacted specimens after varying the aging time. An increase in ITS and a decrease in flow number with aging were reported (Islam et al., 2015). Ziari et al. (2020) evaluated the effects of different aging conditions on the fatigue life of asphalt mixes. In that study, four-point bending beam tests were conducted on both aged and unaged samples, and a reduction in fatigue cracking resistance with aging was reported (Ziari et al., 2020). In recent years, IDEAL-CT has been gaining popularity among the asphalt agencies and industries due to its simplicity in sample preparation, testing and time efficiency. Therefore, in the current study used the IDEAL-CT test to evaluate the fatigue cracking resistance of plastic-modified asphalt mixes before and after laboratory aging.

Generally, degree of aging of asphalt binders are determined using the rate of change of rheological properties, namely viscosity, complex modulus (G*) and phase angle (δ) (Zhao et al. 2016; Zhang et al. 2017; Hu et al. 2016), and chemical functional groups such as sulfoxide index, carbonyl index and butadiene index (Hou et al. 2018a; Hou et al. 2018b; Zhang et al. 2018; Zhang et al. 2011b) before and after aging. Wang et al. (2020) suggested using a Change Rate (CR) parameter for determining the degree of aging of aged binder. The CRs for viscosity, G*, δ, rutting parameter (G*/sinδ), and parameters from Bending Beam Rheometer (BBR) tests (creep stiffness and stress relaxation) were calculated using Equation 4.1. In that study, the CR value for δ was recommended as the most favorable indicator for evaluating the degree of aging (Wang et al. 2020).

$$CR\ (\%) = \frac{Parameter\ of\ aged\ sample - Parameter\ of\ unaged\ sample}{Parameter\ of\ unaged\ sample} \times 100 \qquad (4.1)$$

Kumar et al. (2021) proposed an Aging Index (AI) for evaluating the degree of aging of plastic-modified asphalt binder. The degree of aging was determined by calculating the AI using Equations 4.2. AI was calculated based on DSR-based G*, δ and non-recoverable creep compliance (J_{nr}). A lower value of AI represents a lower susceptibility to aging (Kumar et al. 2021).

$$AI = \frac{\text{Parameter}\ in\ \text{Un}aged\ Condition}{Parameter\ in\ Aged\ Condition} \qquad (4.2)$$

Several studies have investigated asphalt aging using advanced chemical technologies, namely spectrophotometry, fluorescence spectroscopy, Atomic Force Microscopy (AFM), Fourier Transform Infrared Spectroscopy (FTIR) and Gel Permeation Chromatography (GPC)

(Hou et al. 2018a; Hou et al. 2018b; Grosseger et al. 2018; Nazzal et al. 2015). Among these advanced technologies, FTIR is widely used to study aging of asphalt binders due to its sensitivity to chemical functional groups and easy operability (Zhang et al. 2019; Wang et al. 2020). The FTIR is able to detect changes in the type and content of chemical functional groups in the asphalt binder. Generally, carbonyl (C=O) and sulfoxide (S=O) functional groups are used for evaluating the degree of aging of asphalt binder because of their sensitivity to oxidative aging (Ouyang et al. 2006; Hou et al. 2018a; Wang et al. 2020). Using FTIR spectra, aging indices, namely Carbonyl Index (CI) and Sulfoxide Index (SI) are calculated as the ratio of the area of the functional group to the reference area. Differences in the referenced area can lead to significant differences in the aging indices. Wang et al. (2020) recommended using the CR value for functional group indices before and after laboratory aging to eliminate the error associated with the selection of referenced area.

A limited number of studies have addressed the structural performance of asphalt pavement after aging (Baek et al. 2012; Saleh et al. 2020). For example, Baek et al. (2012) evaluated the effect of aging on pavement structure using VECD-FEP++ software by incorporating an aging model developed in that study. Saleh et al. (2020) evaluated the effect of aging on pavement performance using FlexPAVE software. Both studies used Dynamic Modulus (DM) and Simplified Viscoelastic Continuum Damage (S-VECD) data before and after aging for the evaluations. The AASHTOWare Pavement ME Design (PMED) is a useful tool for predicting performance of pavement over its service life (Li et al. 2013; Kim et al. 2007; Ghos et al. 2022b). The PMED software requires the DM values of asphalt mixes only after short-term aging condition. The effect of aging is included in the prediction of pavement performance through the changes in the modulus values of asphalt mix over time (ARA 2004; Saleh et al.

2020). Therefore, in the current study PMED was used to simulate performance of plastic modified mixes on a typical pavement structure over a specific period of service life.

Based on these reviews and gap in the literature, the specific objectives of this study are:

- To study the impact of laboratory aging on the cracking performance of plastic-modified asphalt mixes produced using the dry process;
- To evaluate the impact of plastics on the rheological and chemical properties of asphalt binder;
- To compare the performance of plastic-modified mixes with those of the control mixes in structural level over the service life.

4.2 MATERIALS AND METHODS

Figure 4.1 shows the workflow diagram of this study. An asphalt mix with a Nominal Maximum Aggregate Size (NMAS) of 9.5-mm was designed as the control mix (0%-plastics). This mix was designed following the ODOT BMD Special Provision (ODOT 2023). The optimum binder content of this mix was determined as 5.6%. This mix was then modified using two different PCR plastics, namely, LDPE and LLDPE using the dry process. The optimum LDPE and LLDPE content were determined as 0.5% by the weight of aggregates based on the ODOT BMD Special Provision (ODOT 2023). Properties of these plastics, control mix, details of plastic mixing process and relative position of each mix in the BMD quadrant plot can be found in Chapter 2 (Ghos et al. 2022a).

In this study, both control and plastic-modified mixes were subjected to three different aging protocols, namely, short-, mid- and long-term oven aging conditions. These conditions were as follows:

a) Short-term Oven Aging (STOA): After mixing, loose mixes were aged for 2 hours at compaction temperature (149°C). The specimens were then compacted at 149°C.

b) Mid-term Oven Aging (MTOA): After mixing, loose mixes were placed in the oven for 4 hours at 135°C. Each mix was then heated at compaction temperature for another 30 minutes before compacting specimens.

c) Long-term oven aging (LTOA): After mixing, loose mixes were placed in the oven for 12 hours at 135°C. Then loose mixes were heated at compaction temperature for another 30 minutes and specimens were molded.

These aging protocols were selected based on the discussion with the ODOT personnel. The DM samples were prepared from mixes subjected to STOA. The DM test results were used to simulate pavement performance using PMED. For IDEAL-CT, unaged and aged loose mixes were compacted to prepare cylindrical specimens of 150-mm diameter and 62-mm height using a Superpave Gyratory Compactor (SGC). The IDEAL-CT tests were conducted in accordance with ASTM D8225 (ASTM 2019). In addition, asphalt binders were extracted and recovered from STOA, MTOA and LTOA conditioned mixes for evaluating rheological and chemical properties.

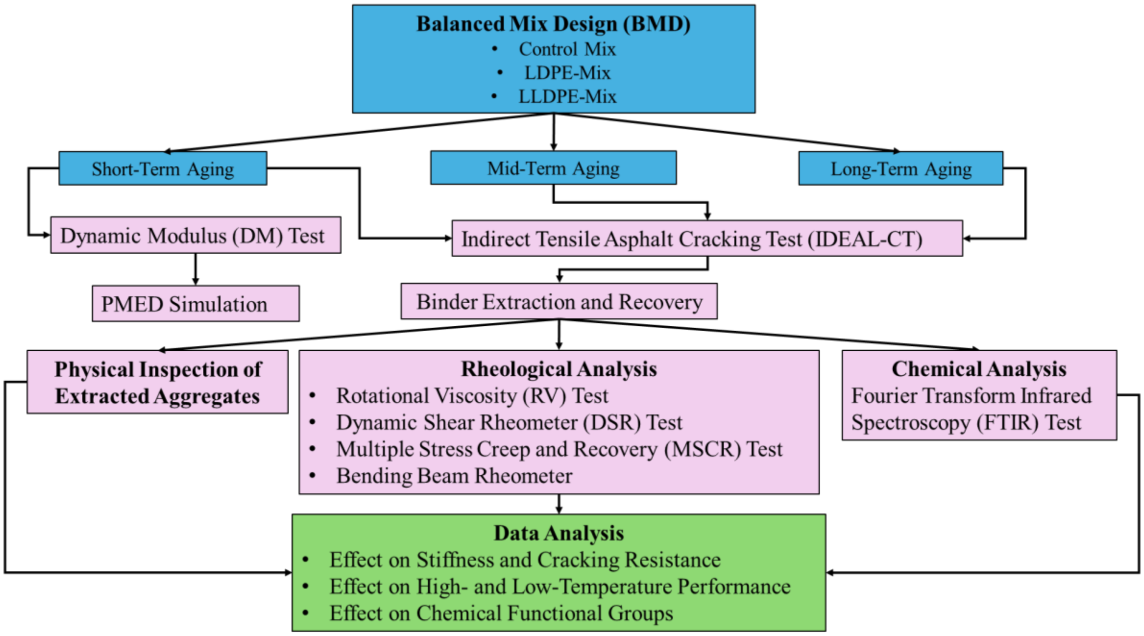

Figure 4.1 Workflow diagram

4.2.1 **Test Methods**

4.2.1.1 ***Indirect Tensile Asphalt Cracking Test (IDEAL-CT)***

The IDEAL-CT tests were conducted on asphalt mix specimens to determine the Cracking Tolerance Index (CT_{Index}), following the ASTM D 8225 (ASTM 2019) test method to evaluate the cracking resistance of the asphalt mixes. The IDEAL-CT tests were performed on the compacted specimens (150-mm in diameter and 62-mm height) by applying a vertical monotonic load at a rate of 50 mm/min until failure at room temperature (25^{o}C). An MTS loading system was used to collect the load and displacement data during testing. For each mix, four cylindrical specimens compacted at 7±0.5% air voids were tested to check repeatability. The load-displacement data were recorded for the entire duration of the test. The CT_{Index} was calculated from the load-displacement curve. Generally, a higher CT_{Index} indicates a better cracking resistance of a mix.

4.2.1.2 ***Dynamic Modulus (DM) Test***

The stiffness of the control and plastic-modified mixes was evaluated using the DM test. For this purpose, an SGC specimen of 150-mm diameter and 170-mm height was prepared for each mix subjected to STOA condition. Specimens were obtained by cutting 100-mm diameter and 150-mm high cores from the compacted specimens. The air voids of each core specimens were determined. The DM test was performed on the specimen having air voids of 7±0.5%. An Asphalt Mixture Performance Tester (AMPT) was used to conduct the DM test. The strain of the specimen during testing was measured using three Linear Variable Displacement Transducers (LVDTs) placed 120° apart. The test was conducted at four different temperatures, namely 4°C, 21°C, 37°C and 54°C with five different frequencies, namely 0.1 HZ, 1.0 Hz, 5 Hz, 10 Hz, and 25 Hz. Dynamic modulus (E*) and phase angles were calculated for each temperature and frequency combination. The data were then further processed to develop the E* master curve for the mixes. The E* values were used to model pavement structure in the PMED software.

4.2.2 **PMED Simulation**

A flexible pavement structure was modeled in the PMED software to carry an Annual Average Daily Truck Traffic (AADTT) of 2000. For this purpose, a 2.5-inch asphalt concrete layer was placed on the top of a 6-inch aggregate base with a Resilient Modulus (M_R) of 30,000-psi followed by a 6-inch A-6 subbase (M_R = 14,000-psi) and A-7-6 subgrade (M_R = 10,000-psi). The annual traffic growth rate was assumed to be 1.5%. In order to simulate the behavior of plastic-modified asphalt mixes, Level 1 inputs were used in the PMED. The required inputs were obtained from the aggregate gradation, volumetric analysis, rheological testing of the binder and DM tests. The Level 3 nationally calibrated values were used for the rest of the inputs in the PMED simulations. Performance of the pavement over 20 years of service life was simulated in terms of International Roughness Index (IRI), rutting, thermal cracking, top-down cracking and bottom-up fatigue cracking.

4.2.3 **Binder Extraction and Recovery**

The asphalt binder was extracted from the aged mixes using a centrifuge extractor in accordance with the AASHTO T 164 (AASHTO 2014) test method. For this purpose, asphalt mix samples were soaked with a solvent (Reagent Grade Trichloroethylene (TCE)) for approximately an hour in a centrifuge bowl to dissolve the binder. The solution with the binder was then separated from the aggregate using a centrifuge extractor. The process was repeated several times to extract all the binder from the mix, as detailed in the test method.

The extracted binder was recovered following the test method in ASTM D 5404M (ASTM 2021) using a rotary evaporator. The extracted solution from the centrifuge extractor was placed in a distillation flask connected with the rotary evaporator. The distillation flask was rotated at the temperatures and vacuum pressures in accordance with ASTM D5404M (ASTM 2021). Nitrogen flow was maintained inside the system throughout the process. At the end of the recovery, temperature was reduced, vacuum was withdrawn, and the binder was poured into a container for further testing. Naming conventions of these binders are presented in Table 4.1. For example, the LDPE-LTOA was used in this manuscript to denote the recovered binder from LDPE-modified mix after LTOA conditioning.

Table 4.1 Naming conventions of recovered binders

Acronyms	**Remarks**
C-ORG	Control binder in unaged condition
C-STOA	Binder extracted and recovered from the control mix after STOA conditioning
C-MTOA	Binder extracted and recovered from the control mix after MTOA conditioning
C-LTOA	Binder extracted and recovered from the control mix after LTOA conditioning
LDPE-STOA	Binder extracted and recovered from the LDPE-modified mix after STOA conditioning
LDPE-MTOA	Binder extracted and recovered from the LDPE-modified mix after MTOA conditioning
LDPE-LTOA	Binder extracted and recovered from the LDPE-modified mix after LTOA conditioning
LLDPE-STOA	Binder extracted and recovered from the LLDPE-modified mix after STOA conditioning
LLDPE-MTOA	Binder extracted and recovered from the LLDPE-modified mix after MTOA conditioning
LLDPE-LTOA	Binder extracted and recovered from the LLDPE-modified mix after LTOA conditioning

4.2.4 **Tests on Recovered Binders**

4.2.4.1 ***Rotational Viscosity (RV)***

In this study, impacts of aging on the viscosity of recovered binders were determined using the Rotational Viscosity (RV) tests following the AASHTO T 316-13 (AASHTO 2019). This test was used to measure the viscosity of both original and recovered binders at 135°C. The torque required to maintain a constant rotational speed of a cylindrical spindle while submerged in binder sample was used to measure the relative resistance to rotation. The torque and speed were used to determine the viscosity of binders in Pascal seconds (Pa.s).

4.2.4.2 ***Dynamic Shear Rheometer (DSR)***

The Dynamic Shear Rheometer (DSR) tests were conducted in accordance with AASHTO T 315 (AASHTO 2022e). The DSR test was conducted on recovered binders to determine complex modulus (G*), phase angle (δ), rutting factor (G*/ sin(δ)) as-well-as the High-Temperature Performance Grade (HPG). The G* is calculated as the ratio of shear stress and shear strain. Phase angle (δ) is the phase difference between applied stress and strain (Wang et al. 2020). In this study, all the binders were tested using the RTFO DSR template for evaluating the effect of aging. The reported HPG is the temperature at which the binder passed the specifications limits but failed at the next 6°C incremental test temperature. Interpolation between two temperatures was used to calculate the PG, "True" Grade (TG). The "True" Grade is also known as Continuous Grade (Tc).

4.2.4.3 ***Multiple Stress Creep Recovery (MSCR)***

In addition to PG grading, Multiple Stress Creep Recovery (MSCR) test was conducted on recovered binders following AASHTO T 350-14 (AASHTO 2017d). This test was used to determine the elastic response of the recovered binders under creep and recovery at two stress levels, namely 0.1kPa and 3.2kPa at 64°C. A 25-mm parallel plate was used with a 1-mm gap setting. The creep portion of the test lasts for 1 second followed by a recovery of 9 seconds. Ten creep and recovery cycles were tested at each stress level. Percent recovery (%R) and the Non-Recoverable Creep Compliance (J_{nr}) were calculated from the test data.

4.2.4.4 ***Bending Beam Rheometer (BBR)***

Bending Beam Rheometer (BBR) tests were conducted in accordance with AASHTO T 313 (AASHTO 2022a). BBR's flexural creep stiffness (S) and the rate of stress relaxation (m-value) and the Low-Temperature PG (LPG) were determined according to AASHTO T 313 (AASHT 2022a). A newly developed parameter called delta Tc (ΔTc) has been gaining attention in the research community. The ΔTc reflects cracking behavior affected by the durability related to aging of binder in an asphalt mix (AI 2019). This parameter (ΔTc) is an indicator of loss of relaxation properties. In this study, ΔTc was calculated from the BBR test results for binders recovered from control, LDPE- and LLDPE-modified mixes. For this purpose, Continuous Low-Temperature PG (Tc) for both stiffness (S) and creep rate (m) were determined exactly at their AASHTO M320 (AASHTO 2022b) limiting values using Equations 4.3 and 4.4, respectively. Further, ΔTc was calculated using Equation 4.5, which is simply the difference between the BBR's *Tc (S)* and *Tc (m)*.

$$Tc(S) = T_1 + \left(\frac{(T_1 - T_2)*(\log 300 - \log S_1)}{\log S_1 - \log S_2}\right) - 10 \qquad (4.3)$$

$$Tc(m) = T_1 + \left(\frac{(T_1 - T_2)*(0.3 - m_1)}{m_1 - m_2}\right) - 10 \qquad (4.4)$$

$$\Delta \mathrm{Tc} = Tc\ (S) - Tc\ (m) \qquad (4.5)$$

where,

$S_1 = creep\ stiffness\ at\ T_1, MPa$

$S_2 = creep\ stiffness\ at\ T_2, MPa$

$m_1 = creep\ rate\ at\ T_1$

$m_2 = creep\ rate\ at\ T_2$

$T_1 = temperature\ at\ which\ S\ and\ m\ passed, {}^0C$

$T_2 = temperature\ at\ which\ S\ and\ m\ failed, {}^0C$

Tc (S) = Continuous low temperature based on BBR's stiffness (S) value, °C;

Tc (m) = Continuous low temperature based on BBR's slope (m) value, °C.

ΔTc = Delta Tc, change in continuous grade sometimes called critical temperature, °C;

4.2.4.5 ***Fourier Transform Infrared (FTIR) Spectroscopy***

In this study, FTIR tests were performed on unaged (control only) binder and binders recovered from STOA, MTOA and LTOA conditioned mixes to determine the changes in chemical functional groups with aging. An Agilent Technologies 4300 Handheld FTIR spectrometer with Diamond Attenuated Total Reflection (ATR) mode was used to collect 1798 scans from each sample in the 650 to 4000 cm^{-1} range. For this purpose, binder samples were heated to 170°C to make them liquid enough to pour a drop on the Diamond ATR sensor. A total of six samples from each binder were tested using the FTIR to ensure repeatability. From the FTIR spectra, carbonyl (C=O) and sulfoxide (S=O) groups were identified for the tested binders. The carbonyl (C=O) and sulfoxide (S=O) groups correspond to peak ranges of 1690-1725 cm^{-1} and 1010-1043 cm^{-1}, respectively (Kumar et al. 2021). The FTIR data were used to calculate the CI and SI using Equations 4.6 and 4.7, respectively (Zargar et al. 2012; Kumar et al. 2021). Values of these indices increase with the aging of asphalt binder (Zargar et al. 2012; Kumar et al. 2021)

$$I_{C=0} = \frac{A_{1690-1725}}{\sum A} \tag{4.6}$$

$$I_{S=0} = \frac{A_{1010-1043}}{\sum A} \tag{4.7}$$

where,

A = area under the peak of a targeted range of FTIR spectra.

$$\sum A = A_{1010-1043} + A_{1350-1510} + A_{1535-1625} + A_{1678-1725}$$

4.3 RESULTS & DISCUSSION

4.3.1 **Testing on Asphalt Mixes**

4.3.1.1 ***Effect on Cracking Resistance***

Cracking resistances of Control, LDPE- and LLDPE-modified mixes were evaluated using the CT_{Index} values from the IDEAL-CT tests. A summary of the IDEAL-CT test results is presented in Figure 4.2. The error bars in Figure 4.2 indicate standard deviation from the average value. Four specimens were tested for each aging condition for all mixes. It was observed that the CT_{Index} values decreased with an increase in the aging time. A similar trend was observed for all three mixes. From Figure 4.2, it was observed that the control mix had better cracking resistance as compared to LDPE- and LLDPE-modified mixes. Higher stiffness of plastic-modified mixes might have contributed to this phenomenon. Also, the rate of change of CT_{Index} with aging is higher for the control mix than LDPE- and LLDPE-modified mixes as evident from Figure 4.2. For example, the rate of change of CT_{Index} from STOA to MTOA was found as 38.6, 35.4, and 22.1% for control, LDPE- and LLDPE-modified mixes, respectively. Partial coating of aggregates with plastics might have reduced the binder absorption of aggregates during MTOA conditioning, and consequently, left more effective binder in plastic-modified mixes. These extra effective binders in plastic-modified mixes might be responsible for the reduced rate of change of CT_{Index} for plastic modified mixes from STOA to MTOA. The rate of change of CT_{Index} from MTOA to LTOA was found as 59.1, 64.3, 70.2% for control, LDPE- and LLDPE-modified mixes, respectively. A portion of plastic particles melted and got mixed with the binder. These melted plastics increased the stiffness of plastic-modified mixes and resulted in a higher rate of change CT_{Index} for plastic-modified mixes as compared to that of the control mix. A more consistent cracking performance can be expected from LLDPE-modified mixes as indicated by the reduced rate of change of CT_{Index} values. A lower aging susceptibility of LLDPE and LDPE than control mixes might be responsible for this phenomenon. This result provides an insight regarding the long-term performance of plastic-modified mixes.

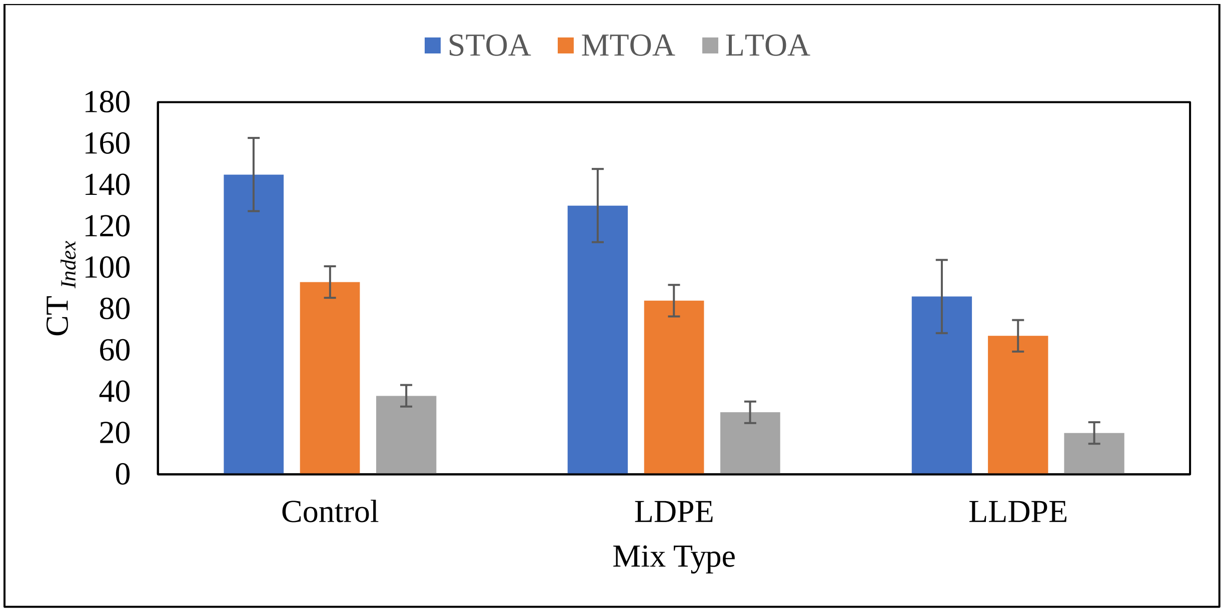

Figure 4.2 Effect of aging on CT_{Index}

4.3.1.2 ***Dynamic Modulus***

Figure 4.3 presents the E* master curves for all three mixes. The addition of plastic is found to shift the master curve to the left. For example, at a reduced frequency of 0.001-Hz, the master curve changes from 124-MPa to 268-MPa with the addition of LDPE. This is primarily caused by the addition of plastic contributing to the increased stiffness of the mix. A similar trend was observed for both LDPE- and LLDPE-modified mixes. However, the changes in stiffness were higher for the LLDPE-modified mix than the LDPE-modified mixes (Figure 4.3). Typically, asphalt mixes with high stiffness exhibit low resistance to cracking (Paul et al. 2016). Therefore, the control mix is expected to produce the highest resistance to cracking followed by the LDPE- and LLDPE-modified mixes. A similar trend was also observed from the IDEAL-CT results, as discussed in the previous section. Several previous studies have reported a similar increase in stiffness with the addition of plastic (see e.g., Moghaddam et al. 2014; Angelone et al. 2016; Ranieri et al. 2017). The dynamic modulus values of the asphalt mixes were also used in the PMED simulations. The results are discussed in the subsequent section.

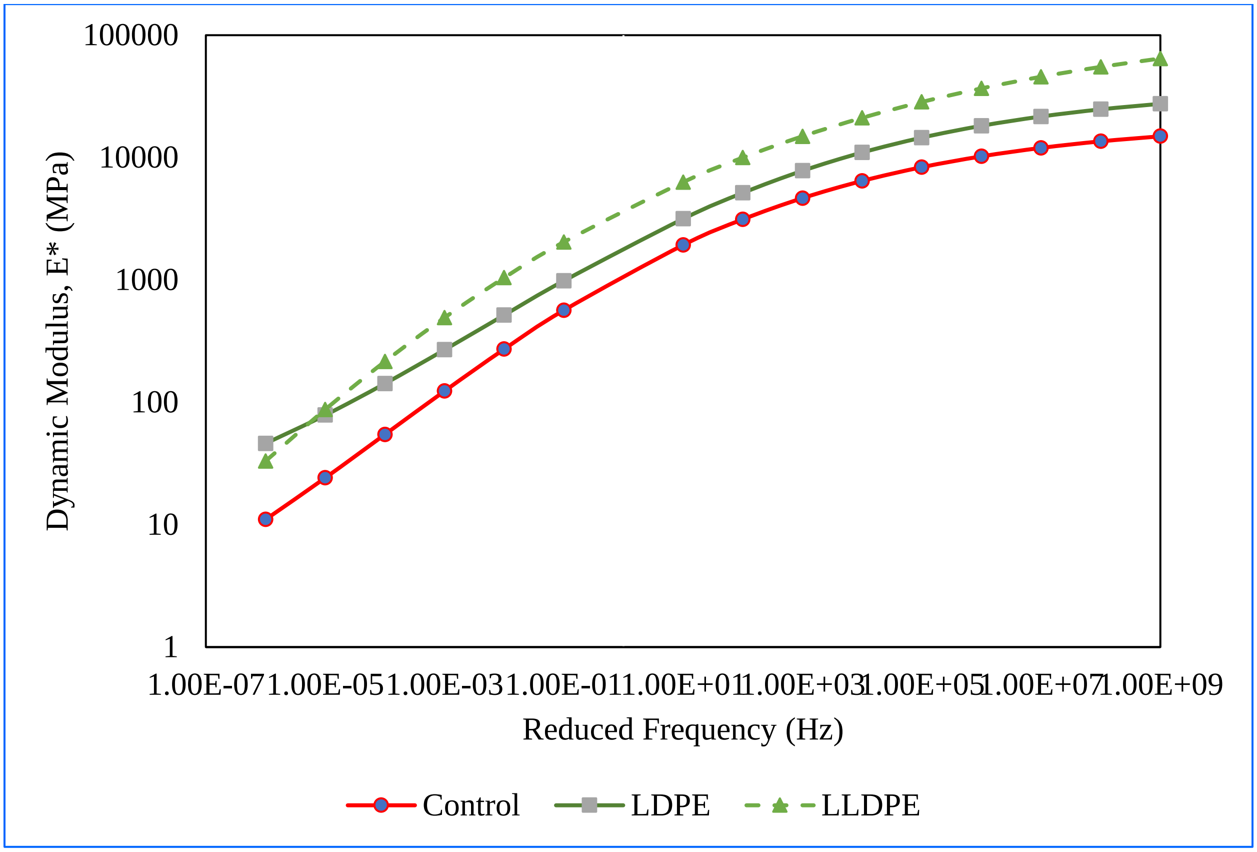

Figure 4.3 DM master curves at the reference temperature (21°C)

4.3.2 **Physical Inspection of Extracted Aggregates**

After extraction of binder from all mixes, extracted aggregates were carefully inspected visually. Figure 4.4 shows the photographic views of the extracted aggregates of the LDPE- and LLDPE-modified mixes after LTOA conditioning. For this purpose, aggregates were washed and air dried to avoid melting of plastic particles. As can be seen in Figure 4.4, a few clumps were formed with plastic and smaller aggregates. In this study, these clumps were named plastic rock. These plastic rocks were found on both LDPE- and LLDPE-modified mixes. These plastic rocks might have acted as coarse aggregates and increased the stiffness of the plastic-modified mixes. Plastic rocks were found in all three aging conditions. In addition, some partially plastic-coated aggregates and distorted plastic particles were found in the extracted aggregates, as shown in Figure 4.4. Therefore, it is evident that plastic particles do not melt fully when using the dry process in preparing mixes.

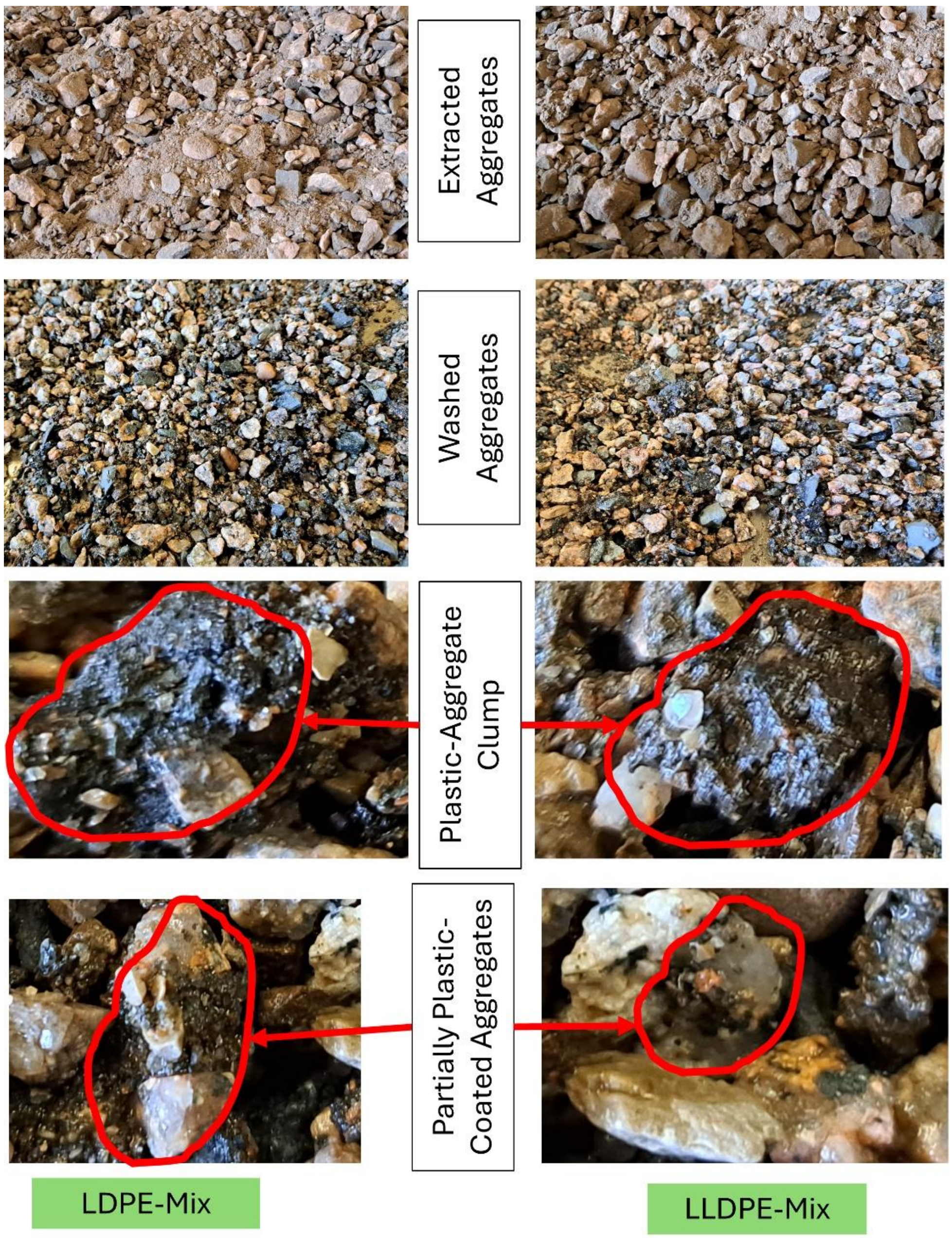

Figure 4.4 Extracted aggregates from plastic-modified mixes after LTOA

4.3.3 **Effect on Extracted Binders**

4.3.3.1 ***Effect on Viscosity***

Viscosity is one of the fundamental properties of asphalt binder which represents the fluidity at a certain temperature (Wang et al. 2020). Table 4.2 presents the variation of viscosities with aging for all extracted binders. The degree of aging of asphalt binder was calculated as the Change Rate of Viscosity (CRV), as suggested by Wang et al. (2020). From Table 4.2, viscosity of asphalt binder increased with an increase in the aging condition. For example, viscosity of control binder increased from 0.433 Pa.s to 1.379 Pa.s (219% increase) after LTOA conditioning. However, binders recovered from MTOA-conditioned mixes showed reduced viscosity as compared to recovered binder from STOA-conditioned mix. Therefore, conditioning of asphalt mixes at 149ºC for 2h can cause more aging than conditioning the mixes at 135ºC for 4h. A similar trend was observed for all three types of binders. As evident from Table 4.2, the highest viscosity was observed for the LLDPE-LTOA binder followed by the LDPE-LTOA and C-LTOA binders. The higher the viscosity, the lesser the workability of binder. Therefore, it would be prudent to use softening agents/ rejuvenators for reducing the viscosity while recycling plastic-modified asphalt mixes at the end of service life.

Table 4.2 Summary of viscosity tests

Binder Type	Viscosity (Pa.s)	Change Rate of Viscosity (CRV)
C-ORG	0.433	--
C-STOA	1.104	155
C-MTOA	0.792	83
C-LTOA	1.379	218
LDPE-STOA	0.742	71
LDPE-MTOA	0.929	114
LDPE-LTOA	2.421	459
LLDPE-STOA	1.384	219
LLDPE-MTOA	1.046	141
LLDPE-LTOA	3.800	777

4.3.3.2 ***Effect on High Temperature Rheological Properties***

The high-temperature performance of recovered binders from all three mixes was determined using the DSR test. In this study, DSR tests were conducted by following RTFO test protocols on recovered binders from STOA-, MTOA- and LTOA-conditioned mixes. The G*, δ and G*/sinδ of unaged binder, and binders recovered from control, LDPE- and LLDPE-modified mixes were determined at 64, 70, 76, 82 and 94ºC. The G* is an indicator of the resistance to permanent deformation of a binder when subjected to a repeated sinusoidal shear load. The δ indicates the ratio of elastic and viscous component of binder (Kumar et al. 2021). A higher G* and a lower δ is desirable for better high-temperature performance (Brown et al. 2009; Jin et al. 2021; Kumar et al. 2021). Table 4.3 presents the Change Rate of Complex Modulus (CRCM) and Change Rate of Phase Angle(CRPA) of binders recovered from control, LDPE and LLDPE-modified mixes. A significant increase in the G* was observed for plastic-modified mixes after LTOA conditioning as evident from the CRCM values in Table 4.3. For example, a CRCM of 2,152% indicates a 2,152% increase of G* for the LDPE- LTOA binder. The δ was found to decrease with an increase in aging as indicated by the CRPA values. For example, a CRPA value of -21.6% indicates a 21.6% decrease in the δ for LDPE-LTOA binder. Wang et al. (2020) recommended using CRPA values in evaluating degree of aging instead of CRCM. The absolute value of CRPA indicates the degree of aging. The lowest CRPA indicates the highest elastic behavior at high temperature. LLDPE-LTOA binder was found to show the highest degree of aging, as presented in Table 4.3.

Figure 4.5 shows the variation of rutting factor (G*/sinδ) with aging and temperature. Overall, the G*/sinδ decreased with an increase in the temperature for all binders. For example, the G*/sinδ of LDPE-LTOA binder decreased from 29.9- to 14.7-kPa with an increase in the temperature from 64 to 70ºC. Reduction in viscosity with an increase in temperature is responsible for this phenomenon. From Figure 4.5, the G*/sinδ was found to increase with an increase in aging time. For example, the G*/sinδ of recovered binders from LLDPE-modified mixes increased from 7.3 to 47.5-kPa at 64ºC for changing the aging from MTOA to LTOA. A similar trend was observed for all samples. Stiffening of binders with aging might have contributed to the increase in the G*/sinδ values. Also, MTOA conditioned samples were found to show a reduced G*/sinδ as compared to the STOA samples. This trend is true for all three types of binders. In addition, the highest G*/sinδ values were observed for the LLDPE-LTOA binder followed by the LDPE-LTOA and C-LTOA binders. Hence, the highest rutting resistance at high temperature can be expected from the LLDPE-modified asphalt mixes.

Figure 4.6 shows the variation of High-Temperature Continuous Grade (High-Tc) of binders recovered from control, LDPE- and LLDPE-modified mixes. The High-Tc value of control binder increased from 66 to 84ºC for conditioning the control mix using LTOA. The High-Tc values of the binders recovered from the LDPE- and LLDPE-modified mixes were found to be 86 and 91ºC, respectively, after LTOA conditioning. The presence of small amount of melted plastic particles in the binder (Vasudevan et al. 2010) might have increased the viscosity and hence increased the High-Tc value.

Table 4.3 Aging indices for complex modulus and phase angle

Binder Type	Change Rate of Complex Modulus (CRCM)	Change Rate of Phase Angle (CRPA)
C-STOA	461	-9.1
C-MTOA	256	-7.0
C-LTOA	1751	-20.7
LDPE-STOA	343	-9.0
LDPE-MTOA	424	-8.3
LDPE-LTOA	2152	-21.6
LLDPE-STOA	937	-13.6
LLDPE-MTOA	485	-9.5
LLDPE-LTOA	3362	-26.7

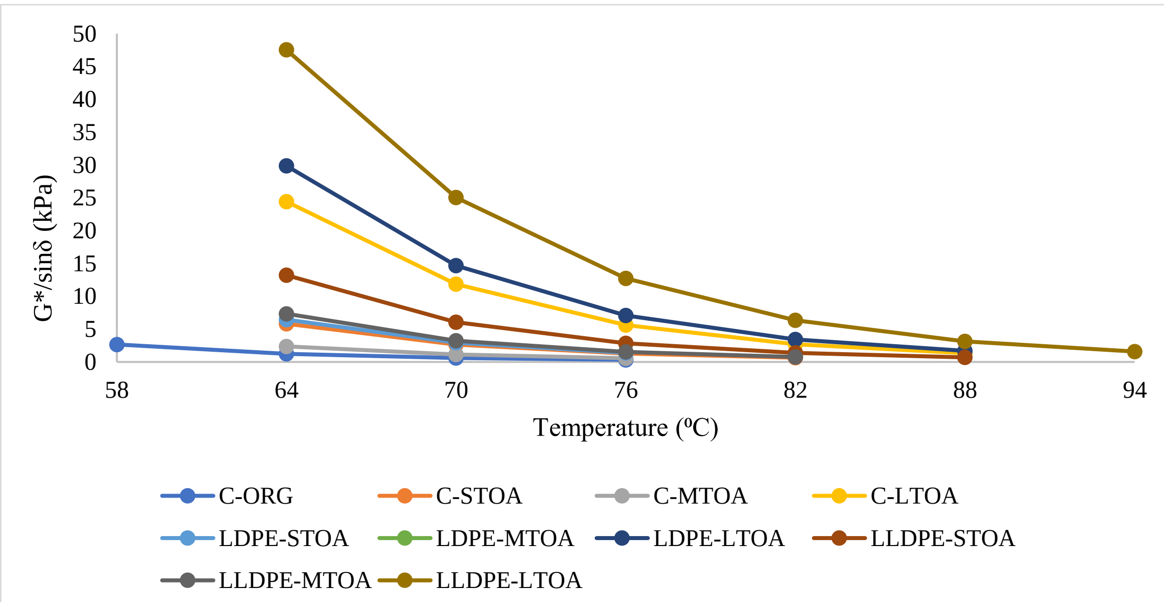

Figure 4.5 Variation of rutting factor with temperature and aging

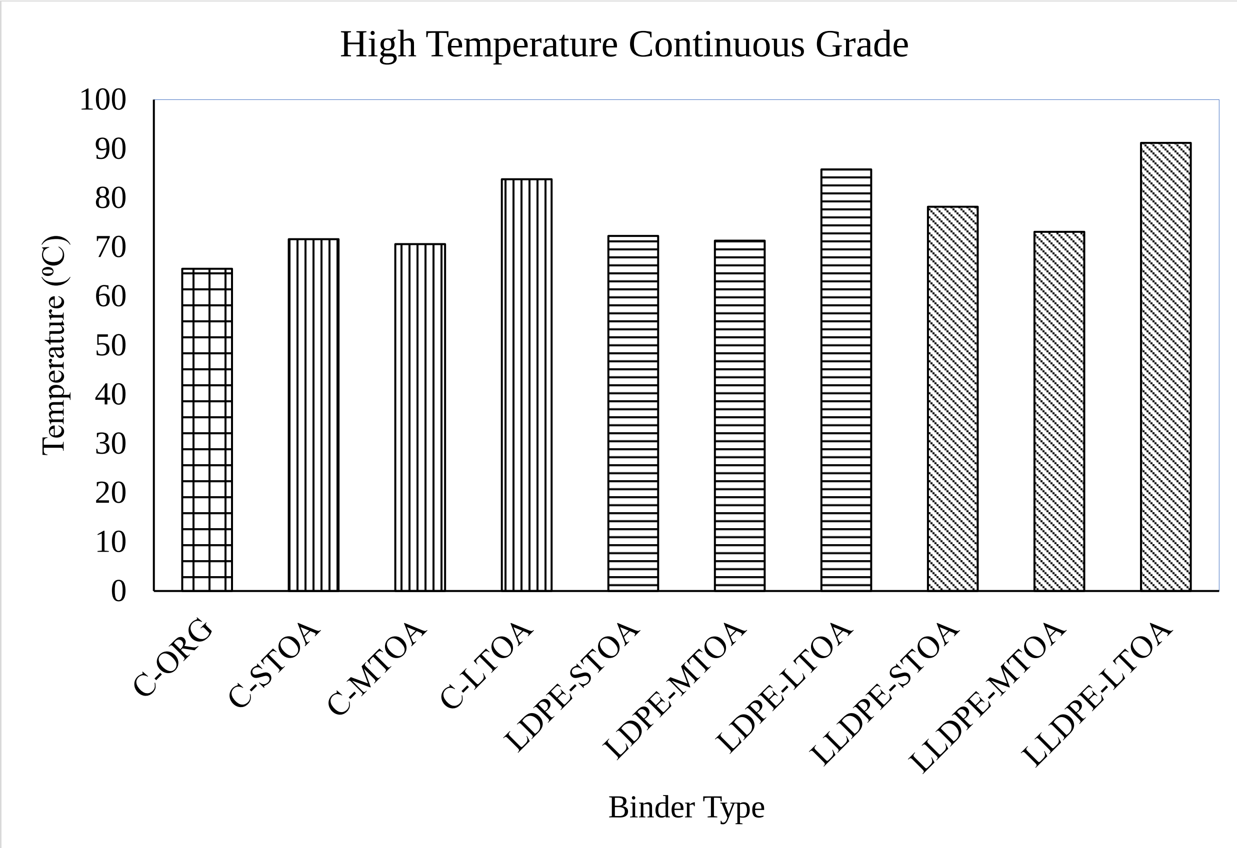

Figure 4.6 Variation of high temperature continuous performance grade with aging

4.3.3.3 ***Effect on Percent Recovery and Nonrecoverable Creep Compliance***

The percent recovery (%R) and Non-recoverable Creep Compliance (J_{nr}) were determined for all recovered binders from control, LDPE- and LLDPE-modified mixes using MSCR tests for all three aging conditions. The MSCR tests were performed following AASHTO T350 (AASHTO 2017d). A summary of the MSCR tests on the binders is presented in Table 4.4. The J_{nr} is an indicator of the resistance of asphalt binder to permanent deformation under repeated loads (AASHTO 2017d). A lower value of J_{nr} indicates better resistance to permanent deformation (Kumar et al. 2021). Overall, the J_{nr} value decreased after LTOA conditioning. Increase in stiffness due to aging is responsible for lowering the J_{nr} values (Kumar et al. 2021). In addition, binders recovered from plastic-modified mixes exhibited reduced J_{nr} values compared to the binder recovered from the control mix at the same aging condition. For example, the J_{nr} of the LLDPE-STOA binder was found to be 0.9159 which is lower than the C-STOA binder (1.2395). A similar trend was observed for all three aging conditions and both plastics. In addition, binders recovered from the MTOA-conditioned mixes were found to exhibit a higher J_{nr} value compared to that of the binders recovered from STOA-conditioned mixes binders. These results are in agreement with the RV and DSR results. The LLDPE-LTOA binder was found to show the lowest J_{nr} value indicating a superior rutting performance.

The %R-value from MSCR test indicates the elastic response and stress dependance of polymer modified and unmodified asphalt binder (AASHTO 2017b). Figure 4.7 shows the plot of %R and J_{nr} at 3.2-kPa at 64°C. According to AASHTO M332 (AASHTO 2017b), a point plotted on or above the reference line on the graph indicates that the asphalt binder is modified with an acceptable elastomeric polymer. Binders recovered from control, and LDPE- and LLDPE-modified mixes were found to fall under reference line, as shown in Figure 4.7. The results indicate no polymerization of binder with plastics during the aging process.

Moreover, the degree of aging of recovered binders from control, LDPE- and LLDPE-modified mixes were calculated in terms of Change Rate of Non-recoverable Creep Compliance (CRNC) using Equation 4.1, as suggested by Wang et al. (2020). The CRNC values were calculated as the percentage change of J_{nr} at 3.2-kPa with respect to that of the unaged control binder. Overall, the CRNC values increased with the aging, as presented in Table 4.4. However, binders recovered from MTOA-conditioned mixes were found to show less CRNC as compared to the binders recovered from STOA-conditioned mixes, indicating less aging occurred in MTOA-conditioned mixes. For example, The CRNC value of C-STOA binder was found as 60%, whereas CRNC of C-MTOA binder was found as 19%. Therefore, the C-STOA binder aged 41% more than the C-MTOA binder. Based on the CRNC values, addition of plastics in asphalt mixes was found to increase the aging sustainability at the same aging conditions. The difference between the degree of aging of binders recovered from control and plastic-modified mixes were evaluated by calculating ΔCRNC values. The ΔCRNC value was calculated as the difference between CRNC of recovered binders from control and plastic-modified mixes at the same temperature. For example, the ΔCRNC of LDPE-STOA binder was found as 10% meaning that the LDPE-modified asphalt mix aged 10% more than the control mix after STOA conditioning. This 10% extra contribution to aging might have come either from the stiffness of dissolved LDPE particles in the recovered binder or change in the chemical functional groups due to oxidation of LDPE. The oxidation of LDPE was further explained in the FTIR section. Also, a similar trend was observed for the recovered binders from LLDPE-modified mixes.

Additionally, binder performance grades at 64°C were determined from the MSCR tests following AASHTO M332 (AASHTO 2017b). Suitability of these binders for different traffic level was determined as follows:

S: Standard traffic situation with Equivalent Single Axel Load (ESAL) < 10 million and traffic speed > 70 km/h

H: Heavy traffic situation with ESAL ranging from 10-30 million and speed 20 to 70km/h

V: Very heavy traffic situation with ESAL>30 million or standing traffic (speed <20 km/h)

E: Extremely heavy traffic with ESAL>30 million and standing traffic (speed <20 km/h)

Overall, all binders are expected to sustain extremely heavy traffic after LTOA conditioning, as evident from Table 4.4. At the same aging conditions, binders recovered from plastic-modified mixes showed a superior performance as compared to the control binder. For example, for MTOA conditioning, the control binder was found to fall on S category whereas, binders recovered from the LDPE- and LLDPE-modified mixes were found to fall on H and V categories, respectively. Relatively, higher numbers of short branches in the LLDPE polymer chain gives superior tensile, impact and puncture strength as compared to LDPE (US Plastics Corp. 2024). For this reason, binders recovered from LLDPE-modified mixes were found to show higher stiffness and superior performance against rutting as compared to binders recovered from control and LDPE-modified mixes.

Table 4.4 Summary of MSCR tests

Sample	J_{nr} (1/kPa)	%R	CRNC (%)	ΔCRNC (%)	Traffic Category
C-STOA	1.2395	2.48	60	--	H
C-MTOA	2.5108	0.45	19	--	S
C-LTOA	0.3502	16.32	89	--	E
LDPE-STOA	0.9159	3.78	71	10	V
LDPE-MTOA	1.5285	1.73	51	32	H
LDPE-LTOA	0.1227	31.33	96	7	E
LLDPE-STOA	0.5857	7.9	81	21	V
LLDPE-MTOA	0.9325	4.06	70	51	V
LLDPE-LTOA	0.0388	52.05	99	10	E

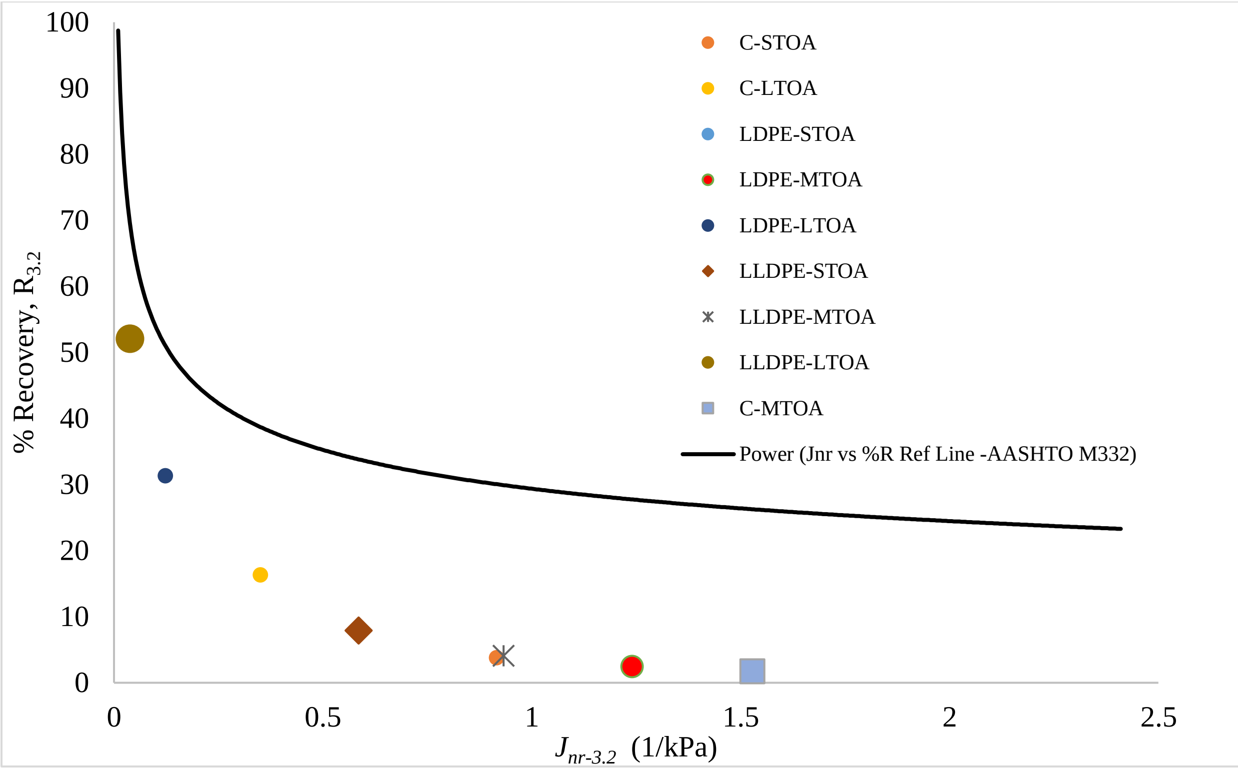

Figure 4.7 J_{nr} vs %R-value plot at 3.2-kPa in different aging conditions

4.3.3.4 ***Effect on Low-Temperature Performance***

Low-Temperature performance of recovered binders from control, LDPE- and LLDPE-modified mixes were evaluated using the BBR test. The BBR tests were only performed on binders recovered from LTOA-conditioned mixes since long-term aging is required for BBR test. A summary of the BBR test results is presented in Table 4.5. A higher stiffness and lower stress relaxation were observed for recovered binders from plastic-modified mixes. Therefore, care should be taken while incorporating plastics in asphalt mixes. A softening agent might be helpful for increasing the low-temperature resistance of plastic-modified mixes. It was observed that the aging bumped the LPG of binders recovered from plastic-modified mixes by one PG.

As previously stated, ΔTc can be used to evaluate the aging of binder in an asphalt mix. A positive ΔTc indicates the binder is governed by stiffness (S-control), whereas negative value indicates the binder is governed by creep rate (m-control) (AI 2019). In this study, all binders were found to be controlled by the m-value. As shown in Table 4.5, ΔTc decreased for binders recovered from plastic-modified mixes compared to the binder recovered from the control mix. The absolute value of ΔTc indicates the degree of aging of the binder (AI 2019). Therefore, the LLDPE-LTOA binder was found to be more susceptible to aging followed by the LDPE-LTOA and C-LTOA binders.

Table 4.5 Summary of the BBR data analysis

Sample ID	Flexural Creep Stiffness, S (MPa)	Creep Rate, m	ΔTc (ºC)	Tc (ºC)	LPG (ºC)
C-LTOA	83	0.33	-6.9	-26.3	-22
LDPE-LTOA	132	0.30	-7.5	-21.6	-16
LLDPE-LTOA	130	0.30	-11.3	-18.0	-16

4.3.3.5 ***Effect on Chemical Functional Groups***

Figure 4.8 shows the FTIR spectra of unaged (control only), binders recovered from the STOA-, MTOA- and LTOA-conditioned mixes. The carbonyl (wave no. 1690-1725 cm^{-1}) and sulfoxide functional groups (wave no. 1010-1043 cm^{-1}) were used for evaluating the aging behavior of the tested binders. Overall, an increase in the FTIR spectra was observed after aging for all binders in the sulfoxide (S=O) and carbonyl (C=O) groups, as shown in Figure 4.8. The changes in S=O group was found to be more distinctive after the STOA and MTOA conditioning than C=O group, as shown in Figure 4.8. Therefore, S=O region is more responsive in FTIR to aging. For quantitative analysis, both carbonyl ($I_{C=O}$) and sulfoxide indices ($I_{S=O}$) were calculated from the FTIR spectra, as presented in Figures 4.9 (a) and 4.9(b), respectively. Figure 4.9(a) shows the variation of $I_{C=O}$ with aging. Overall, $I_{C=O}$ increased with aging for all binders. A similar $I_{C=O}$ was found for binders recovered from mixes after the STOA and MTOA conditioning. For example, the changes in the $I_{C=O}$ of binders recovered from control mixes after the STOA and MTOA conditioning were found to be 2.8% and 2.6% with respect to C-ORG binder, respectively. Considering STOA and MTOA conditionings, the smallest $I_{C=O}$ was found for LLDPE-LTOA binder indicated superior resistance to aging. The $I_{C=O}$ was found to increase further for LTOA conditioning for all binders. The highest $I_{C=O}$ value was found for LDPE-LTOA binder. Formation of C=O on dissolved LDPE plastic particles in binder due to aging could have contributed to the increase of $I_{C=O}$ of LDPE-LTOA binder (Miranda et al. 2021). The lowest $I_{C=O}$ was found for the LLDPE-LTOA binder. Relatively more linear molecular structure with fewer branches of LLDPE, resulted in higher crystallinity and better resistance to oxidative aging as compared to LDPE (Fried 2014). Figure 4.9(b) shows the variation of $I_{S=O}$ with aging. A significant jump in the $I_{S=O}$ was observed from the unaged to STOA/MTOA conditioning for all binders. For example, the $I_{S=O}$ of control binder changed from 0.09 to 0.205 for unaged to the STOA conditioning, respectively. Therefore, a significant amount of sulfoxide groups formed during the mixing and compaction process. During the transition from the STOA/MTOA to LTOA conditioning, the formation of sulfoxide group was not as high as that of the unaged to STOA conditioning. The highest $I_{S=O}$ was observed for LDPE-LTOA binder. As previously noted, a higher thermal oxidative degradation tendency of LDPE could be responsible for significant increase in the $I_{S=O}$ of LDPE-LTOA binder. The lowest $I_{S=O}$ was observed for LLDPE-LTOA binder, as shown in Figure 4.9(b). According to Vasudevan et al. (2010), a certain amount of dry processed plastic melts and gets mixed with the binder in plastic-modified mixes. The LLDPE particles have more organized structures and can prevent penetration of oxygen and other degrading agents in LLDPE-LTOA binder (Hamid 2000; Fried 2014; Andrady

2015). Therefore, the LLDPE-LTOA binder can provide superior resistance to aging as compared to the C-LTOA and LDPE-LTOA binders.

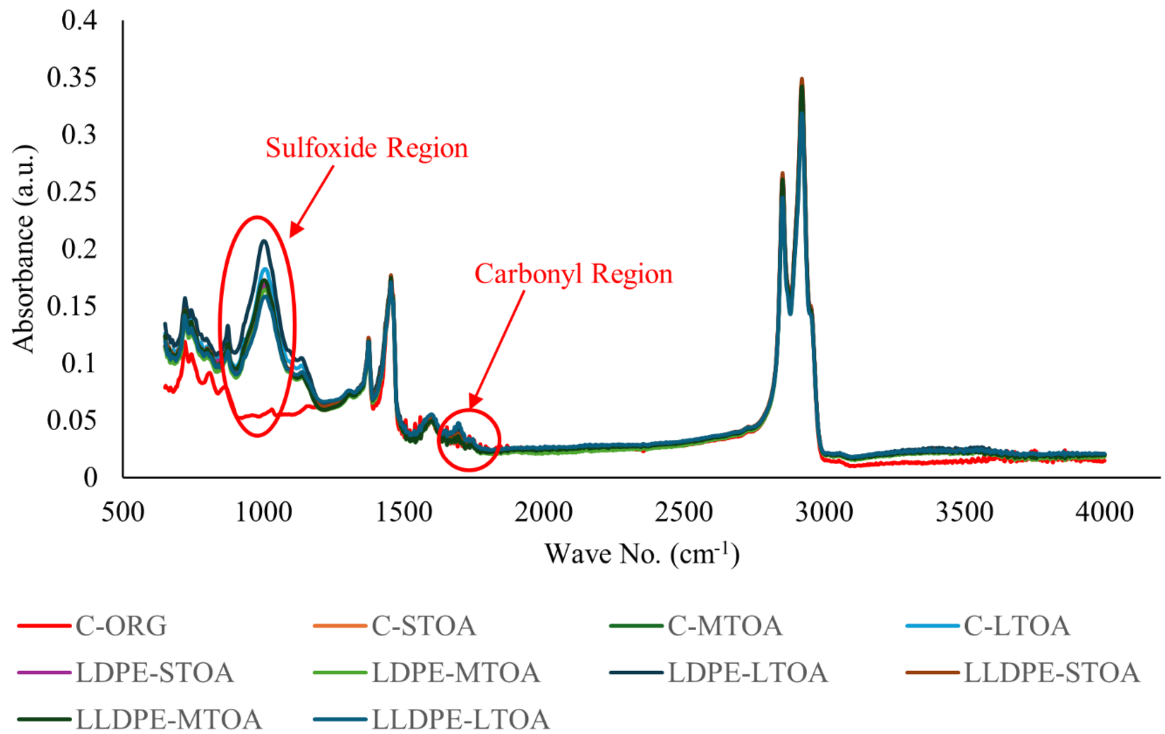

Figure 4.8 Relative plot of FTIR spectra in different aging conditions

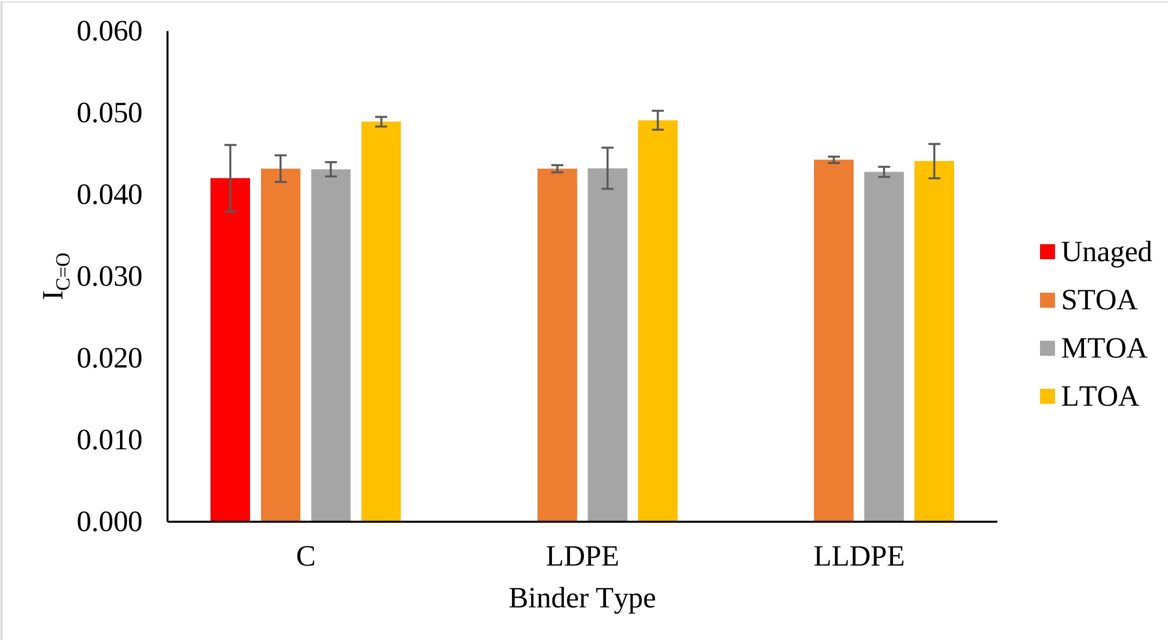

(a)

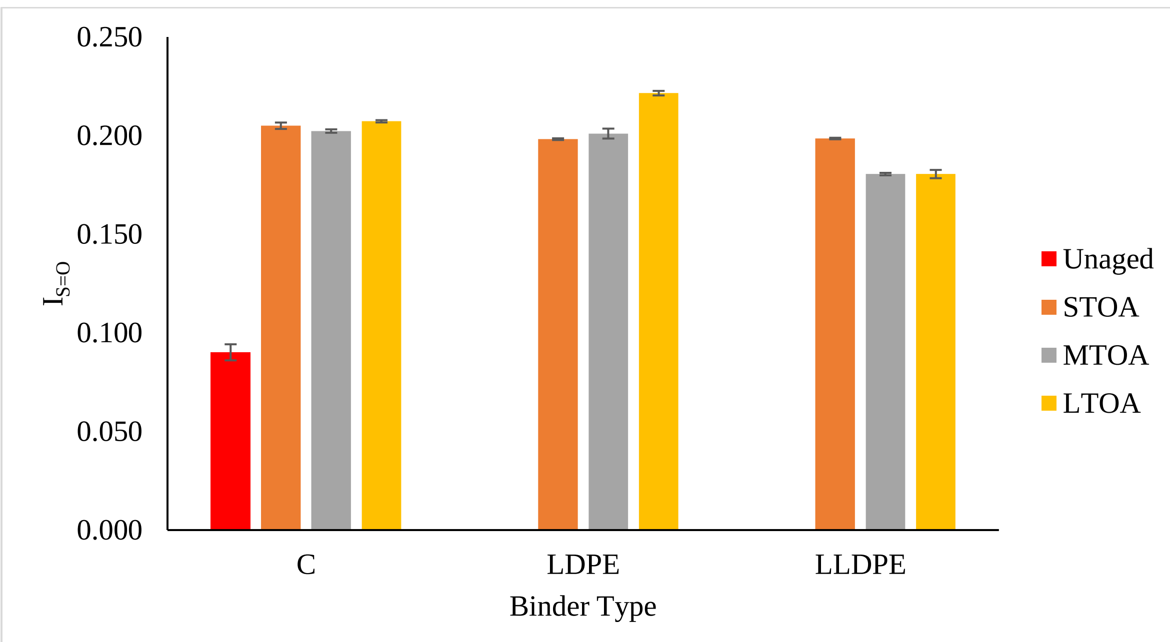

(b)

Figure 4.9 Variation of: (a) Carbonyl Index; and (b) Sulfoxide Index with aging

4.3.4 **PMED Simulation**

Figure 4.10 shows the variation of permanent deformation in asphalt layer of the simulated pavement with different mix types. Permanent deformation (rut depth) decreased for plastic-modified mixes as compared to the control mix. Formation of plastic-rock in the mix and increase in stiffness could have increased the rutting resistance of plastic-modified mixes. The LLDPE-modified mixes were found to provide superior performance as compared to the LDPE-modified mix. Similar trends were found from the dynamic modulus, viscosity, rutting factor (G*/sinδ) and non-recoverable creep compliances (J_{nr}), as discussed in previous sections. Higher structural strength of the LLDPE particles could be responsible for this phenomenon (Fried 2014).

Figure 4.11 presents the variation of top-down and bottom-up fatigue cracking expected after 20 years of service life. Overall, top-down fatigue cracking was found to increase for plastic-modified mixes. This is primarily caused by the stiffness contributed by the addition of plastic. Based on these results, plastic-modified mixes are expected to be more prone to top-down fatigue cracking as compared to non-modified mixes, when the amount of PCR plastic exceeds certain threshold. Top-down cracking was found to reduce for the LLDPE-modified mix as compared to the LDPE-modified mix as shown in Figure 4.11.

Overall, the bottom-up fatigue cracking was found to decrease for plastic-modified mixes, as shown in Figure 4.11. Typically, bottom-up fatigue cracking is related to the number of load repetitions. Tensile stresses develop at the bottom of asphalt layer due to the repetitions of the traffic load. Bottom-up cracking occurs when the tensile stress exceeds the tensile strength of the mix. Therefore, a reduction in bottom-up cracking indicated that the tensile strength and load carrying capacity of the mix increased with the addition of both LDPE and LLDPE plastics.

Also, it was observed that the LLDPE-modified mix lowered the bottom-up fatigue cracking more than the LDPE-modified mix. This is primarily caused by the higher flexibility and strength of the LLDPE compared to the LDPE.

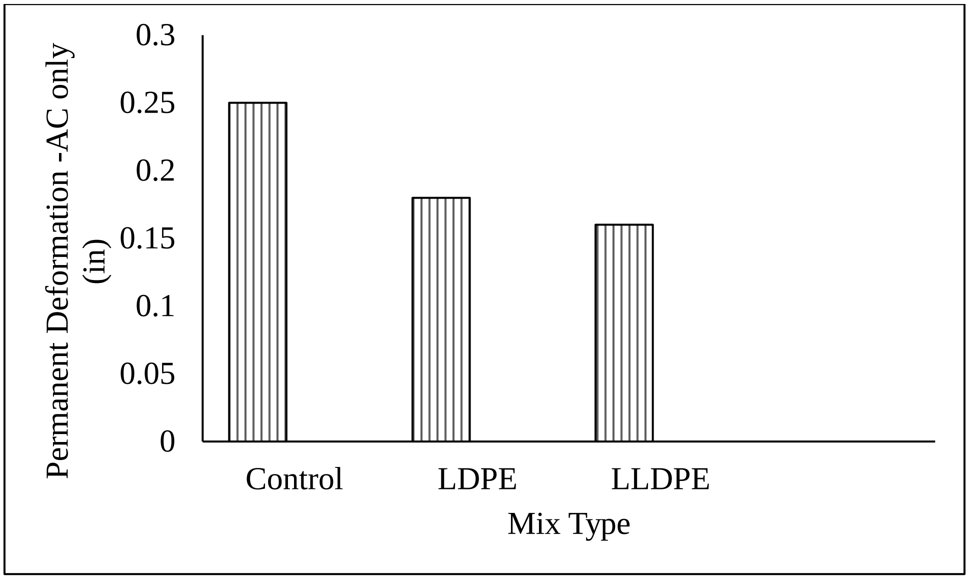

Figure 4.10 Permanent deformation-AC only

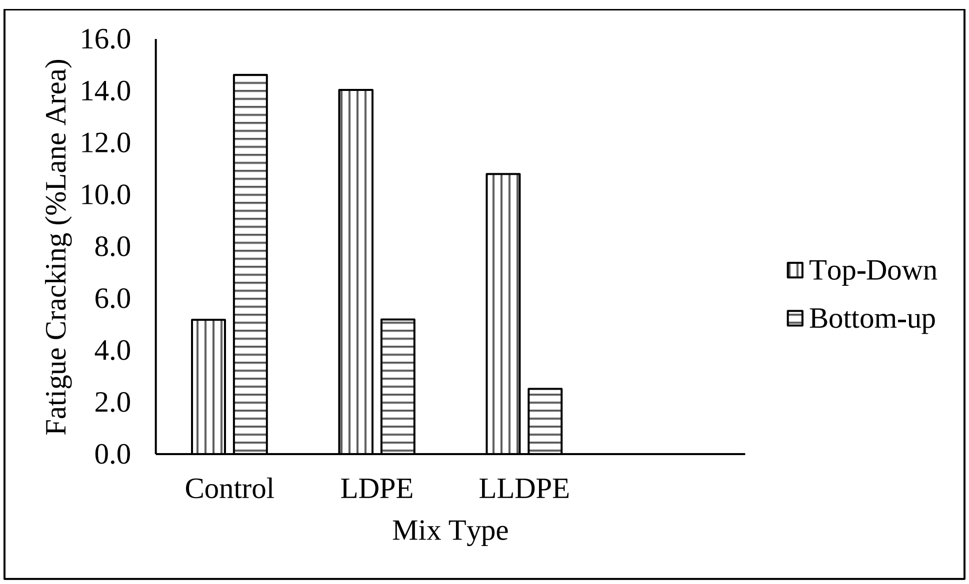

Figure 4.11 Variations of fatigue cracking with mix type

4.4 CONCLUSIONS

This study investigated the aging characteristics of plastic-modified asphalt mixes under three different aging conditions, namely STOA, MTOA and LTOA. For this purpose, a control mix (with no plastic), a LDPE- and a LLDPE-modified mixes designed with BMD approach were prepared in the laboratory and subjected to the abovementioned aging conditions. Asphalt mix performance tests, namely IDEAL-CT and DM tests, were performed to evaluate the effect of aging on the mix performance. Binders were extracted and recovered from these mixes to investigate the effect of aging on binders' rheological and chemical properties. In addition, PMED simulations were performed to predict the pavement performance after 20 years of service life. The following conclusions were drawn based on the results presented in the preceding sections:

- The IDEAL-CT test indicated a superior cracking resistance of the control mix in the early stage (STOA) as compared to the LDPE and LLDPE-conditioned mixes. However, the rate of change of CT_{Index} with aging indicated less aging susceptibility of the LLDPE-modified mix followed by the LDPE-modified mix as compared to that of the control mix. Furthermore, variability of CT_{Index} reduced with an increase in aging time.
- A significant increase in the stiffness of asphalt mixes was observed due to the addition of plastic as indicated by the E* values. This is primarily caused by the formation of plastic rock as observed in the extracted aggregates. Partially plastic-coated aggregates and distorted plastic particles revealed that plastics did not melt fully in the dry processed plastic-modified mixes. The LLDPE-modified mix was found to have highest stiffness followed by the LDPE-modified and control mixes. The LLDPE- modified mix is expected to perform better in rutting compared to the other mixes.

- Polymerization of binders with the addition of LDPE and LLDPE was not evident from the MSCR test. Superior rutting performance of binders recovered from the LDPE- and LLDPE-modified mixes was observed from the DSR and MSCR tests. The presence of dissolved plastic particles might be responsible for increasing in-service high temperature performances of the LDPE- and LLDPE-modified mixes. Rheological characterization indicated a higher aging susceptibility of plastic-modified mixes as indicated by the DSR, MSCR, RV and BBR test results.
- The LDPE-modified mixes were found to be more aging susceptible as compared to the control and LLDPE-modified mixes as indicated by the FTIR results. The more amorphous structure of LDPE allowed oxygen to penetrate easily in its polymer chain and caused formation of C=O and S=O groups contributed to the total $I_{C=O}$ and $I_{S=O}$ of binder. However, the LLDPE-modified mixes showed a better resistance to aging as evident from the $I_{C=O}$ and $I_{S=O}$. Therefore, studying the aging of plastic-modified mixes with mechanical tests is not sufficient. A combination of mechanical tests and chemical tests provides a better understanding of the aging mechanisms.
- Finally, the PMED simulation can provide an insight into the mix performance in structural level. PMED uses the environmental data to simulate aging on the dynamic modulus of a mix over the service life. Both LDPE- and LLDPE-modified mixes were found to provide superior rutting and bottom-up cracking resistances as indicated by the PMED simulations. These results were found to be in agreement with the laboratory test results of mixes and binders.

This study is based on one control mix (NMAS of 9.5-mm and PG 64-22 binder) and two types of PCR plastics, namely LDPE and LLDPE. Effect of laboratory aging may be evaluated on mixes with different aggregate gradations and binders and plastics. Also, a future study may be conducted on the relationship between accelerated laboratory aging protocol used in this study and the AASHTO R30 (AASHTO 2015) aging protocol. The findings of this study are expected to help in understanding the long-term performances of plastic-modified mixes.

CHAPTER 5 EFFECT OF BIO-REJUVENATOR ON POST-CONSUMER RECYCLED (PCR) PLASTIC-MODIFIED ASPHALT MIXES: LABORATORY INVESTIGATION AND ENVIRONMENTAL IMPACT ANALYSIS[§]

ABSTRACT

Incorporation of Post-Consumer Recycled (PCR) plastics in asphalt mixes is reported to improve the mechanical performance of asphalt mixes when used at a lower dosage. However, over stiffening of asphalt mixes due to the addition of higher amounts of plastic has been a serious concern. To this end, this study aims at increasing the percentage of plastic in asphalt mixes by incorporating a bio-rejuvenator. For this purpose, a control mix was designed using the Balanced Mix Design (BMD) approach and then modified with two different types of PCR plastics, namely Low-Density Polyethylene (LDPE) and Linear Low-Density Polyethylene (LLDPE). The asphalt mixes were then further modified by adding bio-rejuvenator. The volumetric properties were determined and the mechanical performances (rutting, cracking and moisture induced damage resistance) of the asphalt mixes were evaluated using the Hamburg Wheel Tracking (HWT) and Indirect Asphalt Tensile Cracking Test (IDEAL-CT). The optimum dosage of plastics was determined using the BMD criteria. In addition, environmental impact analyses were performed on the plastic-modified mixes. A significant reduction in greenhouse gas emission was observed from the use of plastic in asphalt mixes.

Keywords: Post-Consumer Recycled Plastics, Low-Density Polyethylene, Linear Low-Density Polyethylene, Bio-Rejuvenator, Waste Cooking Oil, Green House Gas

[§] This chapter has been submitted to the Journal of Materials in Civil Engineering under the title "Effect of Bio-Rejuvenator on Post-Consumer Recycled (PCR) Plastic-Modified Asphalt Mixes: Laboratory Investigation and Environmental Impact Analysis." The current version has been formatted for this dissertation.

5.1 INTRODUCTION

Plastic recycling in the US has gone down significantly as several countries stopped importing waste plastics from the US (SMART NEWS 2024). According to the US Environmental Protection Agency (EPA), approximately 9% of waste plastics were recycled in 2018 (EPA 2024). The recycling rate further went down to approximately 5% by the end of 2019 (Milbrandt et al. 2022). Landfilling of waste plastics in 2019 was accounted for a loss of $7.2 billion in the market value (Milbrandt et al. 2022). This trend of recycling of waste plastics remained unchanged till this date (The Guardian 2024). The Last Beach Cleanup and Beyond Plastic expressed serious concerns due to the limited plastic recycling facilities in the US (The Guardian 2024). Therefore, the addition of new avenues for utilization of waste plastic is a dare need to tackle the enormous amount of waste plastics in the country. Use of waste plastics in asphalt pavement can save natural resources, conserve energy, reduce carbon footprint and generate economic benefits.

Several studies have reported improvement in the performance of asphalt mixes after the addition of plastics (Vasudevan et al. 2010; Angelone et al. 2016; Lastra-González et al. 2016; Dalhat et al. 2019; Ghos et al. 2022a). For example, Khan et al. (2009) evaluated the rutting performance of Polypropylene (PP)-modified asphalt mixes using Hamburg Wheel Tracking (HWT) tests. Addition of 15% PP by the weight of the binder was reported to improve the rutting resistance (Khan et al. 2009). Lastra-Gonzalez et al. (2016) evaluated the rutting performance of Polyethylene (PE)-, PP-, Polystyrene (PS)-modified asphalt mixes, produced using the dry process, with Wheel Tracking Test (WTT). In that study, 1% of aggregates was replaced by waste plastics. It was reported that the addition of waste plastics improved the rutting resistance (Lastra-Gonzalez et al. 2016). Angelone et al. (2016) conducted a comparative study by adding recycled waste plastics from silo bags (consisting of Low-Density Polyethylene (LDPE) and High-Density Polyethylene (HDPE)) and recycled PP at a rate of 2%, 4% and 6% by the weight of the mix. Increased rutting resistance and stiffness were reported with the addition of waste plastic (Angelone et al. 2016). Ranieri et al. (2017) evaluated the fatigue cracking performance of HDPE-modified asphalt mixes using four-point bending beam and stiffness modulus tests. In that study, the addition of HDPE was reported to increase the stiffness at high temperature (or low frequency) and decrease at low temperature (or high frequency). However, the addition of HDPE was found to reduce the fatigue cracking resistance of asphalt mixes (Ranieri et al. 2017). Zhang et al. (2020a) evaluated the fatigue cracking resistance of PE-modified asphalt mixes using the four-point bending beam test. The addition of waste PE did not produce significant changes in the fatigue performance (Zhang et al. 2020a). Overall, waste plastics were found to improve the rutting resistance, stiffness, and volumetric properties of asphalt mixes (Suaryana et al. 2018; Haider et al. 2020; Ghos et al. 2022). However, plastic-modified mixes were found to adversely affect the fatigue cracking resistance and moisture resistance (Suaryana et al. 2018; Haider et al. 2020; Ghos et al. 2022a; Ghos et al. 2022b; Ghos et al. 2024a). Also, the incorporation of waste plastics using the wet process was found to increase the viscosity of the blends which resulted in a stiff and less workable binder. Consequently, a high mixing and compaction temperature is required during the production of asphalt mix containing waste plastics (Abdelaziz & Mohamed 2010; Al-Abdul Wahhab et al. 2017). Therefore, it is important to take measures to balance performance of asphalt mixes containing waste plastics. To this end, Balanced Mix Design (BMD) is a useful tool for designing asphalt mixes containing plastics by ensuring a balanced performance in terms of rutting and cracking (Ghos et al. 2022a). The current study aimed to increase the plastic content in asphalt mixes using a bio-rejuvenator without sacrificing the cracking resistance.

Several studies have been conducted to reduce the stiffness and restore the flowability of asphalt binder containing recycled materials (Shen et al. 2005; Shen et al. 2007; Mogawer et al. 2012; Nazzal et al. 2015; Zhou et al. 2018). It was found that the application of asphalt rejuvenators allows the incorporation of recycled materials in asphalt mixes (Shen et al. 2005; Shen et al. 2007; Mogawer et al. 2012; Nazzal et al. 2015). Rejuvenators are recycling agents with a high proportion of light components (Nazzal et al. 2015; Zeng et al. 2018; Zhou et al. 2018). The purpose of using a rejuvenator is to restore the rheological and chemical properties of the aged binder to a level close to the virgin binder (Zhou et al. 2018). Rejuvenators can also be added to highly viscous binders to reduce stiffness and improve engineering properties (Behnood 2019). Until now, rejuvenators have been used for incorporating Reclaimed Asphalt Pavement (RAP) and Recycled Asphalt Shingles (RAS) in asphalt mixes (Zeng et al. 2018; Zhou et al. 2018; Fang et al. 2019; Behnood 2019)). Several studies were conducted on the use of rejuvenators with other recycled materials, including PCR plastics (Buttlar et al. 2019; Nizamuddin et al. 2022). In that study, rejuvenator was used as a softening agent to reduce stiffness and improve fatigue cracking performance of asphalt mixes.

Traditional rejuvenators are either softer asphalt binders or some extracts from petroleum (for example, aromatic oils, paraffinic oils, and naphthenic oils) (Zhou et al. 2018). The use of these petroleum-based rejuvenators poses several challenges. For example, the lighter components of the rejuvenators volatilize easily at high temperatures. Also, rejuvenators are found to oxidize quickly and reduce the aging resistance of the binders in the long term (Fang et al. 2021). Therefore, emphasis has been given to developing bio-material-based rejuvenators to promote sustainable construction. In recent years, a variety of bio-rejuvenators has been developed from non-petroleum-based sources, such as vegetable oils, wood fibers, and livestock manures. (Fini et al. 2012; Yang & Suciptan 2016; Fang et al. 2021). Recent studies have reported significant improvements in the Performance Grade (PG), fatigue cracking resistance, low-temperature cracking resistance, and thermal stability with the use of bio-rejuvenators (Fini et al. 2013; Qu et al. 2018; Behnood 2019; Fang et al. 2021).The use of bio-rejuvenators in asphalt mixes containing PCR plastics are expected to improve cracking performance and results in economic and environmental benefits. In this regard, Waste Cooking Oil (WCO) is one of the most widely studied bio-rejuvenators (Zargar et al. 2012; Asli et al. 2012; Chen et al. 2014; Zhang et al. 2017; Chang et al. 2023). For example, Zargar et al. (2012) investigated the possibility of WCO as a rejuvenating agent for aged binders. It was found that using 3-4% of WCO in the aged binder could result in physical and rheological properties close to the original binder (Zargar et al. 2012). Chen et al. (2014) reported restoration of the rheological properties of aged asphalt binder with the incorporation of 5% WCO by the weight of the original binder (Chen et al. 2014). Dugan et al. (2020) evaluated the performance of RAP binders rejuvenated with Waste Vegetable Oil (WVO). In that study, binder blends were prepared with 40% net PG 64-22 binder and 60%-RAP binder. A 10% WVO dose was found to exhibit lower viscosity and rutting factor as compared to the net PG 64-22 binder (Dugan et al. 2020). The current study used WCO as a softening agent for reducing stiffness and increasing the resistance to cracking of plastic-modified asphalt mixes.

In addition to performance evaluation, assessing environmental impact is equally important to using waste plastics and bio-rejuvenators in asphalt mixes. Environmental impacts of asphalt mixes have been determined in the past studies using the reduced energy generation and CO_2 emission approach (also known as the Greenhouse Gas (GHG) emission approach), as well as the Life Cycle Assessment (LCA) approach (Wu et al. 2021; Belc et al. 2021; Santos et al. 2021; Yao et al. 2022). Wu et al. (2021) evaluated the environmental impact of WMA using the reduced energy consumption and CO_2 emission approaches. In that study, heat reduction due to WMA production was calculated as compared to the same amount of HMA production. The reduced heat was then converted into Carbon Dioxide Equivalent (CO_2e). A significant reduction in CO_2e was reported for using WMA. Santos et al. (2021) evaluated the environmental impact of PP- and PE-modified asphalt mixes using the LCA approach. In that study, LCA was conducted by considering several replacement ratios of virgin materials by their recycled counterparts. The plastic-modified binders and mixes were found to be more environmentally advantageous compared to the virgin materials (Santos et al. 2021). Yao et al. (2022) evaluated the environmental impact of a wet processed PET-modified asphalt mix using the CO_2 emission approach. It was reported that a reduction of 26.2% in the GHG emission could be achieved by incorporating PET in asphalt mixes (Yao et al. 2022). In the current study, the GHG emission approach is used for evaluating the environmental impact of plastic-modified mixes.

The present study evaluated the feasibility of using PCR plastics in asphalt mixes considering volumetric properties, mechanical performance, and environmental impact. The specific objectives were as follows:

- To evaluate the properties and performance of asphalt mixes containing two types of PCR plastics and a WCO rejuvenator;
- To determine the optimum dosage of PCR plastics and WCO relative to the BMD criteria; and

- To assess the environmental impact of using PCR plastic and WCO-modified asphalt mixes in terms of GHG Emissions.

5.2 MATERIALS AND METHODS

Figure 5.1 shows the workflow diagram followed in this study. A control mix (0%-plastic) with a Performance Grade (PG) 64-22 binder and aggregates of Nominal Maximum Aggregate Size (NMAS) of 9.5-mm was selected following the ODOT BMD Special Provision (ODOT 2023). Gradation, aggregate types and volumetric properties of the control mix can be found in Chapter 2 (Ghos et al. 2022a). The optimum binder content of the control mix was found to be 5.6%. The control mix was then modified by adding two different types of PCR plastics (LDPE and LLDPE) and a WCO as the rejuvenator. Asphalt mixes with and without WCO-modified mixes were prepared with three different percentages (1%, 1.5% and 2%) of LDPE and LLDPE. For the purpose of this study, 2.36-mm diameter LDPE and LLDPE pellets were incorporated in asphalt mixes using the dry process. The properties of these plastics and the process of adding plastic can be found in Chapter 2 (Ghos et al. 2022a). This study was conducted in two steps. At first, a set of Superpave Gyratory Compacted (SGC) samples were prepared for the control, LDPE- and LLDPE-modified mixes. The volumetric properties and mechanical performances of the asphalt mixes were determined. It was observed that the asphalt mixes stiffened with the addition of plastic. According to the ODOT BMD provision, a softer grade binder can be used for producing BMD mixes containing recycled materials (e.g., RAP) (ODOT 2023). Therefore, in this study, a softer grade binder was used to reduce the stiffness of the plastic-modified mixes. In step two, WCO was added in plastic-modified mixes as a softening agent. For this purpose, WCO was collected and mixed with the preheated binder at three different percentages (1%, 2% and 3% by the weight of binder). The high-temperature rheological characteristics of WCO-binder blends were determined using the Dynamic Shear Rheometer (DSR) test. Fourier Transform Infrared Spectroscopy (FTIR) test was conducted on the WCO-binder blend to check for any chemical interactions between WCO and binder. For this purpose, chemical functional groups namely, carbonyl and sulfoxide groups were determined from the FTIR spectra. The amount of WCO required to lower the high-temperature performance grade by one grade was selected as the optimum WCO dose. The binder was then modified with the optimum WCO dose and used for preparing the LDPE- and LLDPE-modified mixes using the dry process. Table 5.1 shows the naming conventions of all mixes used in this study. For example, 1-LDPE is used to represent the asphalt mix prepared with LDPE by replacing 1% aggregate. The 1-LDPE-WCO is used to denote the asphalt mix prepared with WCO-binder blend and 1% LDPE. Necessary tests were conducted to determine the volumetric properties and mechanical performances of the mixes. The optimum doses of LDPE and LLDPE were selected based on the ODOT BMD criteria (ODOT 2023). In addition, the GHG emission for producing the control and WCO-plastic-modified mixes was calculated using the methodology suggested by the National Asphalt Pavement Association (NAPA) (Williams et al. 2022).

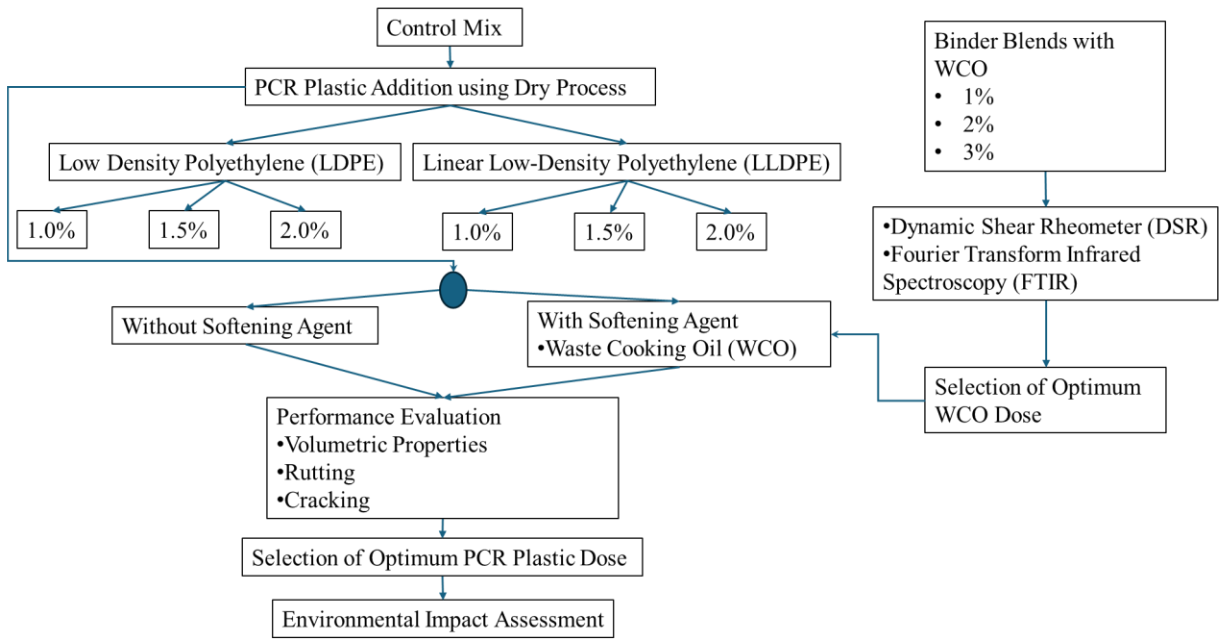

Figure 5.1 Workflow diagram

Table 5.1 Naming conventions of plastic-modified mixes

ID	Remarks
C	Control mix
1.0-LDPE	Plastic-modified mixes prepared by replacing 1.0% of total aggregates by LDPE
1.5-LDPE	Plastic-modified mixes prepared by replacing 1.5% of total aggregates by LDPE
2.0-LDPE	Plastic-modified mixes prepared by replacing 2.0% of total aggregates by LDPE
1.0-LLDPE	Plastic-modified mixes prepared by replacing 1.0% of total aggregates by LLDPE
1.5-LLDPE	Plastic-modified mixes prepared by replacing 1.5% of total aggregates by LLDPE
2.0-LLDPE	Plastic-modified mixes prepared by replacing 2.0% of total aggregates by LLDPE
1.0-LDPE-WCO	Binder modified by WCO, and plastic-modified mixes prepared by replacing 1.0% of total aggregates by LDPE
1.5-LDPE-WCO	Binder modified by WCO, and plastic-modified mixes prepared by replacing 1.5% of total aggregates by LDPE
2.0-LDPE-WCO	Binder modified by WCO, and plastic-modified mixes prepared by replacing 2.0% of total aggregates by LDPE
1.0-LLDPE-WCO	Binder modified by WCO, and plastic-modified mixes prepared by replacing 1.0% of total aggregates by LLDPE
1.5-LLDPE-WCO	Binder modified by WCO, and plastic-modified mixes prepared by replacing 1.5% of total aggregates by LLDPE
2.0-LLDPE-WCO	Binder modified by WCO, and plastic-modified mixes prepared by replacing 2.0% of total aggregates by LLDPE

5.2.1 **Test Methods**

5.2.1.1 ***Dynamic Shear Rheometer (DSR)***

The Dynamic Shear Rheometer (DSR) tests were conducted in accordance with AASHTO T 315 (AASHTO 2022e). The DSR test was conducted on all three WCO-binder blends to determine complex modulus (G*), phase angle (δ), rutting factor (G*/ sin(δ)) as-well-as the High-Temperature Performance Grade (HPG). The G* is calculated as the ratio of shear stress and shear strain. Phase angle (δ) is the phase difference between applied stress and strain (Wang et al. 2020). In this study, all binders were tested using the original DSR template for evaluating the effect of WCO. The temperature at which the binder passed the specifications limits but failed at the next 6°C increment was considered HPG. Interpolation between two temperatures was used to calculate the “True” Grade (TG) or Continuous Grade (Tc).

5.2.1.2 ***Fourier Transform Infrared Spectroscopy (FTIR)***

In this study, FTIR test was performed on control and WCO-binder blends to determine the changes in chemical functional groups due to the addition of WCO. An Agilent Technologies 4300 Handheld FTIR spectrometer with Diamond Attenuated Total Reflection (ATR) mode was used to collect 1798 scans from each sample in the 650 to 4000 cm^{-1} range. For this purpose, binder samples were heated to 170°C to make them liquid enough to pour a drop on the Diamond ATR sensor. From the FTIR spectra, carbonyl (C=O) and sulfoxide (S=O) groups were identified for the tested binder blends. The carbonyl (C=O) and sulfoxide (S=O) groups correspond to peak ranges of 1690-1725 cm^{-1} and 1010-1043 cm^{-1}, respectively (Kumar et al. 2021). The Carbonyl Index (CI) and Sulfoxide Index (SI) were determined using Equations 5.1 and 5.2 (Zargar et al. 2012; Kumar et al. 2021).

$$I_{C=0} = \frac{A_{1690-1725}}{\sum A} \tag{5.1}$$

$$I_{S=0} = \frac{A_{1010-1043}}{\sum A} \tag{5.2}$$

where,

A = area under the peak of a targeted range of FTIR spectra.

$$\sum A = A_{1010-1043} + A_{1350-1510} + A_{1535-1625} + A_{1678-1725}$$

5.2.1.3 ***Volumetric Analysis***

To evaluate volumetric properties, the theoretical maximum specific gravity of asphalt mix (G_{mm}) was determined for each mix following AASHTO T209-12 (AASHTO 2016b). For this purpose, approximately 1500-gm of loose, oven-dried sample was placed in a tared vacuum flask at 25°C. Sufficient water having the same temperature was added to the flask so that the asphalt sample was completely submerged. Vacuum was applied for 15±2-mintues with a vacuum pressure of 30 psi. The flask was then filled completely by adding water. The mass of the flask filled with the mix and water was measured in air. From these data, the G_{mm} was calculated. The bulk specific gravity (G_{mb}) was determined for each mix following AASHTO T166 (AASHTO 2016c). For this purpose, compacted specimens having a diameter of 150-mm, and a height of 115-mm were prepared from each mix using a Superpave Gyratory Compactor (SGC) using 50-gyrations. The mass of the sample under dry, submerged, and saturated conditions was measured, and G_{mb} was calculated from these data. Using the G_{mm} and G_{mb} values, % densities, air voids, Voids in Mineral Aggregates (VMA), and Voids Filled with Asphalt (VFA) were calculated for each mix. The compactability of plastic-modified mixes was calculated following ASTM D6925-15 (ASTM 2015) and AASHTO R 35 (AASHTO 2022c) test methods to assess any issues pertaining to the densification of dry processed mixes.

5.2.1.4 ***Hamburg Wheel Tracking (HWT)***

For evaluating rutting performance, HWT tests were conducted on a pair of 150-mm diameter and 62-mm thick saw-cut specimens from the laboratory produced mixes, following the AASHTO T 324 (AASHTO 2011) method. The specimens for the HWT tests were compacted at 7±0.5% air voids. The tests were conducted at 50 °C with a wheel pass frequency of 52 passes/minute. The tests were terminated after reaching a maximum rut depth of 20-mm or 20,000-load cycles, whichever reached first. A typical rut depth vs load cycle plot is presented in Figure 5.2.

The HWT data from each test were first analyzed using the AASHTO T 324 (AASHTO 2011) method. The rut depth at 10,000-load cycle and the Stripping Inflection Point (SIP) were directly obtained from the rut depth vs load cycle plot according to the AASHTO T324 method (AASHTO 2011). The rut depth at 10,000-load cycle was used as a measure of the rutting resistance. The SIP was determined as the intersection between the creep phase and stripping phase. The SIP was used as a measure of the resistance to moisture induced damage. The HTW results were then further analyzed using the Texas A&M University (TAMU) method for more mechanistic evaluation, as suggested by Yin et al. (2014). The measured data were fitted as described by Yin et al. (2014) and shown in Figure 5.2(a). The inflection point of the fitted curve is termed as Stripping Number (SN) and the number of load cycle at SN is defined as the (LC_{SN}). The LC_{SN} denotes the number of load cycles at which adhesive fracture starts between aggregates and binder. The strain was calculated for each test by dividing the rut depth by the specimen thickness and fitted using the Tseng-Lytton model as shown in Figure 5.2(b). The strain up to SN is called the visco-plastic strain (ε^{vp}) and after SN is called the stripping strain (ε^{st}). The number of load cycles from SN to ε^{st} corresponding to 12.5-mm rut depth is defined as the stripping life (LC_{ST}), as shown in Figure 5.2(c). The resistance to moisture damage of each mix was evaluated by using LC_{SN} and LC_{ST}. A higher LC_{SN} indicates a better resistance to moisture induced damage. The rut depth vs load cycle plot consists of two phases, namely creep phase and stripping phase. The portion of the curve after inflection point represents the stripping phase. The stripping of binder from aggregates occurs during this phase. Mixes with a higher LC_{ST} are expected to provide better resistance to moisture induced damage. Yin et al. (2014) suggested to use a parameter called the visco-plastic strain increment at stripping number ($\Delta\varepsilon^{vp}_{LCsn}$) to account for the contribution of rutting from visco-plastic deformation only. The

$\Delta\varepsilon_{LCsn}^{vp}$ was calculated using Equation 5.3. The $\Delta\varepsilon_{LCsn}^{vp}$ isolated the visco-plastic strain during the creep phase and discarded the contribution of mix after stripping of binder from aggregates during calculating rutting resistance. A lower $\Delta\varepsilon_{LCsn}^{vp}$ indicates a higher resistance to rutting (Yin et al. 2014).

$$\Delta\varepsilon_{LC_{SN}}^{vp} = \alpha^{\lambda}\lambda\varepsilon_{\infty}^{vp} exp\left[-\left(\frac{\alpha}{LC_{SN}}\right)^{\lambda}\right](LC_{SN})^{-(\lambda+1)} \qquad (5.3)$$

where,

$\varepsilon_{\infty}^{vp}$ = saturated visco-plastic strain of HWT specimen

α and λ = model parameters

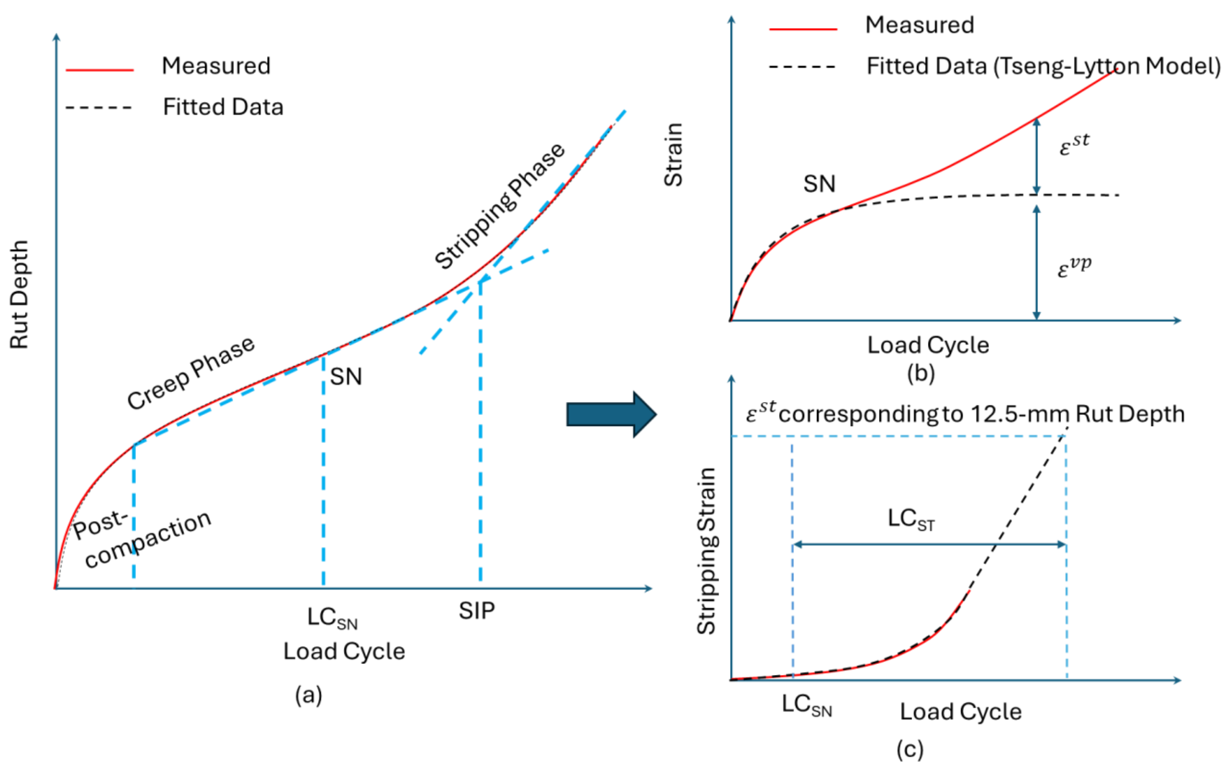

Figure 5.2 Typical rutting profile of HWT test

5.2.1.5 ***Indirect Asphalt Tensile Cracking Test (IDEAL-CT)***

The IDEAL-CT tests were conducted on asphalt mix specimens to determine the Cracking Tolerance Index (CT_{Index}) following the ASTM D 8225 (ASTM 2019) test method to evaluate the cracking resistance of the asphalt mixes. The IDEAL-CT tests were performed on the compacted specimens (150-mm in diameter and 62-mm in height) by applying a vertical monotonic load at a rate of 50 mm/min until failure at room temperature (25ºC). An MTS loading system was used to collect the load and displacement data during testing. For each mix, four cylindrical specimens compacted at 7±0.5% air voids were tested to ensure repeatability. The load-displacement data were recorded for the entire duration of the test. The load-displacement data was used to calculate the cracking resistance of the asphalt mixes in terms of CT_{Index}. Generally, a higher CT_{Index} indicates a better cracking resistance for a mix.

5.2.2 **Green House Gas (GHG) Emission**

The environmental impact of plastic-modified mixes was evaluated in terms of the reduction of GHG emissions. In this study, the GHG emission calculations were conducted by using the methodology suggested by Williams et al. (2022). The GHG emissions were quantified by calculating the avoided upstream emissions that would be associated with the mineral aggregates replaced by the plastics and binders reduced by the combined effect of WCO and plastics in asphalt mixes. Table 5.2 shows the factors used for calculating the GHG emission associated with the producing plastic-modified mixes. According to Williams et al. (2022), emission factors for virgin aggregates production, transportation and fuel combustion are 1.761 kg CO_2e/ton, 0.185 kg CO_2e/ton-mile and 12.25 kg CO_2e/gal, respectively. Emission factor for extraction, processing and production of net asphalt binder was assumed as 577.9 kg CO_2e/ton (Wildnauer et al. 2019; Williams et al. 2022). These emission factors are consistent with Environmental Product Declaration (EPD) of asphalt mixes (Williams et al. 2022). A total of 3 alternative scenarios were evaluated for waste plastics in this study. Scenario 1: waste plastics, used for producing asphalt mixes, to be disposed through landfilling; Scenario 2: waste plastics used for producing asphalt mixes would be incinerated for ultimate disposal; and Scenario 3: waste plastics would be disposed by the combination of landfilling (85%) and incineration (15%). The rates in Scenario 3 were decided based on the current rate of waste plastic disposal (SMART NEWS 2024). Following assumptions were made during the calculation of GHG:

1. The calculations were performed based on the asphalt mix production and construction in Oklahoma only.
2. A total of 5.1 million tons of asphalt mixes was produced in Oklahoma in 2021 (Williams et al. 2022). In this study, approximately, 85% of these mixes were considered as the surface mix for calculating the GHG emissions.
3. The average transport distance was assumed to be 40-miles for aggregates, binders, plastics and WCO.
4. This study used a cradle-to gate approach for calculating the GHG emissions. End-of-life for plastic-modified mixes were not considered in this study.

Net GHG emissions for each mix were calculated using Equation 5.4.

$$GHG_{CO_2e} = \sum_{i}^{n} E_i \, M_i \qquad (5.4)$$

where,

E_i = Emission factor for binder, aggregates and other inputs

M_i= Mass of corresponding items

In calculating the net GHG emissions, GHG overburdens were assumed as positive and avoided GHG emissions were considered as negative.

Table 5.2 Emission factors for GHG calculations

Item	Emission Factor	Reference
Aggregate Production	1.761 kg CO_2e/ton	Williams et al. (2022)
Aggregate Transportation	0.185 kg CO_2e/ton-mile	Williams et al. (2022)
Fuel Combustion	12.25 kg CO_2e/gal	Williams et al. (2022)
Net Binder	577.9 kg CO_2e/ton	Wildnauer et al. 2019; Williams et al. 2022
LDPE/LLDPE Recycling	272 kg CO_2e/ton	Hopewell et al. (2009)
WCO	0.1-0.3 kg CO_2e/liter	NREL (2009)
Landfilling of LDPE/LLDPE	181 kg CO2e/ton	EPA (2020)
Incineration of LDPE/LLDPE	1.7-2.5 kg CO2e/kg	Plastic Europe (2020)

5.3 RESULTS AND DISCUSSION

5.3.1 **Effect of WCO on Binder Performance**

Effect of WCO dosage on the high-temperature rheological properties of the control binder was evaluated using the DSR test. For this purpose, the complex modulus (G*), phase angle (δ), and the rutting factor (G*/sinδ) for the control binder and WCO-binder blends were obtained at 52, 58, 64 and 70ºC. Figure 5.3 shows the variation of G*/sinδ with the WCO dosage level. Overall, G*/sinδ was found to reduce with an increase in the WCO percentages and temperature. For example, the G*/sinδ value was found to decrease from 1.45- to 0.64-kPa with an increase in the WCO percentage from 2 to 3%. The main chemical component of WCO is triglyceride. Softening of binder with the addition of triglycerides from WCO is primarily responsible for reducing the G*/sinδ values. The G*/Sinδ value is an indicator of the resistance to permanent deformation or rutting at in-service high temperature (AASHTO 2022e). A higher G*/sinδ value indicates better rutting resistance of the binder. As the use of WCO reduced the G*/sinδ value of the binder blend, care should be taken in using an appropriate amount of WCO in producing asphalt mixes.

Figure 5.4 shows the variation of high-temperature continuous grades of binder blends with the WCO percentages. As expected, the high-temperature continuous grade decreased with an increase in the WCO percentage. For example, the continuous grade decreased from 66.8 to 61.1°C with an increase in the WCO amount from 0 to 2%. The HPG of the binder-WCO blends was selected based on the AASHTO M 320 (AASHTO 2022b) specification. The HPGs of 1%-, 2%- and 3%-WCO blends were found as 64°, 58° and 52°C, respectively. The amount of WCO required to lower the binder grade by one PG was considered as the optimum dose. The addition of 2%WCO was found to be optimum and was used for producing asphalt mixes. The volumetric properties and mechanical performances of the plastic-WCO-modified mixes are discussed in the subsequent sections.

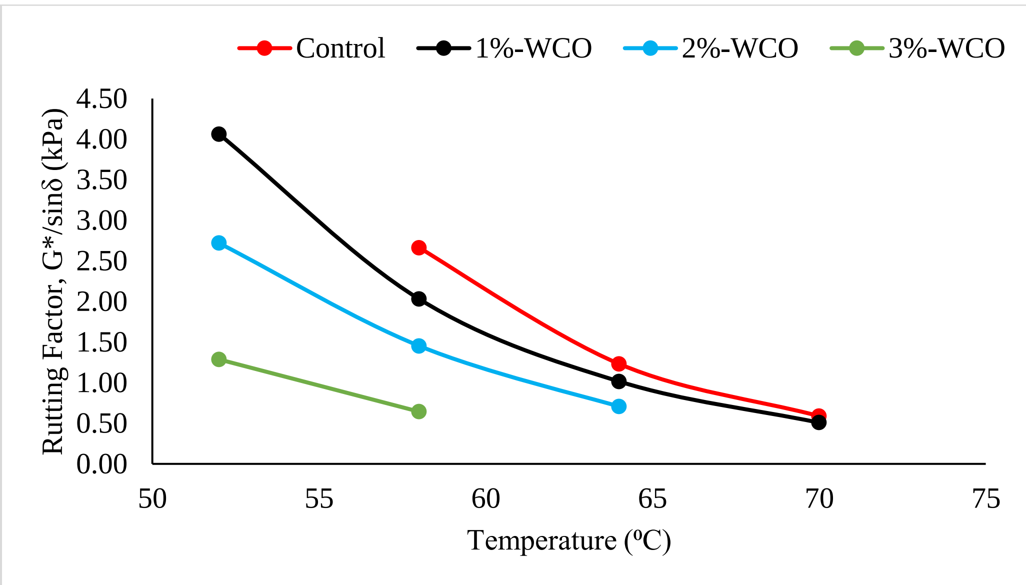

Figure 5.3 Variation of rutting factor with WCO dosage

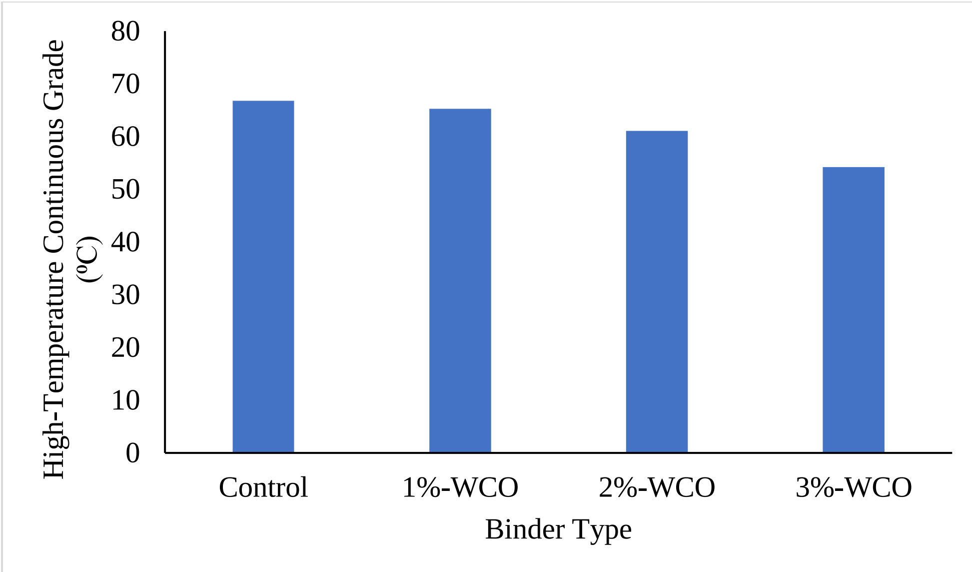

Figure 5.4 Variation of high-temperature performance grade with WCO dosage

5.3.2 **Effect of WCO on Chemical Functional Groups of Binder**

As previously mentioned, FTIR tests were performed on WCO-binder blends to check if the addition of WCO causes any chemical change to the asphalt binder. A summary of the FTIR analysis is presented in Table 5.3. Both CI and SI were calculated for the control binder, and 2%-WCO- and 3%-WCO- binder blends. No difference in the CI and SI indices were observed due to the addition of WCO. For example, the CI values of all the binder samples were found to remain as 0.049, as evident from Table 5.3. It can be concluded that the WCO worked as a softening agent and no chemical interactions occurred between WCO and binder.

Table 5.3 Effect of WCO on binder's chemical functional groups

Sample ID	Carbonyl Index (CI)	Sulfoxide Index (SI)
C	0.049	0.094
2%-WCO	0.049	0.094
3%-WCO	0.049	0.094

5.3.3 **Effect on Asphalt Mix Performances**

5.3.3.1 ***Effect on Compactibility***

The effects of LDPE, LLDPE and WCO on the densification was evaluated using the compaction curve. Figures 5.5(a) and 5.5(b) show the variation of relative densities with the number of gyrations during the compaction process. Overall, the addition of plastics was found to improve the densification as indicated by the upward shift of the compaction curves from that of the control mix. The LLDPEs showed a relatively higher shift in the compaction curve as compared to the LDPEs, as evident from Figures 5.5(a) and 5.5(b). The higher Melt Flow Index (MFI) of LLDPE as compared to LDPE is primarily responsible for relatively higher shift in compaction curves (Xu et al. 2023). The addition of WCO was found to shift the curve downward from the plastic-modified mixes. The chemical compatibility of LDPE and LLDPEs with WCO retarded the melting of these plastic particles (CP Lab Safety 2024). The reduction in the melting of plastic particles in the presence of WCO might be responsible for reducing the densification of plastic-WCO-modified mixes.

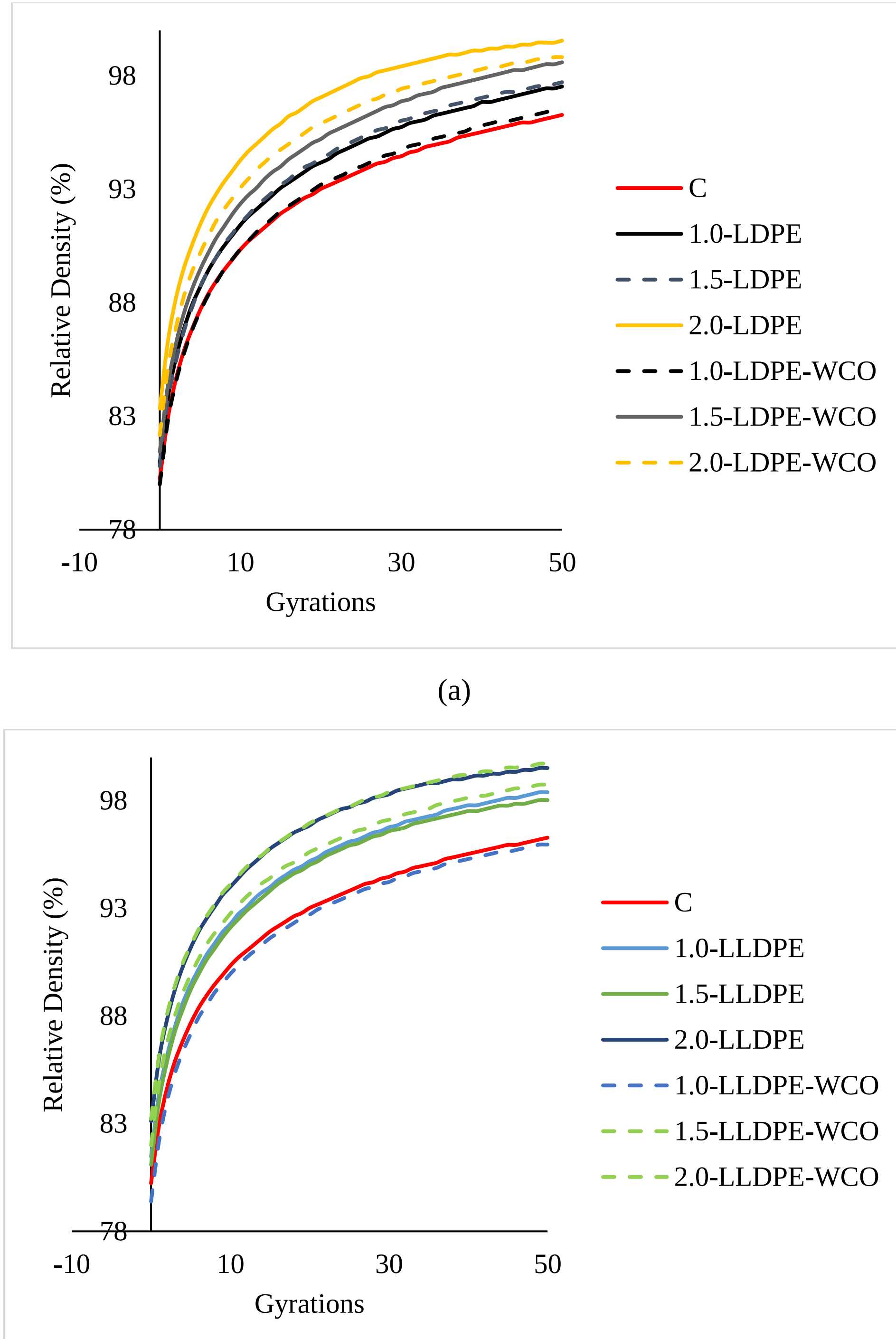

(a)

(b)

Figure 5.5 Variation of relative density with gyrations: (a) LDPE-modified mixes; and (b) LLDPE-modified mixes

5.3.3.2 ***Effect on Volumetric Properties***

Effects on the volumetric properties, namely G_{mm}, G_{mb}, VMA, VFA, Percent Binder Absorbed (P_{ba}) and Effective Binder Content (P_{be}) due to plastic and WCO addition were evaluated in this study. Figures 5.6, 5.7, 5.8, 5.9, 5.10, 5.11 and 5.12 show the variations of G_{mm}, G_{mb}, %density, VMA, VFA, P_{ba} and P_{be}, respectively. Overall, G_{mm} was found to decrease with an increase in the plastic percentage. For example, G_{mm} of the asphalt mix was found to decrease from 2.472 to 2.431 with an increase in the LDPE from 0 to 1%. A similar trend was also observed for LLDPE, as evident from Figure 5.6. The reduction in G_{mm} is even higher with the addition of WCO. Low specific gravities of LDPE, LLDPE and WCO compared to mineral aggregates and binders are primarily responsible for reducing the Gmm of plastic- and plastic-WCO-modified mixes. However, at higher plastic percentages (1.5% and 2.0%), plastic- and plastic-WCO-modified mixes resulted in similar G_{mm} values.

Figure 5.7 shows the variation of G_{mb} with the addition of plastics and WCO. Overall, G_{mb} decreased with an increase in the plastic content for plastic-modified mixes. For example, the G_{mb} was found to decrease from 2.371 to 2.355 with an increase in the LDPE percentage from 1 to 1.5%. A similar trend was observed for LLDPE-modified mixes. As previously noted, low specific gravities of LDPE, LLDPE and WCO as compared to mineral aggregates and binders are primarily responsible for this phenomenon. However, it is interesting to note that the addition of WCO, G_{mb} started increasing with the increase of plastic percentages, as evident from Figure 5.7. The higher G_{mm} of plastic-WCO modified mixes allowed more mix to be compacted in the same size specimens resulted in higher G_{mb} values of plastic-WCO-modified mixes as compared to the plastic-modified mixes.

Figure 5.8 shows the variation of %densities with the addition of plastics and WCO. Overall, %densities increased with an increase in the amounts of plastics. A similar trend was observed for both plastic- and plastic-WCO-modified mixes. For example, the %density value of asphalt specimen was found to increase from 97.2 to 98.2% with an increase in the LDPE from 1.5 to 2% for LDPE-WCO-modified mixes.

Figure 5.9 shows the variations of VMA in plastic- and plastic-WCO-modified mixes. The VMA was found to increase with an increase in the plastic percentage. For example, VMA was found to increase from 13.0 to 13.7% for an increase in the LLDPE percentage from 1.0 to 1.5%. Replacement of aggregates by one size of plastic particles might have increased the voids in the overall aggregate blend. The plastic-WCO-modified mixes were found to exhibit higher VMA as compared to plastic-modified mixes. Higher chemical compatibility of LDPE and LLDPE with WCO provided stability to plastic particles resulted in higher voids in the aggregate blends (CP Lab Safety 2024). However, at higher plastic percentages, (for example, at 2% LLDPE), more plastic particles might have melted and reduced the VMA. The WCO has higher heat retention capacity (2.0-2.2 J/g^{o}C) than asphalt binder (0.92-1.2 J/g^{o}C) (Berk 2018; Somayaji 1985). Therefore, the binder-WCO blend retained less heat than net binder alone and reduced the melting of plastics at lower plastic percentages. However, at higher plastic percentages, there were not enough WCO to retard the melting process and consequently, a higher VMA value was observed at lower plastic percentages.

Figures 5.10, 5.11 and 5.12 show the variation of VFA, P_{ba} and P_{be} with the addition of LDPE, LLDPE and WCO. It was observed that the VFA increased with an increase in the LDPE and LLDPE percentages with and without the addition of WCO. For example, VFA increased from 82 to 82.4% with an increase in the LLDPE percentage from 1 to 1.5%. This increased

VFA was found to reduce P_{ba} in plastic-modified mixes as evident from Figure 5.11. Reduction in P_{ba} resulted in increase in the P_{be} as evident from Figure 5.13. Partial coating of aggregates with melted plastic particles might have reduced absorption of binder by the aggregates and left more effective binders in the mix as evident from Figures 5.11 and 5.12 (Vasudevan et al. 2010; Ghos et al. 2024a). This trend is true for both plastic- and plastic-WCO-modified mixes.

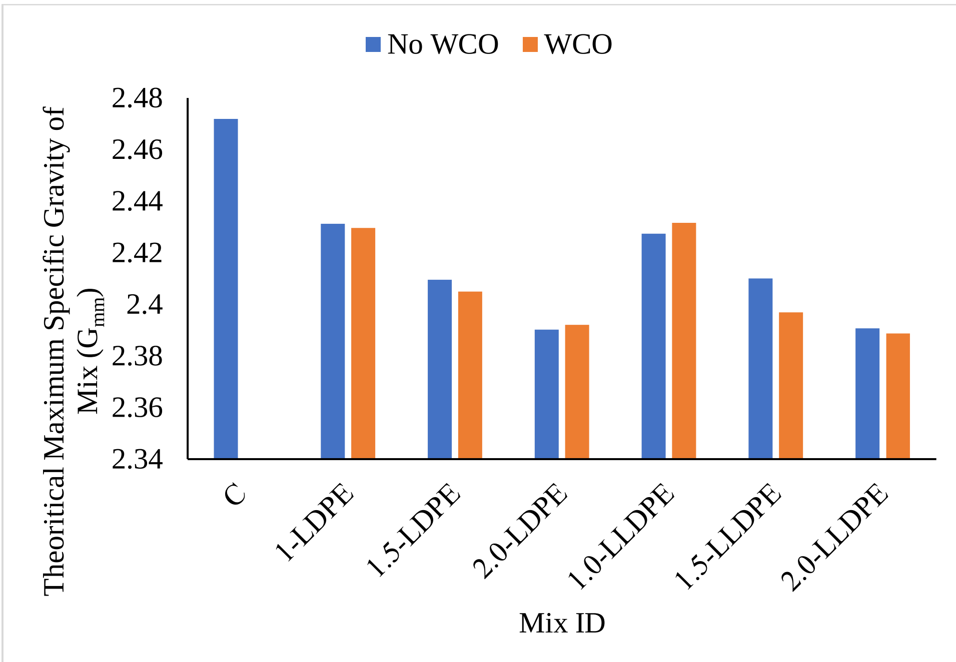

Figure 5.6 Variation of Theoretical Maximum Specific Gravity of Mix (G_{mm}) with mix type

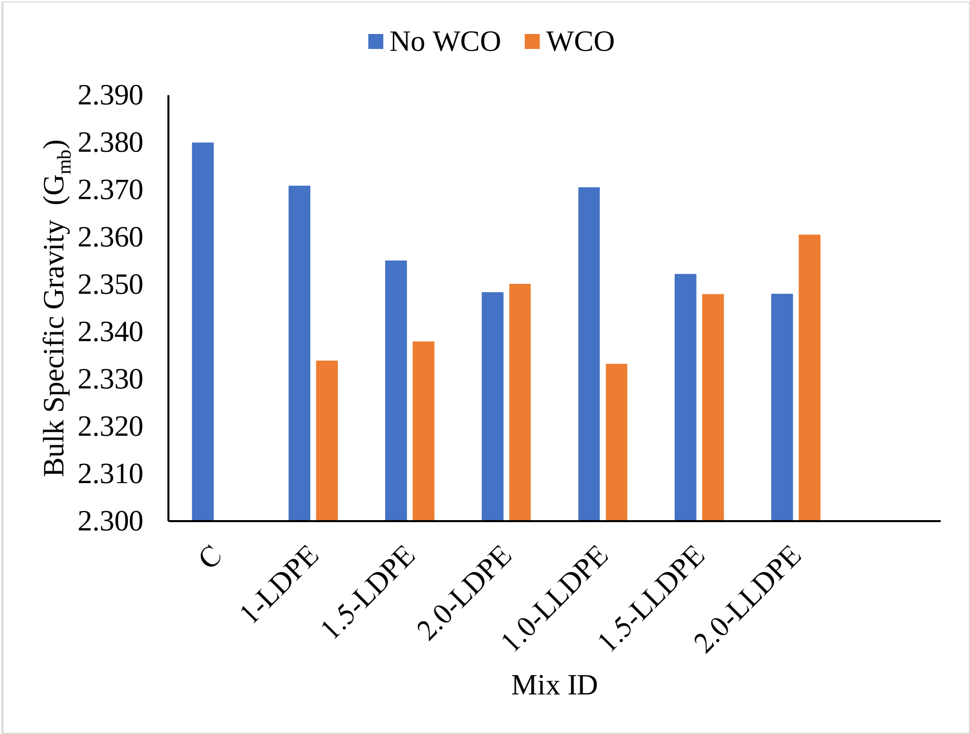

Figure 5.7 Variation of Bulk Specific Gravity of Mix (G_{mb}) with mix type

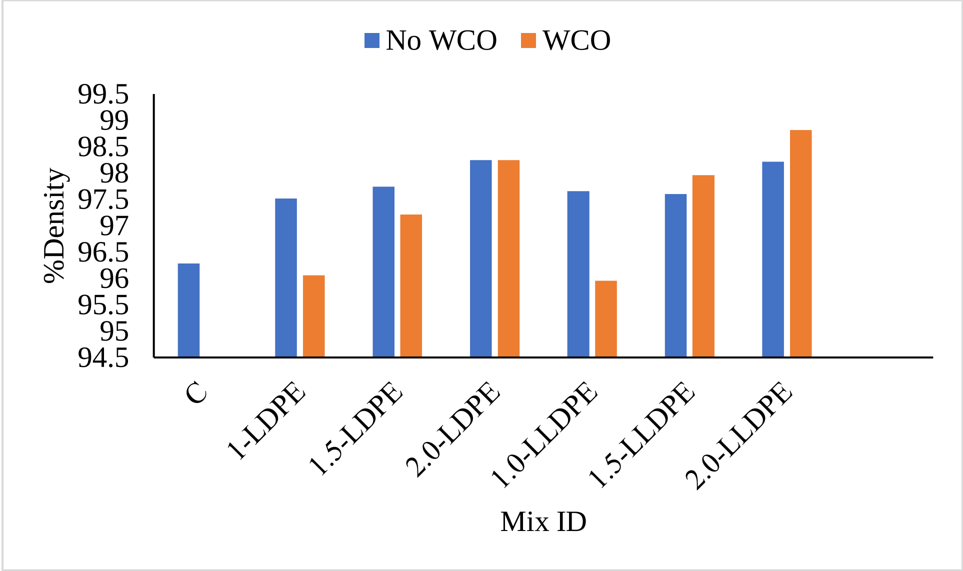

Figure 5.8 Variation of density with mix type

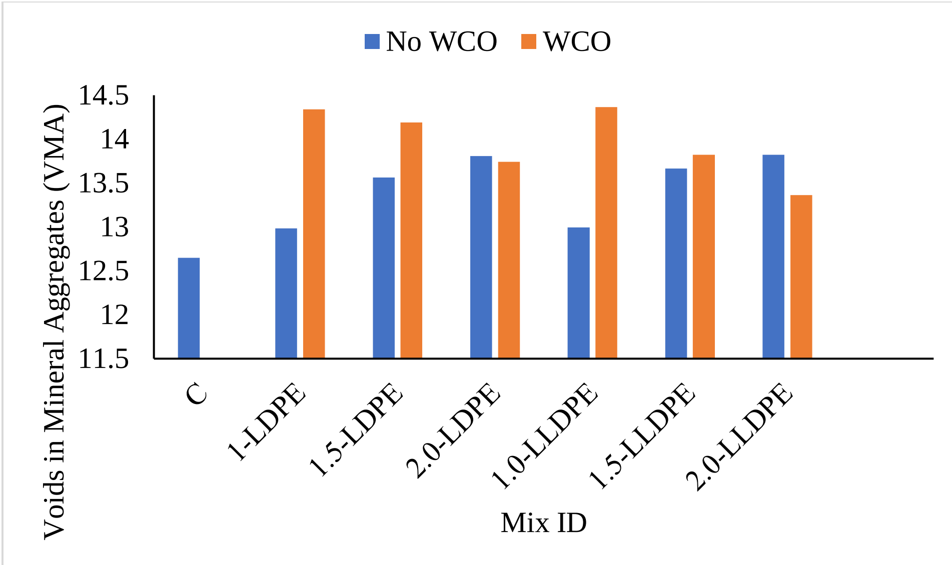

Figure 5.9 Variation of Voids in Mineral Aggregates (VMA) with mix type

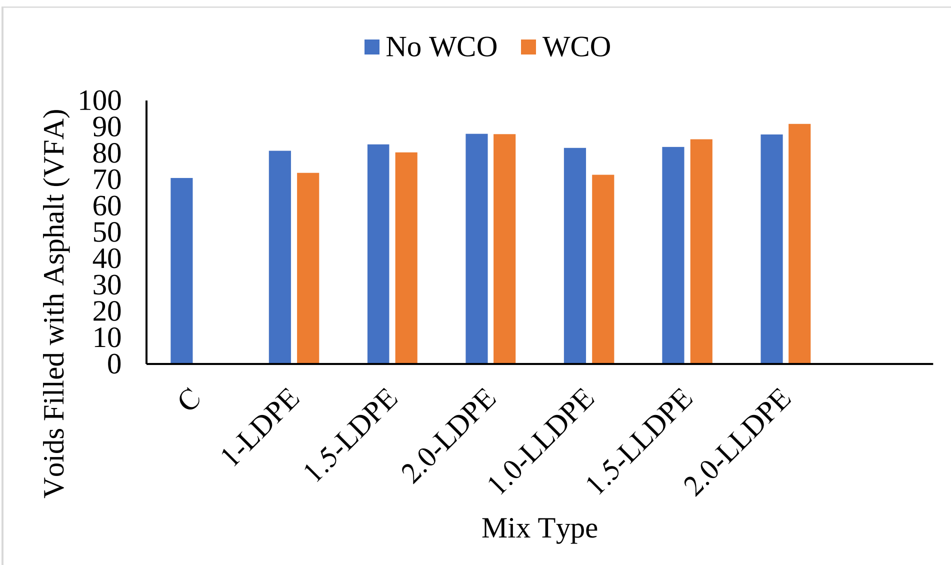

Figure 5.10 Variation of Voids Filled with Asphalt (VFA) with mix type

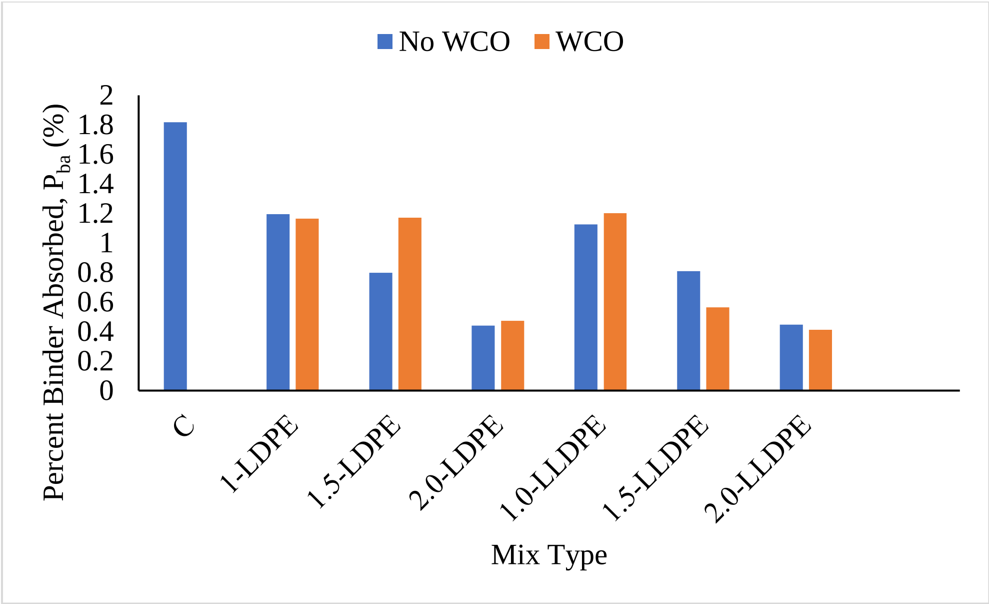

Figure 5.11 Variation of Percent Binder Absorbed (P_{ba}) with mix type

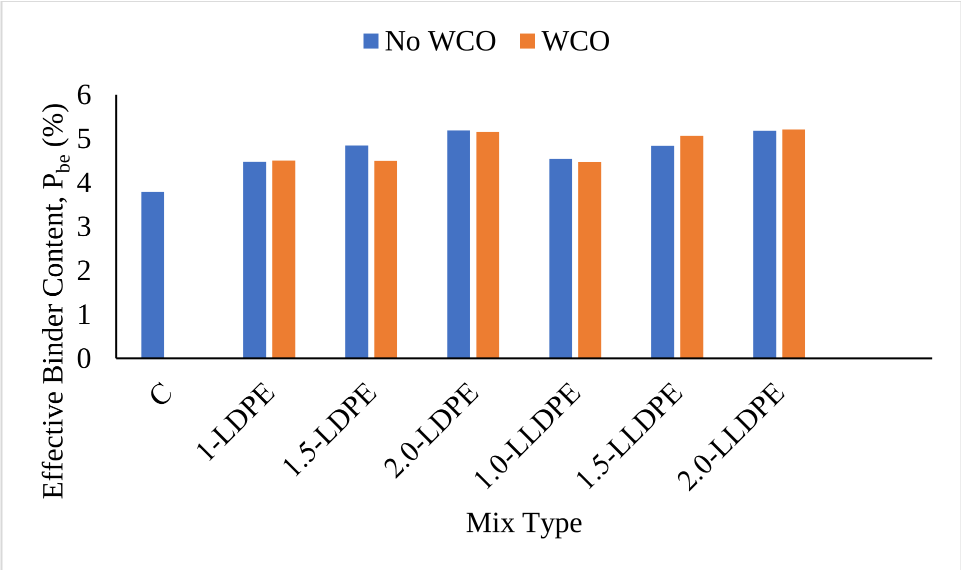

(g)

Figure 5.12 Variation of Effective Binder Content (P_{be}) with mix type

5.3.3.3 ***Effect on Rutting and Moisture Resistance***

Effects of LDPE, LLDPE and WCO on the rutting and moisture-induced damage resistance were evaluated using the HWT test. The rut depth vs load cycle data was recorded for each test and analyzed using both AASHTO 324 Method (AASHTO 2011) and Texas A&M

University (TAMU) method (Yin et al. 2014). Distinct parameters, namely rut depth at 10,000-wheel path, SIP, stripping slope, creep slope, LC_{SN}, $\Delta\varepsilon^{vp}_{LCsn}$ and LC_{ST} were used in this evaluation. A summary of the HWT results is presented in Table 5.4. Overall, rutting resistance was found to improve with the addition of LDPE and LLDPE as evident from Table 5.4. For example, the rut depth was found to decrease from 4.5-mm to 1.6-mm and 2.77-mm with the addition of 1% LDPE and 1% LLDPE, respectively. A similar trend was also observed from the $\Delta\varepsilon^{vp}_{LCsn}$ values. A higher value of $\Delta\varepsilon^{vp}_{LCsn}$corresponds to a lower resistance to rutting. Increase in the stiffness of plastic-modified mixes due to the formation of plastic rocks as mentioned in Chapter 4 (Ghos et al. 2024a) and the presence of plastic particles in the binder (Vasudevan et al. 2010; Ghos et al. 2024a) are primarily responsible for increasing the rutting resistance. It is interesting to observe that the rutting resistance increased up to the addition of 1.5% LDPE and decreased for 2% LDPE -modified mixes. A similar trend was observed for LLDPE-modified mixes. Therefore, replacement of a higher amount of aggregates (2% in this case) with plastic particles might produce a tender mix and hence reduce the rutting resistance. The addition of WCO was found to reduce the rutting resistance, as evident from Table 5.4. For example, rut depth was found as 1.64-mm and 5.67-mm for 1.0-LLDPE and 1.0-LDPE-WCO mixes, respectively. These results are consistent with the expectation that WCO reduces the stiffness of plastic-modified mixes. In addition to softening the mix, WCO might have prevented or reduced melting of plastics due to its chemical compatibility with LDPE and LLDPE and resulted in reduced modification of the binder (CP Lab Safety 2024). Therefore, care should be taken while using WCO in plastic-modified mixes as it may result in excessive rutting.

The resistance to moisture-induced damage was evaluated by SIP, stripping slope, LC_{SN} and LC_{ST}. It was observed that the addition of LDPE and LLDPE eliminated the inflection points in the rut depth vs load cycle plots. A mix without inflection point is expected to provide robust resistance to moisture-induced damage (Yin et al. 2014). A similar trend was obtained from both AASHTO T324 (AASHTO 2011) and TAMU methods (Yin et al. 2014). For example, SIP and LC_{SN} of all mixes were found to be more than 20,000 load cycles. As presented in Table 5.4, the LC_{ST} could not be calculated for plastic-modified mixes as the stripping phase did not exist. Therefore, plastic-modified mixes are expected to perform better against moisture induced damage. However, the addition of WCO was found to reduce the resistance to moisture induced damage. As previously mentioned, the use of WCO resulted in reduced melting of plastic particles. This phenomenon might have decreased the coating of aggregates with plastics and reduced the presence of melted plastics in binder.

Table 5.4 Summary of rutting and moisture induced damage performances

Parameter	Softening Agent	Mix Type						
		Control	1.0-LDPE	1.5-LDPE	2.0-LDPE	1.0-LLDPE	1.5-LLDPE	2.0-LLDPE
Rut Depth	No WCO	4.1	1.64	1.56	2.25	2.77	0.84	2.54
	WCO	--	5.67	1.9	5.81	2.4	1.88	1.9
SIP	No WCO	>20000	>20000	>20000	>20000	>20000	>20000	>20000
	WCO	--	10100	>20000	12620	14401	>20000	>20000
Creep Slope	No WCO	0.66	0.04	0.05	0.07	0	0	0
	WCO	----	0.0	0.1	0.43	0.12	0.1	0.02
Stripping Slope	No WCO	0	0	0	0	0	0	0
	WCO	--	--	0	6.04	0.22	0	0
LC_{SN}	No WCO	>20000	>20000	>20000	>20000	>20000	>20000	>20000
	WCO	--	0	>20000	2675	6285	>20000	>20000
LC_{ST}	No WCO	13475	--	--	--	--	--	--
	WCO	--	115	--	11705	>20000	--	--
$\Delta\varepsilon^{vp}_{LCsn}$	No WCO	6.7E-06	3.1E-07	3.2E-07	3.6E-07	0	0	0
	WCO	--	1.4E-10	5.9E-07	6.0E-06	1.4E-06	5.E-07	--

5.3.3.4 ***Effect on Cracking Resistance***

Figure 5.13 shows the variation of CT_{Index} with LDPE, LLDPE and WCO addition. Overall, the addition of LDPE and LLDPE was found to reduce the CT_{Index}. For example, CT_{Index} was found to reduce from 61 to 38 with an increase in LLDPE percentage from 1.0 to 1.5%. Increase in stiffness of mixes due to plastic addition is primarily responsible for reduced CT_{Index}. Increasing the amount of LLDPE from 1.5% to 2.0%, the CT_{Index} was found to increase from 36 to 38. Excessive plastics might have reduced the stiffness of asphalt mix as compared to the aggregates. A similar trend was observed for the LDPE-modified mixes. Nevertheless, all plastic-modified mixes were found to exhibit lower CT_{Index} as compared to the control mix. As previously mentioned, the main objective of this study was to increase the cracking resistance by incorporating WCO. A significant improvement in the cracking resistance was observed for WCO-LDPE-modified mixes, as evident from Figure 5.13. For example, the CT_{Index} was found to be 332 for the 1.5-LDPE mix after adding WCO, whereas the CT_{Index} was only 55 for the 1.5-LDPE mix without WCO. Softening of binder due to WCO is primarily responsible for increasing the CT_{Index} values. These results are also in agreement with DSR and HWT results. The CT_{Index} values of LLDPE mixes were also increased but not significantly. Therefore, WCO can be a great softening agent for LDPE-modified mixes but not significant for LLDPE-modified mixes.

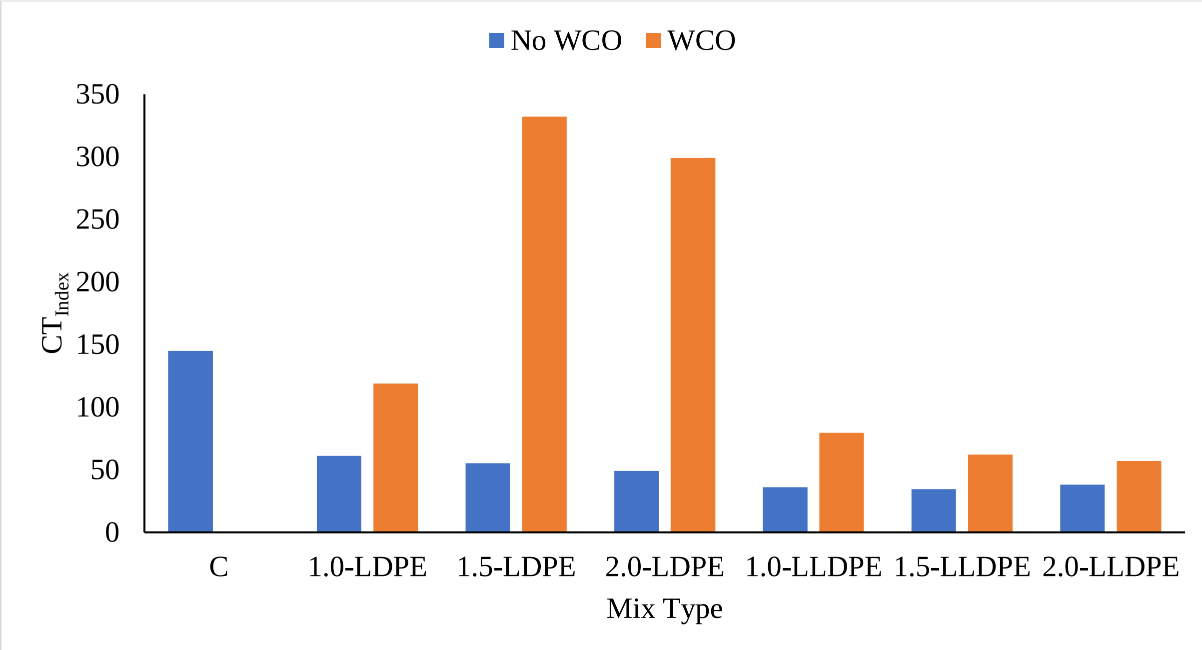

Figure 5.13 Variation of CT_{Index} of plastic- and WCO-plastic -modified mixes

5.3.4 **Selection of Optimum Plastic Dosage**

The optimum dosage of LDPE and LLDPEs were selected based on the 2023 ODOT's BMD Special Provision (ODOT 2023). Table 5.5 presents a summary of volumetric and performance properties of control, plastic- and WCO-plastic-modified mixes along with the ODOT BMD requirements. According to the 2023 ODOT BMD Special Provision, to be considered as a BMD surface course, a mix needs to have a CT_{Index} of at least 100 and a maximum rut depth of 12.5-mm (ODOT 2023). In addition, the %density of a BMD mix should vary between 96.0 and 97.0%. As presented in Table 5.5, the control mix satisfied all three ODOT's BMD criteria, namely %density, cracking and rutting. The LDPE and LLDPE-modified mixes, however, did not satisfy the ODOT's BMD criteria in at least one of the three categories. For example, 1.0-LDPE mix was found to fail in volumetric (density = 97.5>97.0%) and cracking criteria (CT_{Index} = 83<100). As previously mentioned, incorporation of WCO provided a significant improvement in the cracking resistance of LDPE-modified mixes. From Table 5.5, 1.0-LDPE-WCO and 1.5-LDPE-WCO-modified mixes were found to satisfy all three ODOT's BMD criteria. Therefore, the optimum doses of LDPE were selected as 1.5% with 2% WCO-modified binder. The WCO improved the properties of LLDPE-modified mixes to some extent but could not reach the BMD thresholds.

Table 5.5 Summary of the volumetric properties and mechanical performance along with ODOT BMD requirements

Parameter	Softening Agent	Sample ID						
		Control	1-LDPE	1.5-LDPE	2.0-LDPE	1.0-LLDPE	1.5-LLDPE	2.0-LLDPE
%Density	No WCO	96.3	97.5	97.7	98.3	97.6	97.6	98.2
	WCO	--	96	97	98.2	96	98	98.8
Cracking Tolerance Index (CT_{Index})	No WCO	145	61	55	49	36	35	38
	WCO	--	119	332	299	79.5	62	57
Rut Depth (mm)	No WCO	4.1	1.64	1.56	2.25	2.77	0.84	2.54
	WCO	--	5.67	1.9	5.81	2.4	1.88	1.9
ODOT %Density Requirement: 96.0-97.0%	No WCO	YES	NO	NO	NO	NO	NO	NO
	WCO	--	YES	YES	NO	YES	NO	NO
ODOT Cracking Requirements: CT_{Index} >=100	No WCO	YES	NO	NO	NO	NO	NO	NO
	WCO	--	YES	YES	YES	NO	NO	NO
ODOT Rutting Requirement: Rut Depth <=12.5-mm	No WCO	YES	YES	YES	YES	YES	YES	YES
	WCO	YES	YES	YES	YES	YES	YES	YES

*Satisfied ODOT Requirements: YES

* Did not Satisfy ODOT Requirements: NO

5.3.5 **Effect on Green House Gas (GHG) Emissions**

As previously noted, the environmental impacts of using plastic- and plastic-WCO-modified mixes were evaluated in terms of the net GHG emissions for each mix type. Figure 5.14(a) shows the variation of initial GHG emission amount for each mix type. As expected, the addition of waste plastics increased the initial GHG burdens. The increase in the plastic percentage further increased the GHG burdens. For example, the GHG burdens increased from 0.176 to 0.188 million tons CO_{2e} per year with an increase in the LDPE percentage from1 to 2%. The extra GHG emissions were associated with the recycling of waste plastics and transporting to asphalt plants. Figure 5.14(b) shows the avoided GHG emissions by incorporating PCR plastics in asphalt mixes. As previously mentioned, plastics are usually disposed of by landfilling or incineration. Incineration of plastics emits more GHG compared to landfilling. For instance, using a 1.5-LDPE mix can prevent 0.012 million tons of CO_2e emissions through landfilling and 0.153 million tons CO_2e through incineration. It was observed that the GHG emissions reduced significantly by adding PCR plastics in asphalt mixes. The addition of WCO further reduced GHG emissions. For example, avoided GHG emissions were found to be 0.102- and 0.205-million tons of CO_2e for 1.0-LDPE-WCO and 2.0-LDPE-WCO mixes, respectively. Figure 5.14(c) shows the net GHG emissions of control, plastic- and plastic-WCO-modified mixes. The net GHG emissions were calculated as the summation of GHG burden and avoided GHG emissions. It was observed that the addition of waste plastics significantly reduced the net GHG emissions as compared to the control mixes. For example, the net GHG emission of control and 1.5-LDPE mixes were found as 0.16 and 0.15 million tons of CO_2e, respectively, for Scenario 1 which considers landfilling. The rate of reduction in GHG emission was calculated as 7.5%. This rate was significantly higher for Scenario 2 and Scenario 3. The rates of reduction of GHG emission for 1.5-LDPE mix were found as 94% and 20% for Scenarios 2 and 3, respectively. It is interesting to note that the addition of 2% LDPE moved the mix production to carbon negative meaning that more GHG emissions could be avoided than produced. The avoided GHG emissions related to incineration of wastes plastic is primarily responsible for getting negative value for 2%-LDPE and LLDPE-modified mixes. Moreover, the addition of WCO further decreased the GHG emission.

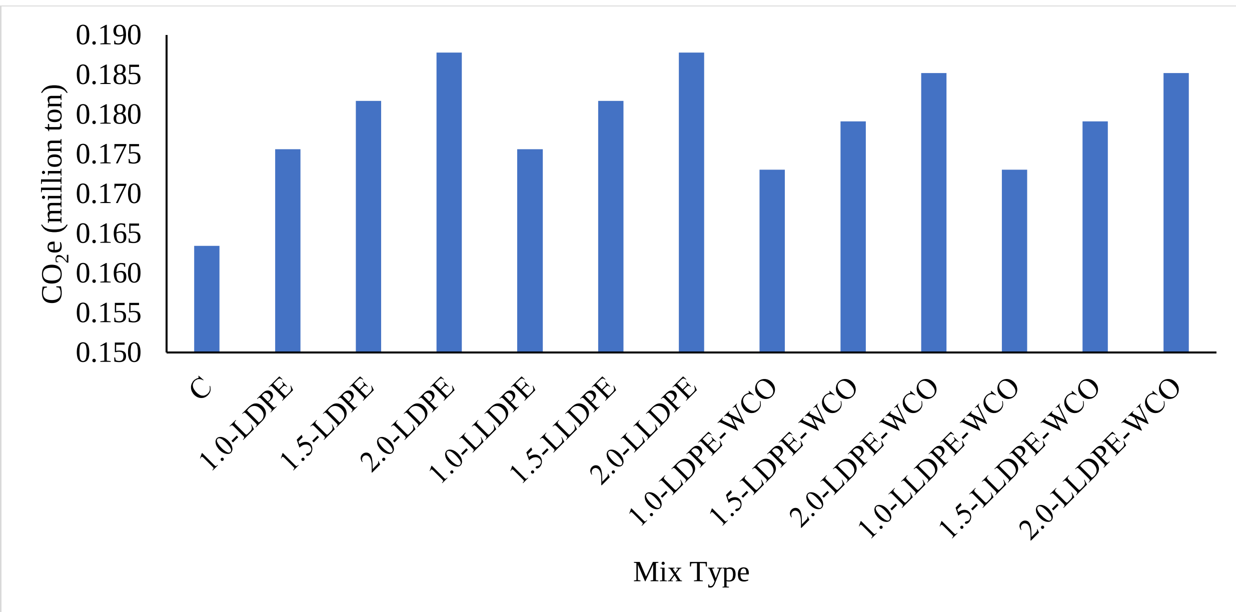

(a)

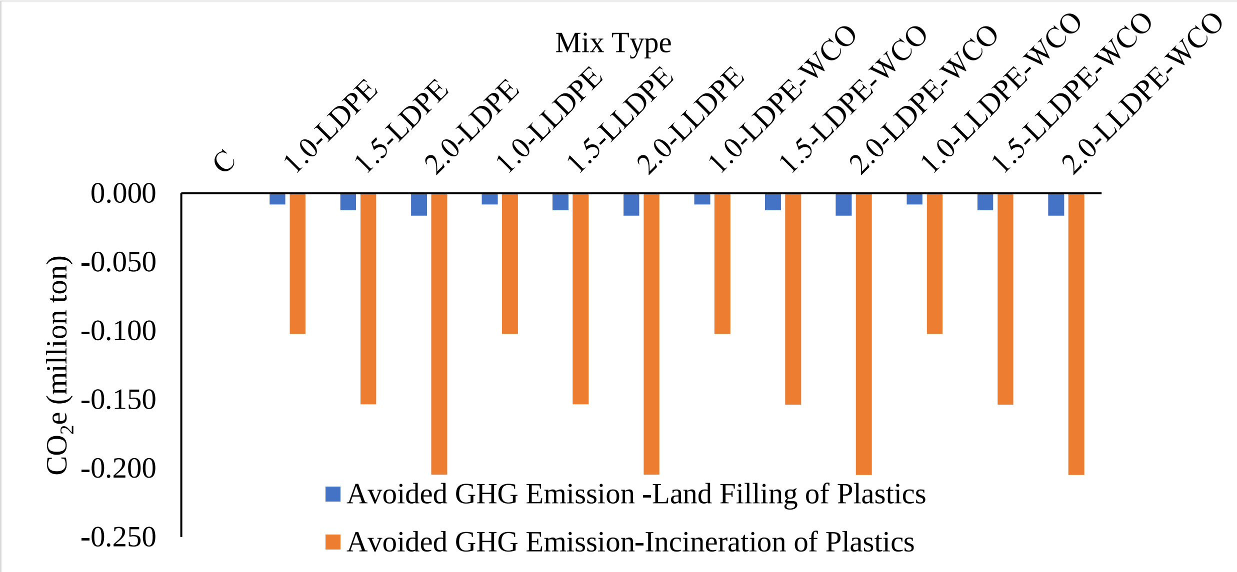

(b)

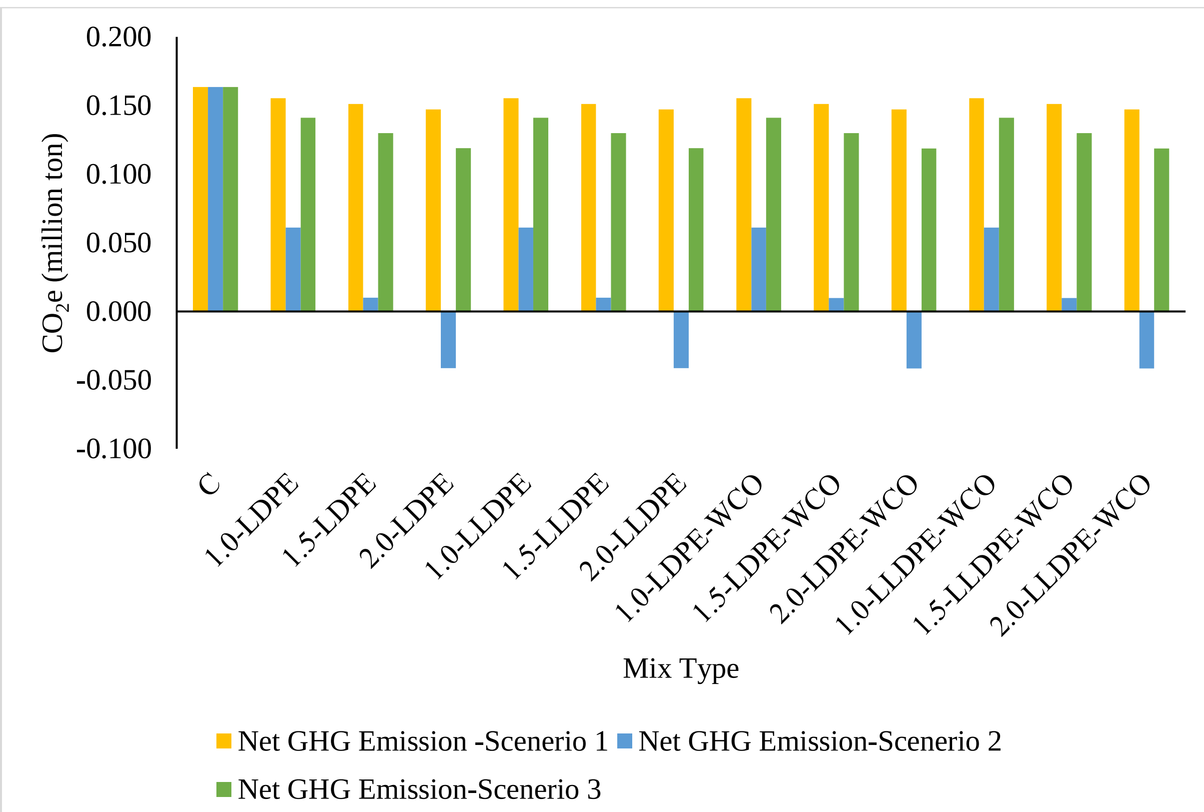

(c)

Figure 5.14 Variation of GHG emissions: (a) GHG burdens; (b) Avoided GHG emissions; and (c) Net GHG emissions considering three alternative scenarios

5.4 CONCLUSIONS

This study is aimed at increasing the plastic content in asphalt mixes by satisfying the BMD criteria. For this purpose, two different types of PCR plastics, namely LDPE and LLDPE, and a bio-rejuvenator (WCO in this case) was used for modifying a control asphalt mix. Both volumetric properties and mechanical performances of control, plastic- and plastic-WCO-modified mixes were evaluated in this study. Optimum dosage of plastic dosage was selected based on the ODOT's BMD threshold. In addition, environmental benefits of using plastic-modified mixes were quantified using GHG emission reduction. The following conclusions could be drawn from the results presented in the preceding sections:

- Addition of LDPE and LLDPE increase the rutting and moisture resistance as indicated by the HWT results. However, a significant reduction in the cracking resistances was observed due to increase in the plastic content, as indicated by the IDEAL-CT. Modification of binder with WCO resulted in a softer grade binder and latter improved the cracking resistance of plastic-modified mixes. Softening of binder with WCO was observed to be a physical phenomenon. No chemical interactions between binder and WCO were observed as evident from the FTIR results.
- A significant improvement in the cracking performance of LDPE-modified mix was observed after WCO addition. However, rutting resistance was reduced due to WCO addition. Therefore, care should be taken while using WCO in plastic-modified mixes. The optimum dosage of LDPE was found to be 1.5% by considering the ODOT's BMD criteria.
- A significant reduction in the GHG emissions was observed for plastic-modified mixes as compared to the control mix. A mix prepared with 1.5% LDPE and 2%-WCO modified

binder is expected to reduce the GHG emissions by 0.16 million tons of CO_2e for Oklahoma.

Findings of this study are based on one control mix (NMAS of 9.5-mm and PG 64-22 binder), two types of PCR plastics (LDPE and LLDPE) and one bio-rejuvenator (WCO). The effect of other bio-rejuvenators and commercial rejuvenators may be evaluated on different plastic-modified mixes. This study may be repeated using different grades of binders. In this study, environmental impacts of plastic- and WCO-plastic-modified mixes were evaluated using the CO_2e emission approach. Future studies may be conducted using Life Cycle Assessment (LCA). In addition, the environmental impacts may be evaluated using other environmental impact indicators, namely, ozone layer depletion, acidification, eutrophication and photochemical ozone formation.

CHAPTER 6 CONCLUSIONS AND RECOMMENDATIONS

6.1 CONCLUSIONS

In this dissertation, the effects of incorporating two types of Post-Consumer Recycled (PCR) plastics, namely LDPE and LLDPE, in asphalt mixes were evaluated with respect to changes in volumetric properties, rutting, cracking and moisture-induced damage. Also, the effects of loading rate and notch depth on the fracture properties of plastic-modified asphalt mixes were examined using three commonly used cracking tests. In addition, the effects of accelerated laboratory aging on plastic-modified mixes and extracted binders were evaluated using mix performance testing, binder rheology and advanced chemical characterization. An attempt was made to increase the plastic percentages by incorporating a bio-rejuvenator (Waste Cooking Oil (WCO)). The volumetric and mechanical performances of asphalt mixes with and without WCO were evaluated. Moreover, environmental impact assessments of plastic- and WCO-plastic-modified mixes were conducted using CO_2e emissions as the indicator. Also, the suitability of the plastic-modified mixes as a BMD was evaluated. Specific conclusions pertaining to a given topic were covered in each chapter. The major findings of this study are summarized in this chapter.

6.1.1 **Volumetric and Mechanical Performances of PCR Plastic-modified Mixes**

i. Adding PCR plastic at room-temperature during mixing with heated aggregate and binder was found to be a feasible way for incorporation of plastic in asphalt mixes using the dry process.

ii. The addition of LDPE and LLDPE plastics increased the density (% of G_{mm}) and decreased the G_{mm} and G_{mb} of the mixes.

iii. Rutting resistance improved with the use of the LDPE and LLDPE plastics. The LDPE-modified mixes exhibited a better rutting resistance than the LLDPE-modified mixes.

iv. Incorporation of plastic reduced the cracking resistance as indicated by the lower CT_{Index} in IDEAL-CT tests. However, the LLDPE-modified mixes performed better on cracking than the LDPE-modified mixes.

v. Based on the TSR values, the addition of LDPE and LLDPE reduced the resistance to moisture-induced damage of asphalt mixes. However, the LDPE-modified mixes were found to have a higher resistance to moisture-induced damage compared to the LLDPE-modified mixes.

vi. The mixes with 0.25%-LLDPE and 0.25%-LLDPE satisfied the requirements for a balanced mix, as per ODOT specification for BMD. Mixes with higher plastic percentages (0.5 and 1.0%) did not satisfy the BMD criteria. Specifically, two volumetric criteria (% density and Voids Filled with Asphalt (VFA)) and cracking resistance were difficult to meet at higher plastic percentages.

6.1.2 **Fracture Characteristics of PCR Plastic-modified Mixes**

i. The IFIT, L-SCB and IDEAL-CT tests showed that the ranking of mixes for cracking resistance is different for different test methods.

ii. The post-peak behavior of tested specimens had a significant influence on the ranking of cracking performance of the mixes. The L-SCB test was found to be more conservative than other tests. It only deals with the load-displacement curve up to crack initiations and does not account for the post-peak behavior. Situations where slower traffic loads are expected, plastic-modified mixes can be expected to provide superior performance as evident by the J_c-values from the L-SCB tests. The IDEAL-CT test is a more simplified test from practical considerations. However, the post-peak behavior is well captured by the IFIT test.

iii. The fracture parameters, namely SEF, Jc, FI and G_f, with loading rate and notch depth are influenced by the plastic content. At slower loading rate, the L-SCB was found to provide more consistent results. Variations in FI with loading rates are more distinguishable at slower loading rates and FI becomes asymptomatic at higher loading rates. Therefore, FI may be a better parameter at higher loading rates and Jc may be a better parameter at slower loading rates regardless of plastic contents.

6.1.3 **Aging and Long-Term Performance of Plastic-modified Mixes**

i. The IDEAL-CT test indicated a superior cracking resistance of the control mix in the early stage (STOA) compared to the LDPE and LLDPE-conditioned mixes. However, the rate of change of CT_{Index} with aging indicated reduced aging susceptibility of the LLDPE-modified mix followed by the LDPE-modified mix as compared to the control mix.

ii. The formation of plastic rock was a likely contributor to the stiffness of plastic-modified mixes. Partially plastic-coated aggregates and distorted plastic particles revealed that plastics did not melt fully in the dry processed plastic-modified mixes.

iii. Rheological characterization indicated superior rutting performance of plastic-modified mixes. No polymerization due to plastic addition was observed from the binder rheology. A higher aging susceptibility of plastic-modified mixes was evident from the rheological characterization of recovered binders.

iv. The LDPE-modified mixes were found to be more aging susceptible as compared to the control and LLDPE-modified mixes, as indicated by the FTIR results. Studying only the aging of plastic-modified mixes with mechanical tests is not sufficient. A combination of mechanical tests and chemical tests provides a better understanding of the aging mechanisms.

v. The PMED simulation can provide an insight into the mix performance at the structural level. Both LDPE- and LLDPE-modified mixes were found to provide superior rutting and bottom-up cracking resistances as indicated by the PMED simulations.

6.1.4 **Effect of WCO on Plastic-modified Mixes and Environmental Impact Assessment**

i. Addition of LDPE and LLDPE increased the rutting and moisture resistance. However, a significant reduction in the cracking resistance was observed due to increased plastic content. Modification of binder with WCO resulted in a softer grade binder which improved the cracking resistance of plastic-modified mixes.

ii. Softening of binder with WCO was observed to be a physical phenomenon. No chemical interactions between binder and WCO were observed, as evident from the FTIR results.

iii. A significant improvement in the cracking performance of LDPE-modified mixes was observed after WCO addition. However, rutting resistance was reduced due to WCO addition. Therefore, care should be taken while using WCO in plastic-modified mixes. The optimum dosage of LDPE was found to be 1.5% according to the ODOT's BMD criteria.

iv. A significant reduction in the GHG emissions was observed for plastic-modified mixes as compared to the control mix. A mix prepared with 1.5% LDPE and 2%-WCO modified binder is expected to reduce the GHG emissions by 0.16 million tons of CO_2e per year for Oklahoma.

6.2 Limitations and Recommendations

i. In this study, it was assumed that the plastic particles will act as a replacement of aggregate. However, in reality, a portion of the plastic is expected to melt during the mixing and compaction process. Due to the limited scope of this study, the effect of melted plastic was not investigated in this study. Also, for the purpose of this study, all the plastic modified mixes were considered uniform, i.e., similar distribution of materials throughout the compacted specimens. It should be noted that the findings of this study were based on a surface mix (NMAS of 9.5-mm) and two types of PCR plastics (LDPE and LLDPE). Effects of other PCR plastics on mixes with different aggregate gradations and different binder grades may be evaluated in future studies. Also, future studies may include plastics of different shapes and sizes.

ii. Investigations of chemical interactions between the asphalt binder and plastic particles are recommended for future studies. In addition, characterization of bond between the asphalt binder and plastics and between aggregates and plastics may be evaluated in future studies.

iii. Expanding the database by including more plant and laboratory mixes is recommended for future studies. Also, the incorporation of Finite Element Analysis (FEA) would be helpful in understanding these cracking tests, namely IFIT, IDEAL-CT and L-SCB.

iv. The aging of plastic-modified mixes was investigated using three aging protocols decided in consultation with the Oklahoma Department of Transportation (ODOT) personnel. Establishing relationships between the existing mix aging protocol (AASHTO R30 (AASHTO (2015)) and the proposed aging protocol for asphalt mixes may be pursued in future studies. Also, future studies may be conducted to establish relationships between the extracted binders from aged mixes and laboratory simulated aged binders using rheological and chemical properties.

v. In this study, aging was simulated using a force draft oven. A future study may be conducted using ultraviolet (UV) oven to simulate the UV aging of plastic-modified mixes.

vi. Structural performance of a flexible pavement was simulated in this study using a commonly used software, PMED. Properties of the plastic-modified mixes were used to model the asphalt layer of this flexible pavement. The effect of different pavement structures, for example, asphalt overlay on the top of a concrete pavement may be evaluated in future studies.

vii. This study did not examine the source and properties of WCO. Future studies may examine WCOs from known sources and assess their quality.

viii. In this study, environmental impacts of plastic- and WCO-plastic-modified mixes were evaluated using the CO_2e emission approach. Future studies may be conducted using Life Cycle Assessment (LCA). In addition, the environmental impacts may be evaluated using other environmental impact indicators, namely, ozone layer depletion, acidification, eutrophication and photochemical ozone formation.

ix. This study was based on laboratory investigations. Construction of pavement sections with plastic-modified mixes and monitoring the field performance are recommended for future studies.

REFERENCES

AASHTO (2007). T283: Standard Method of Test for Resistance of Compacted Asphalt Mixtures to Moisture-Induced Damage. American Association of State Highway and Transportation Officials. Washington D.C.

AASHTO (2011). T 324: Standard Method of Test for Hamburg Wheel-Track Testing of Compacted Hot Mix Asphalt (HMA). American Association of State Highway and Transportation Officials. Washington D.C.

AASHTO (2013). TP105: Standard Method of Test for Determining the Fracture Energy of Asphalt Mixtures Using the Semicircular Bend Geometry (SCB). American Association of State Highway and Transportation Officials, Washington, D.C.

AASHTO (2014). T164 Standard Method of Test for Quantitative Extraction of Asphalt Binder from Hot Mix Asphalt (HMA). American Association of State Highway and Transportation Officials. Washington D.C.

AASHTO (2015). R30-02: Standard Practice for Mixture Conditioning of Hot Mix Asphalt (HMA). American Association of State Highway and Transportation Officials. Washington D.C.

AASHTO (2016a). R28-12: Standard Method of Test for Accelerated Aging of Asphalt Binder Using a Pressurized Aging Vessel (PAV). American Association of State Highway and Transportation Officials. Washington D.C.

AASHTO (2016b). T209: Standard Method of Test for Theoretical Maximum Specific Gravity (G_{mm}) And Density of Hot Mix Asphalt (HMA). American Association of State Highway and Transportation Officials. Washington D.C.

AASHTO (2016c). T166: Standard Method of Test for Bulk Specific Gravity (G_{mb}) of Compacted Hot Mix Asphalt (HMA) Using Saturated Surface-Dry Specimens. American Association of State Highway and Transportation Officials. Washington D.C.

AASHTO (2017a). M323: Standard Specification for Superpave Volumetric Mix Design. American Association of State Highway and Transportation Officials. Washington D.C.

AASHTO (2017b). M 332-14: Standard Specifications for Performance-Graded Asphalt Binder Using Multiple Stress Creep Recovery (MSCR) Test. American Association of State Highway and Transportation Officials. Washington D.C.

AASHTO (2017c). T240-13: Standard Method of Test for Effect of Heat and Air on a Moving Film of Asphalt Binder (Rolling Thin-Film Oven Test). American Association of State Highway and Transportation Officials. Washington D.C.

AASHTO (2017d). T350-14: Standard Method of Test Multiple Stress Creep Recovery (MSCR) Test of Asphalt Binder Using a Dynamic Shear Rheometer (DSR)for Determining the Rheological Properties of Asphalt Binder Using a Dynamic Shear Rheometer (DSR). American Association of State Highway and Transportation Officials. Washington D.C.

AASHTO (2019). T 316: Standard Method of Test for Viscosity Determination of Asphalt Binder Using Rotational Viscometer. American Association of State Highway and Transportation Officials. Washington D.C.

AASHTO (2022a). T 313-22: Standard Method of Test for Determining the Flexural Creep Stiffness of Asphalt Binder Using the Bending Beam Rheometer (BBR). American Association of State Highway and Transportation Officials. Washington D.C.

AASHTO (2022b). M 320-22: Standard Specification for Performance-Graded Asphalt Binder. American Association of State Highway and Transportation Officials. Washington D.C.

AASHTO (2022c). R35-12: Standard Practice for Superpave Volumetric Design for Hot-Mix Asphalt (HMA). American Association of State Highway and Transportation Officials. Washington D.C.

AASHTO (2022d). T 393: Standard Method of Test for Determining the Fracture Potential of Asphalt Mixtures Using the Flexibility Index Test (FIT). American Association of State Highway and Transportation Officials. Washington D.C.

AASHTO (2022e). T315-22: Standard Method of Test for Determining the Rheological Properties of Asphalt Binder Using a Dynamic Shear Rheometer (DSR). American Association of State Highway and Transportation Officials. Washington D.C.

Abdulshafi, A. A., & Majidzadeh, K. (1985). J-integral and Cyclic Plasticity Approach to Fatigue and Fracture of Asphaltic Mixtures. Transportation Research Record, 1034, 112-123.

Abdelaziz, M., & Mohamed Rehan, K. (2010). Rheological Evaluation of Bituminous Binder Modified with Waste Plastic Material.

Abukhettala, M. (2016). Use of Recycled Materials in Road Construction. In Proceedings of the 2nd International Conference on Civil, Structural and Transportation Engineering (ICCSTE'16), Ottawa, Canada (138-1).

Adegoke, D. D., Ogundairo, T. O., Olukanni, D. O., & Olofinnade, O. M. (2019). Application of Recycled Waste Materials for Highway Construction: Prospect and Challenges. In Journal of Physics: Conference Series (Vol. 1378, 022058). IOP Publishing.

Al-Abdul Wahhab, H. I., Dalhat, M. A., & Habib, M. A. (2017). Storage Stability and High-Temperature Performance of Asphalt Binder Modified with Recycled Plastic. Road Materials and Pavement Design, 18(5), 1117-1134.

Aliha, M. M., Behbahani, H., Fazaeli, H., & Rezaifar, M. H. (2014). Study of Characteristic Specification on Mixed Mode Fracture Toughness of Asphalt Mixtures. Construction and Building Materials, 54, 623-635.

Almeida, A., Capitão, S., Bandeira, R., Fonseca, M., & Picado-Santos, L. (2020). Performance of AC Mixtures Containing Flakes of LDPE Plastic Film Collected from Urban Waste Considering Ageing. Construction and Building Materials, 232, 117253.

Ameri, M., Mansourian, A., Pirmohammad, S., Aliha, M. R. M., & Ayatollahi, M. R. (2012). Mixed Mode Fracture Resistance of Asphalt Concrete Mixtures. Engineering Fracture Mechanics, 93, 153-167.

Andrady, A. L. (2015). Plastics and Environmental Sustainability. John Wiley & Sons.

Angelone, S., Cauhapé Casaux, M., Borghi, M., & Martinez, F. O. (2016). Green Pavements: Reuse of Plastic Waste in Asphalt Mixtures. Materials and Structures, 49, 1655-1665.

Asphalt Institute (AI) (2019). IS-240: Use of the Delta Tc Parameter to Characterize Asphalt Binder Behavior.

Applied Research Associates (ARA) (2004). Guide for Mechanistic-Empirical Design of New and Rehabilitated Pavement Structures. Transportation Research Board, Washington, D.C

ASTM (2013). D5630-13: Standard Test Method for Ash Content in Plastics, ASTM International, West Conshohocken, PA.

ASTM (2015). D6925-15: Standard Test Method for Preparation and Determination of the Relative Density of Asphalt Mix Specimens by Means of the Superpave Gyratory Compactor. ASTM International, West Conshohocken, PA.

ASTM (2016). D8044-16: Standard Test Method for Evaluation of Asphalt Mixture Cracking Resistance using the Semi-Circular Bend Test (SCB) at Intermediate Temperatures. ASTM International West Conshohocken.

ASTM (2017). D6980-17: Standard Test Method for Determination of Moisture in Plastics by Loss in Weight, ASTM International, West Conshohocken, PA.

ASTM (2019). D8225-19: Standard Test Method for Determination of Cracking Tolerance Index of Asphalt Mixture Using the Indirect Tensile Cracking Test at Intermediate Temperature, ASTM International, West Conshohocken, PA.

ASTM (2020a). D1238-20: Standard Test Method for Melt Flow Rates of Thermoplastics by Extrusion Plastometer, ASTM International, West Conshohocken, PA.

ASTM (2020b). D792-20: Standard Test Methods for Density and Specific Gravity (Relative Density) of Plastics by Displacement, ASTM International, West Conshohocken, PA.

ASTM (2021). D 5404M: Standard Practice for Recovery of Asphalt Binder from Solution Using the Rotary Evaporator. ASTM International, West Conshohocken, PA.

Asli, H., Ahmadinia, E., Zargar, M., & Karim, M. R. (2012). Investigation on Physical Properties of Waste Cooking Oil–Rejuvenated Bitumen Binder. Construction and Building Materials, 37, 398-405.

Azam, A. M., El-Badawy, S. M., & Alabasse, R. M. (2019). Evaluation of Asphalt Mixtures Modified with Polymer and Wax. Innovative Infrastructure Solutions, 4(1), 43.

Baek, C., Underwood, B. S., & Kim, Y. R. (2012). Effects of Oxidative Aging on Asphalt Mixture Properties. Transportation Research Record, 2296(1), 77-85.

Behnood, A. (2019). Application of Rejuvenators to Improve the Rheological and Mechanical Properties of Asphalt Binders and Mixtures: A Review. Journal of Cleaner Production, 231, 171-182.

Belc, A. L., Ciutina, A., Buzatu, R., Belc, F., & Costescu, C. (2021). Environmental Impact Assessment of Different Warm Mix Asphalts. Sustainability, 13(21), 11869.

Berk, Z. (2018). Food Process Engineering and Technology. Academic Press.

Brown, E. R., Kandhal, P. S., Roberts, F. L., Kim, Y. R., Lee, D. Y., & Kennedy, T. W. (2009). Hot Mix Asphalt Materials, Mixture Design, and Construction. NAPA Research and Education Foundation.

Buchanan S. (2017). Balanced Mix Design (BMD). In Annual Conference of the Association of Asphalt Paving Technologies, CA, USA.

Buttlar, W. G., Meister, J., Jahangiri, B., Majidifard, H., & Rath, P. (2019). Performance Characteristics of Modern Recycled Asphalt Mixes in Missouri, Including Ground Tire Rubber, Recycled Roofing Shingles, and Rejuvenators (No. cmr 19-002).

Chang, Q., Edgar III, A. O., Ghos, S., Zaman, M., Huang, L., & Wu, X. (2023). An Atomistic Model of Aged Asphalt Guided by the Oxidation Chemistry of Benzylic Carbon with Application to Asphalt Rejuvenated with a Triglyceride. Construction and Building Materials, 400, 132743.

Chen, M., Xiao, F., Putman, B., Leng, B., & Wu, S. (2014). High Temperature Properties of Rejuvenating Recovered Binder with Rejuvenator, Waste Cooking and Cotton Seed Oils. Construction and Building Materials, 59, 10-16.

Costa, L. M., Peralta, J., Oliveira, J. R., & Silva, H. M. (2017). A New Life for Cross-Linked Plastic Waste as Aggregates and Binder Modifier for Asphalt Mixtures. Applied Sciences, 7(6), 603.

CP Lab Safety (2024).

url: https://www.calpaclab.com/ldpe-chemical-compatibility-chart/ (Accessed Date: 9/16/2024)

Cooper, S. B., King, W., & Kabir, S. (2016). Testing and Analysis of LWT and SCB Properties of Asphalt Concrete Mixtures (No. Final Report 536).

Costa, L. M., Silva, H. M., Oliveira, J. R., & Fernandes, S. R. (2013). Incorporation of Waste Plastic in Asphalt Binders to Improve Their Performance in the Pavement. International Journal of Pavement Research and Technology, 6(4), 457.

Costa, L. M., Silva, H. M., Peralta, J., & Oliveira, J. R. (2019). Using Waste Polymers as a Reliable Alternative for Asphalt Binder Modification–Performance and Morphological Assessment. Construction and Building Materials, 198, 237-244.

Dalhat, M. A., & Al-Abdul Wahhab, H. I. (2017). Performance of Recycled Plastic Waste Modified Asphalt Binder in Saudi Arabia. International Journal of Pavement Engineering, 18(4), 349-357.

Dalhat, M. A., Al-Abdul Wahhab, H. I., & Al-Adham, K. (2019). Recycled Plastic Waste Asphalt Concrete via Mineral Aggregate Substitution and Binder Modification. Journal of Materials in Civil Engineering, Vol. 31(8), 04019134.

Domke, C. H., Davison, R. R., & Glover, C. J. (2000). Effect of Oxygen Pressure on Asphalt Oxidation Kinetics. Industrial & Engineering Chemistry Research, 39(3), 592-598.

Dugan, C. R., Sumter, C. R., Rani, S., Ali, S. A., O'Rear, E. A., & Zaman, M. (2020). Rheology of Virgin Asphalt Binder Combined with High Percentages of RAP Binder Rejuvenated with Waste Vegetable Oil. ACS Omega, 5(26), 15791-15798.

El Khatib, A. K. (2016). Development of a Performance-Based Test Method for Quantification of Cracking Potential in Asphalt Pavement Materials. Doctoral Dissertation, University of Illinois at Urbana-Champaign.

Elseifi, M. A., Mohammad, L. N., Ying, H., & Cooper III, S. (2012). Modeling and Evaluation of the Cracking Resistance of Asphalt Mixtures Using the Semi-Circular Bending Test at Intermediate Temperatures. Road Materials and Pavement Design, 13(sup1), 124-139.

Environmental Protection Agency (EPA). 2020

https://www.epa.gov/facts-and-figures-about-materials-waste-and-recycling/plastics-material-specific-data#PlasticsOverview (Accessed Date: 7/25/2020)

Environmental Protection Agency (EPA) (2024) url: https://www.epa.gov/facts-and-figures-about-materials-waste-and-recycling/plastics-material-specific-data (Accessed Date: 8/26/2024)

Fang, C., Liu, P., Yu, R., & Liu, X. (2014). Preparation Process to Affect Stability in Waste Polyethylene-Modified Bitumen. Construction and Building Materials, 54, 320-325.

Fang, J.M., Han, Z.Y., Tu, J.S. (2019). Study on the Rheological Properties and Regeneration Mechanism of Biomass Heavy Oil Recycled Asphalt. Bulletin of the Chinese Ceramic Society 38 (04), 1024–1029.

Fang, Y., Zhang, Z., Yang, J., & Li, X. (2021). Comprehensive Review on the Application of Bio-Rejuvenator in the Regeneration of Waste Asphalt Materials. Construction and Building Materials, 295, 123631.

Fini, E. H., Al-Qadi, I. L., You, Z., Zada, B., & Mills-Beale, J. (2012). Partial Replacement of Asphalt Binder with Bio-Binder: Characterisation and Modification. International Journal of Pavement Engineering, 13(6), 515-522.

Fini, E. H., Oldham, D., & Abu-Lebdeh, T. (2013). Synthesis and Characterization of Bio-Modified Rubber (BMR) Asphalt: A Sustainable Waste Management Solution for Scrap Tire and Swine Manure. J. Environ. Eng, 10, 1454-1461.

Fried, J. R. (2014). Polymer Science and Technology. Pearson Education.

Ghos, S., Sumter, C. R., Arevalo, P. C., Ali, S. A., Zaman, M., Hobson, K. R., ... & Metzer, D. (2022a). Performance of Asphalt Mixes Containing Postconsumer Recycled Plastic Using Balanced Mix Design Approach and Dry Process. Transportation Research Record, 2676(9), 720-732.

Ghos, S., Ali, S. A., Zaman, M., Arevalo, P. F. C., & Hobson, K. R. (2022b). Evaluation of Stiffness and Fatigue Cracking Resistance of Post-Consumer Recycled (PCR) Plastic-Modified Asphalt Mixes. In International Conference on Transportation and Development 2022 (201-211).

Ghos, S., Ali, S. A., Zaman, M. & Hobson, K. R. (2024a). Fracture Characterization of Asphalt Mixes Containing Post-Consumer Recycled (PCR) Plastics using Different Cracking Tests. Submitted in International Journal of Pavement Research and Technology (Under Review).

Ghos, S., Ali, S. A., Hobson, K. R. & Zaman, M. (2024b). Aging of Post Consumer Recycled (PCR) Plastic-Modified Asphalt Mixes and Binders: A Laboratory Study. Submitted in Transportation Geotechnics (Under Review).

Ghos, S., Ali, S. A., Urbina, L. G., Segura, A., Hobson, K. R. & Zaman, M. (2024c). Effect of Bio-Rejuvenator on Post-Consumer Recycled (PCR) Plastic-Modified Asphalt Mixes: Laboratory Investigation and Environmental Impact Analysis. Submitted in Journal of Materials in Civil Engineering (Under Review).

Goli, A., Rout, B., Cyril, T., & Govindaraj, V. (2023). Evaluation of Mechanical Characteristics and Plastic Coating Efficiency in Plastic-Modified Asphalt Mixes. International Journal of Pavement Research and Technology, 16(3), 693-704.

Grossegger, D., Grothe, H., Hofko, B., & Hospodka, M. (2018). Fluorescence Spectroscopic Investigation of Bitumen Aged by Field Exposure Respectively Modified Rolling Thin Film Oven Test. Road Materials and Pavement Design, 19(4), 992-1000.

Haider, S., Hafeez, I., & Ullah, R. (2020). Sustainable Use of Waste Plastic Modifiers to Strengthen the Adhesion Properties of Asphalt Mixtures. Construction and Building Materials, 235, 117496.

Hamid, S. H. (2000). Handbook of Polymer Degradation. CRC Press.

Haslett, K. E. (2018). Evaluation of Cracking Indices for Asphalt Mixtures Using SCB Tests at Different Temperatures and Loading Rates. Senior Honors Thesis, University of New Hampshire.

Heydari, S., Javadi, N. H. S., Bayat, H., & Hajimohammadi, A. (2024). Assessment of Binder Modification in Dry-Added Waste Plastic Modified Asphalt. Polymers, 16(14).

Hou, X., Lv, S., Chen, Z., & Xiao, F. (2018a). Applications of Fourier Transform Infrared Spectroscopy Technologies on Asphalt Materials. Measurement, 121, 304-316.

Hou, X., Xiao, F., Wang, J., & Amirkhanian, S. (2018b). Identification of Asphalt Aging Characterization by Spectrophotometry Technique. Fuel, 226, 230-239.

Hu, K. & Wang, S. (2016). Study on Rheological Properties of Asphalt Based on Different Aging Methods, Highways & Automotive Applications 5, pp 73–75.

Hopewell, J., Dvorak, R., & Kosior, E. (2009). Plastics Recycling: Challenges and Opportunities. Philosophical Transactions of the Royal Society B: Biological Sciences, 364(1526), 2115-2126.

Islam, M. R., Hossain, M. I., & Tarefder, R. A. (2015). A Study of Asphalt Aging Using Indirect Tensile Strength Test. Construction and Building Materials, 95, 218-223.

Indian Road Congress (IRC) (2013) SP: 98-2013. Guidelines For the Use of Waste Plastic in Hot Bituminous Mixes (Dry Process) in Wearing Course.

Jin, X., Han, R., Cui, Y., & Glover, C. J. (2011). Fast-Rate–Constant-Rate Oxidation Kinetics Model for Asphalt Binders. Industrial & Engineering Chemistry Research, 50(23), 13373-13379.

Jin, D., Ge, D., Chen, S., Che, T., Liu, H., Malburg, L., & You, Z. (2021). Cold in-Place Recycling Asphalt Mixtures: Laboratory Performance and Preliminary ME Design Analysis. Materials, 14(8), 2036.

Kim, Y. R., Castorena, C., Elwardany, M., Rad, F. Y., Underwood, B. S., Gundla, A., ... & Glaser, R. R. (2018). Long-Term Aging of Asphalt Mixtures for Performance Testing and Prediction.

Kim, S., Ceylan, H., and Gopalakrishnan, K. (2007). Effect of ME Design Guide Inputs on Flexible Pavement Performance Predictions. Road Materials and Pavement Design, 8(3), pp. 375-397.

Khan A.S. (2016). Displacement Rate and Temperature Effect on Asphalt Concrete Cracking Potential.MS Thesis, University of Illinois at Urbana-Champaign.

Khan TA, Sharma DK & Sharma BM. (2009). Performance Evaluation of Waste Plastic/Polymer Modified Bituminous Concrete Mixes. Journal of Scientific and Industrial Research, Vol 68, 975-979.

Kole, P. J., Löhr, A. J., Van Belleghem, F. G., & Ragas, A. M. (2017). Wear and Tear of Tires: A Stealthy Source of Microplastics in the Environment. International Journal of Environmental Research and Public Health, 14(10), 1265.

Kumar V, Singh R, Ahuja IP (2020). Use of Thermosetting Polymers for Smart Civil Structures. In Reference Module in Materials Science and Materials Engineering. DOI: 10.1016/B978-0-12-820352-1.00067-5.

Kumar, A., Choudhary, R., & Kumar, A. (2021). Aging Characteristics of Asphalt Binders Modified with Waste Tire and Plastic Pyrolytic Chars. PLoS One, 16(8), e0256030.

Lastra-González, P., Calzada-Pérez, M. A., Castro-Fresno, D., Vega-Zamanillo, Á., & Indacoechea-Vega, I. (2016). Comparative Analysis of the Performance of Asphalt Concretes Modified by Dry Way with Polymeric Waste. Construction and Building Materials, 112, 1133-1140.

Lee, S. J., Amirkhanian, S. N., & Kim, K. W. (2009). Laboratory Evaluation of the Effects of Short-Term Oven Aging on Asphalt Binders in Asphalt Mixtures Using HP-GPC. Construction and Building Materials, 23(9), 3087-3093.

Leng, Z., Padhan, R. K., & Sreeram, A. (2018). Production of A Sustainable Paving Material Through Chemical Recycling of Waste PET into Crumb Rubber Modified Asphalt. Journal of Cleaner Production, 180, 682-688.

Lesueur, D. (2009). The Colloidal Structure of Bitumen: Consequences on the Rheology and on the Mechanisms of Bitumen Modification. Advances in Colloid and Interface Science, 145(1-2), 42-82.

Li, R., Schwartz, C. W., and Forman, B. (2013). Sensitivity of Predicted Pavement Performance to Climate Characteristics. In Airfield and Highway Pavement 2013: Sustainable and Efficient Pavements (pp. 760-771).

Li X, & Marasteanu M. (2010). The Fracture Process Zone in Asphalt Mixture at Low Temperature. Engineering Fracture Mechanics.77(7):1175-90.

Martin-Alfonso, J. E., Cuadri, A. A., Torres, J., Hidalgo, M. E., & Partal, P. (2019). Use of Plastic Wastes from Greenhouse in Asphalt Mixes Manufactured by Dry Process. Road Materials and Pavement Design, 20(sup1), S265-S281.

Mashaan, N. S., Chegenizadeh, A., Nikraz, H., & Rezagholilou, A. (2021). Investigating the Engineering Properties of Asphalt Binder Modified with Waste Plastic Polymer. Ain Shams Engineering Journal, 12(2), 1569-1574.

Meroni, F., Flintsch, G. W., Diefenderfer, B. K., & Diefenderfer, S. D. (2020). Application of Balanced Mix Design Methodology to Optimize Surface Mixes with High-RAP Content. Materials, 13(24), 5638.

Menaria, Y., & Sankhla, R. (2015). Use of Waste Plastic in Flexible Pavements-Green Roads. Open Journal of Civil Engineering, 5(03), 299.

Miranda, M. N., Sampaio, M. J., Tavares, P. B., Silva, A. M., & Pereira, M. F. R. (2021). Aging Assessment of Microplastics (LDPE, PET and uPVC) Under Urban Environment Stressors. Science of the Total Environment, 796, 148914.

Milbrandt, A., Coney, K., Badgett, A., & Beckham, G. T. (2022). Quantification and Evaluation of Plastic Waste in the United States. Resources, Conservation and Recycling, Vol. 183, 106363.

Mishra, B., & Gupta, M. K. (2020,). Use of Plastic Waste in Bituminous Mixes by Wet and Dry Methods. In Proceedings of the Institution of Civil Engineers-Municipal Engineer (Vol. 173, 2, 87-97). Thomas Telford Ltd.

Modarres, A., & Hamedi, H. (2014). Effect of Waste Plastic Bottles on the Stiffness and Fatigue Properties of Modified Asphalt Mixes. Materials & Design, 61, 8-15.

Mogawer, W., Bennert, T., Daniel, J. S., Bonaquist, R., Austerman, A., & Booshehrian, A. (2012). Performance Characteristics of Plant Produced High RAP Mixtures. Road Materials and Pavement Design, 13(sup1), 183-208.

Moghaddam, T. B., Soltani, M., & Karim, M. R. (2014). Experimental Characterization of Rutting Performance of Polyethylene Terephthalate Modified Asphalt Mixtures Under Static and Dynamic Loads. Construction and Building Materials, 65, 487-494.

Nazzal, M. D., Abu-Qtaish, L., Kaya, S., & Powers, D. (2015). Using Atomic Force Microscopy to Evaluate the Nanostructure and Nanomechanics of Warm Mix Asphalt. Journal of Materials in Civil Engineering, 27(10), 04015005.

Nizamuddin, S., Baloch, H. A., Jamal, M., Madapusi, S., & Giustozzi, F. (2022). Performance of Waste Plastic Bio-Oil as a Rejuvenator for Asphalt Binder. Science of the Total Environment, 828, 154489.

National Renewable Energy Laboratory (NERL). (2009). Life Cycle Analysis of Waste Cooking Oil Biodiesel Production.
url: https://www.nrel.gov/ (Accessed Date: 7/12/2024)

Newcomb, D., Arámbula-Mercado, E., Martin, A. E., Yuan, M., Tran, N., & Yin, F. (2019). Field Verification of Proposed Changes to the AASHTO R 30 Procedures for Laboratory Conditioning of Asphalt Mixtures (No. NCHRP Project 09-52A).

Nouali, M., Ghorbel, E., & Derriche, Z. (2020). Phase Separation and Thermal Degradation of Plastic Bag Waste Modified Bitumen During High Temperature Storage. Construction and Building Materials, 239, 117872.

Oklahoma Department of Transportation (ODOT) (2009). 2009 Oklahoma Department of Transportation Specification.

Oklahoma Department of Transportation (ODOT) (2014). OHD L-55: Method of Test for Hamburg Rut Testing of Compacted Hot-Mix Asphalt (HMA).

Oklahoma Department of Transportation (ODOT) (2020). ODOT Balanced Mix Design Special Provision.

Oklahoma Department of Transportation (ODOT) (2023). ODOT Balanced Mix Design Special Provision.

Ouyang, C., Wang, S., Zhang, Y., & Zhang, Y. (2006). Improving the Aging Resistance of Styrene–Butadiene–Styrene Tri-Block Copolymer Modified Asphalt by Addition of Antioxidants. Polymer Degradation and Stability, 91(4), 795-804.

Ozer H, Al-Qadi IL, Singhvi P, Khan T, Rivera-Perez J, El-Khatib A. Fracture Characterization of Asphalt Mixtures with High Recycled Content Using Illinois Semicircular Bending Test Method and Flexibility Index. Transportation Research Record. 2016;2575(1):130-7.

Paul, D. K., Sirin, O., & Kassem, E. (2016). Laboratory Investigation of Asphalt Mixture Aging. In Proceedings of 6th Eurasphalt & Eurobitume Congress (pp. 1-7).

Plastics Europe. (2020). Eco-profiles and Environmental Product Declarations of the European Plastics Manufacturers: Low-Density Polyethylene (LDPE). url: https://plasticseurope.org/sustainability/circularity/life-cycle-thinking/eco-profiles-set/ (Accessed Date: 7/12/2024)

Plastic Industry Association (PLASTICS). 2020 (url: https://www.plasticsindustry.org/sites/default/files/2020-Size%20%26%20Impact%20Report-Executive%20Summary.pdf)

Plastic Technology. 2021 url: https://www.ptonline.com/articles/density-molecular-weight-in-polyethylene, (Accessed Date: 7-26-21)

Qu, X., Liu, Q., Wang, C., Wang, D., & Oeser, M. (2018). Effect of Co-Production of Renewable Biomaterials on the Performance of Asphalt Binder in Macro and Micro Perspectives. Materials, 11(2), 244.

Ranieri, M., Costa, L., M. Oliveira, J. R., RD Silva, H. M., & Celauro, C. (2017). Asphalt Surface Mixtures with Improved Performance Using Waste Polymers via Dry and Wet Processes. Journal of Materials in Civil Engineering, 29(10), 04017169.

Radeef, H. R., Hassan, N. A., Mahmud, M. Z. H., Abidin, A. R. Z., Ismail, C. R., Abbas, H. F., & Al-Saffar, Z. H. (2021). Characterisation of Cracking Resistance in Modified Hot Mix Asphalt Under Repeated Loading Using Digital Image Analysis. Theoretical and Applied Fracture Mechanics, 116, 103130.

Radeef, H. R., Hassan, N. A., Abidin, A. Z., Mahmud, M. Z. H., Ismail, C. R., Abbas, H. F., ... & Redha, S. (2022). Impact of Ageing and Moisture Damage on the Fracture Properties of Plastic Waste Modified Asphalt. In IOP Conference Series: Earth and Environmental Science (Vol. 971, No. 1, p. 012009). IOP Publishing.

Radeef, H. R., Hassan, N. A., Mahmud, M. Z. H., Al Saffar, Z. H., Abass, H. F., Abidin, A. R. Z., & Ismail, C. R. (2023). Fracture Resistance of Polymeric Wastes Modified Asphalt Using R-Curve and Digital Image Correlation. Theoretical and Applied Fracture Mechanics, 123, 103691.

Saha G, & Biligiri KP. (2016). Fracture Properties of Asphalt Mixtures Using Semi-Circular Bending Test: A State-of-the-Art Review and Future Research. Construction and Building Materials.105:103-12.

Sabouri M (2020). Evaluation of Performance-Based Mix Design for Asphalt Mixtures Containing Reclaimed Asphalt Pavement (RAP). Construction and Building Materials. 235:117545.

Saleh, N. F., Keshavarzi, B., Rad, F. Y., Mocelin, D., Elwardany, M., Castorena, C., ... & Kim, Y. R. (2020). Effects of Aging on Asphalt Mixture and Pavement Performance. Construction and Building Materials, 258, 120309.

Santos, J., Pham, A., Stasinopoulos, P., & Giustozzi, F. (2021). Recycling Waste Plastics in Roads: A Life-Cycle Assessment Study Using Primary Data. Science of the Total Environment, 751, 141842.

Shen, J., Amirkhanian, S., & Lee, S. J. (2005). The Effects of Rejuvenating Agents on Recycled Aged CRM Binders. The International Journal of Pavement Engineering, 6(4), 273-279.

Shen, J., Amirkhanian, S., & Aune Miller, J. (2007). Effects of Rejuvenating Agents on Superpave Mixtures Containing Reclaimed Asphalt Pavement. Journal of Materials in Civil Engineering, 19(5), 376-384.

Spiegelberg, S., Kozak, A., & Braithwaite, G. (2016). Characterization of Physical, Chemical, and Mechanical Properties of UHMWPE. In UHMWPE Biomaterials Handbook (pp. 531-552). William Andrew Publishing.

Somayaji, S. (1985). Civil Engineering Materials. Pearson Education India.

Suaryana, N., Nirwan, E., & Ronny, Y. (2018). Plastic Bag Waste on Hot Mixture Asphalt as Modifier. Key Engineering Materials, 789, 20-25.

SMART NEWS (2024)
url: https://www.smithsonianmag.com/smart-news/the-us-recycled-just-5-percent-of-its-plastic-in-2021-180980052/ (Accessed Date: 8/26/2024)

The Guardian (2024)
url: https://www.theguardian.com/us-news/2022/may/04/us-recycling-plastic-waste (Accessed Date: 8/26/2024)

Unice, K. M., Weeber, M. P., Abramson, M. M., Reid, R. C. D., Van Gils, J. A. G., Markus, A. A., ... & Panko, J. M. (2019). Characterizing Export of Land-Based Microplastics to the Estuary-Part I: Application of Integrated Geospatial Microplastic Transport Models to Assess Tire and Road Wear Particles in the Seine Watershed. Science of the Total Environment, 646, 1639-1649.

United State Plastic Corporation (2024) Link: https://www.usplastic.com/knowledgebase/article.aspx?contentkey=508 (Accessed Date: 8/24/2024)

Vasudevan, R. N. S. K., Nigam, S. K., Velkennedy, R., Sekar, A. R. C., & Sundarakannan, B. (2010). Utilization of Waste Polymers for Flexible Pavement and Easy Disposal of Waste Polymers. International Journal of Pavement Research and Technology, 3(1), 34-42.

Vogelsang, C., Lusher, A., Dadkhah, M. E., Sundvor, I., Umar, M., Ranneklev, S. B., ... & Meland, S. (2019). Microplastics in Road Dust–Characteristics, Pathways and Measures. NIVA-Report.

Wang, F., Xiao, Y., Cui, P., Lin, J., Li, M., & Chen, Z. (2020). Correlation of Asphalt Performance Indicators and Aging Degrees: A Review. Construction and Building Materials, 250, 118824.

Wang, Y., Wang, W., & Wang, L. (2022). Understanding the Relationships Between Rheology and Chemistry of Asphalt Binders: A Review. Construction and Building Materials, 329, 127161.

West, R., Rodezno, C., Leiva, F., & Yin, F. (2018). Development of a Framework for Balanced Mix Design. Project NCHRP, 20-07.

Wildnauer, M., Mulholland, E., & Liddie, J. (2019). Life Cycle Assessment of Asphalt Binder. Asphalt Institute, Lexington, KY.

Willis R, Yin F, Moraes R. (2020). Recycled Plastics in Asphalt Part A: State of the Knowledge. National Asphalt Pavement Association (NAPA).

Williams, B. A., Willis, J. R., & Shacat, J. (2020). Asphalt Pavement Industry Survey on Recycled Materials and Warm-Mix Asphalt Usage: 2019 (No. IS 138 (10e)).

Williams, B.A., J.R. Willis, & Shacat, J. (2022). Annual Asphalt Pavement Industry Survey on Recycled Materials and Warm-Mix Asphalt Usage: 2021, 12th Annual Survey (IS 138). National Asphalt Pavement Association, Greenbelt, Maryland. DOI:10.13140/RG.2.2.23149.26081

Wu, S., Tahri, O., Shen, S., Zhang, W., & Muhunthan, B. (2021). Environmental Impact Evaluation and Long-Term Rutting Resistance Performance of Warm Mix Asphalt Technologies. Journal of Cleaner Production, 278, 123938.

Xu, K., Wen, Y., & Xu, X. (2023). Melt Flow Ratio: A Way to Identify the Type of Polyethylene. Advanced Industrial and Engineering Polymer Research, 6(1), 79-82.

Yang, S. (2016). Quantification and Characterization of Fracture Resistance in Asphalt Concrete Based on R-Curve Method. Doctoral Dissertation, University of Arkansas.

Yang, S. H., & Suciptan, T. (2016). Rheological Behavior of Japanese Cedar-Based Bio-Binder as Partial Replacement for Bituminous Binder. Construction and Building Materials, 114, 127-133.

Yao, L., Leng, Z., Lan, J., Chen, R., & Jiang, J. (2022). Environmental and Economic Assessment of Collective Recycling Waste Plastic and Reclaimed Asphalt Pavement into Pavement Construction: A Case Study in Hong Kong. Journal of Cleaner Production, 336, 130405.

Yin, F., Arambula, E., Lytton, R., Martin, A. E., & Cucalon, L. G. (2014). Novel Method for Moisture Susceptibility and Rutting Evaluation Using Hamburg Wheel Tracking Test. Transportation Research Record, 2446(1), 1-7.

Zhao, X., Wang, S., Wang, Q., & Yao, H. (2016). Rheological and Structural Evolution of SBS Modified Asphalts Under Natural Weathering. Fuel, 184, 242-247.

Zhang, Q., Goh, S. W., & You, Z. P. (2011a). Study on Dynamic Modulus of Waste Plastic Modified Asphalt Mixture Using Waste Plastic Bag Chips. Advanced Materials Research, 261, 824-828.

Zhang, F., Yu, J., & Han, J. (2011b). Effects of Thermal Oxidative Ageing on Dynamic Viscosity, TG/DTG, DTA and FTIR of SBS-and SBS/Sulfur-Modified Asphalts. Construction and Building Materials, 25(1), 129-137.

Zhang, D., Zhang, H., & Shi, C. (2017). Investigation of Aging Performance of SBS-Modified Asphalt with Various Aging Methods. Construction and Building Materials, 145, 445-451.

Zhang, H., Chen, Z., Xu, G., & Shi, C. (2018). Physical, Rheological and Chemical Characterization of Aging Behaviors of Thermochromic Asphalt Binder. Fuel, 211, 850-858.

Zhang, P., Guo, Q., Tao, J., Ma, D., & Wang, Y. (2019). Aging Mechanism of a Diatomite-Modified Asphalt Binder Using Fourier-Transform Infrared (FTIR) Spectroscopy Analysis. Materials, 12(6), 988.

Ziari, H., Amini, A., & Goli, A. (2020). The Effect of Different Aging Conditions and Strain Levels on Relationship Between Fatigue Life of Asphalt Binders and Mixtures. Construction and Building Materials, 244, 118345.

Zhou, B., Pei, J., Zhang, J., Guo, F., Wen, Y., & Luo, P. (2020). Comparison of Fracture Test Methods for Evaluating the Crack Resistance of Asphalt Mixture. Arabian Journal for Science and Engineering, 45, 8745-8758.

Zhou, F., Im, S., Sun, L., & Scullion, T. (2017). Development of an IDEAL Cracking Test for Asphalt Mix Design and QC/QA. Road Materials and Pavement Design, 18(sup4), 405-427.

Zhang, J., Li, H., Liu, P., Liang, M., Jiang, H., Yao, Z., & Airey, G. (2020a). Experimental Exploration of Influence of Recycled Polymer Components on Rutting Resistance and Fatigue Behavior of Asphalt Mixtures. Journal of Materials in Civil Engineering, 32(6), 04020129.

Zhang, W., Tang, J., Dong, Z., Ma, T., Akber, M. A., Huang, X., ... & Luan, Y. (2020b). Performance Characterization of Recycled-Asphalt Pavement with Stabilized Rubber–Modified Asphalt Using Balanced Mix Design Method. Journal of Materials in Civil Engineering, 32(12), 04020387.

Zhou, F., Karki, P., Xie, S., Yuan, J. S., Sun, L., Lee, R., & Barborak, R. (2018). Toward the Development of Performance-Related Specification for Bio-rejuvenators. Construction and Building Materials, 174, 443-455.

Zargar, M., Ahmadinia, E., Asli, H., & Karim, M. R. (2012). Investigation of the Possibility of Using Waste Cooking Oil as a Rejuvenating Agent for Aged Bitumen. Journal of Hazardous Materials, 233, 254-258.

Zeng, M., Li, J., Zhu, W., & Xia, Y. (2018). Laboratory Evaluation on Residue in Castor Oil Production as Rejuvenator for Aged Paving Asphalt Binder. Construction and Building Materials, 193, 276-285.